Journal of Medicinal Chemistry

pubs.acs.org/jmc

Perspective

Targeting SARS-CoV-2 Proteases and Polymerase for COVID-19 Treatment: State of the Art and Future Opportunities

Rolando Cannalire, Carmen Cerchia, Andrea R. Beccari, Francesco Saverio Di Leva, and Vincenzo Summa*

Cite This: J. Med. Chem. 2022, 65, 2716−2746

Read Online

ACCESS | Metrics & More | Article Recommendations | Supporting Information

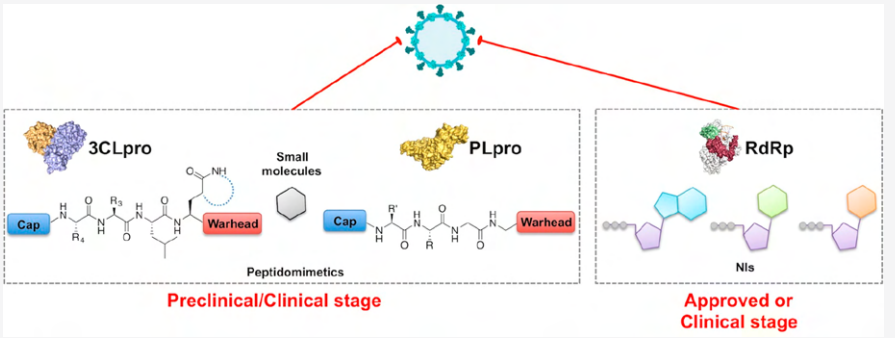

ABSTRACT: The newly emerged coronavirus, called SARS-CoV-2, is the causing pathogen of pandemic COVID-19. The identification of drugs to treat COVID-19 and other coronavirus diseases is an urgent global need, thus different strategies targeting either virus or host cell are still under investigation. Direct-acting agents, targeting protease and polymerase functionalities, represent a milestone in antiviral therapy. The 3C-like (or Main) protease ($3CL^{pro}$) and the nsp12 RNA-dependent RNA-polymerase (RdRp) are the best characterized SARS-CoV-2 targets and show the highest degree of conservation across coronaviruses fostering the identification of broad-spectrum inhibitors. Coronaviruses also possess a papain-like protease, another essential enzyme, still poorly characterized and not equally conserved, limiting the identification of broad-spectrum agents. Herein, we provide an exhaustive comparative analysis of SARS-CoV-2 proteases and RdRp with respect to other coronavirus homologues. Moreover, we highlight the most promising inhibitors of these proteins reported so far, including the possible strategies for their further development.

INTRODUCTION

RNA viruses represent a large and heterogeneous group of human pathogens that periodically jeopardize the public health because of apparent sudden epidemic outbreaks. In the recent years, the World Health Organization (WHO) prioritized the most threatening viral diseases worldwide including Middle East respiratory syndrome (MERS), severe acute respiratory syndrome (SARS), Ebola, Zika, and Dengue[1] while advancing the theory of Disease X, a disease associated with pandemic risk caused by a still unknown pathogen.[2] Lastly, at the end of 2019, an outbreak of severe pneumonia with an uncertain etiopathology in China was indicated as the Disease X by WHO that soon after announced the identification of a new coronavirus (CoV), called 2019-nCoV, as the etiologic agent of COVID-19 disease.[3,4] Genomic sequence of 2019-nCoV has highlighted 79.5% identity to SARS-CoV genome and thereafter the new CoV is known as SARS-CoV-2. The infection has rapidly spread in many countries across Asia, Europe, and Americas, causing the pandemic COVID-19 disease, as announced by WHO on March 11 2020, that currently has caused almost 35 million cases, many hospitalizations and more than one million deaths.[5] The current scenario has highlighted major gaps in the abilities of most countries to face new virulent pathogens. In fact, the most effective procedure to control the spread of the infection is the social distancing: as a consequence, billions of people's lives have been impacted following such countermeasures.[6−8] Moreover, COVID-19 will likely burden on worldwide health systems and on the global economy due to the lock-down measures, and the damage will be uncountable if the spread of the virus is not effectively controlled.[9] However, together with the social distancing and the lock-down, the availability of effective antiviral drugs would have an enormous beneficial impact on the control of the health emergency and the possibility to come back to normal life.

Special Issue: COVID-19

Received: July 2, 2020
Published: November 13, 2020

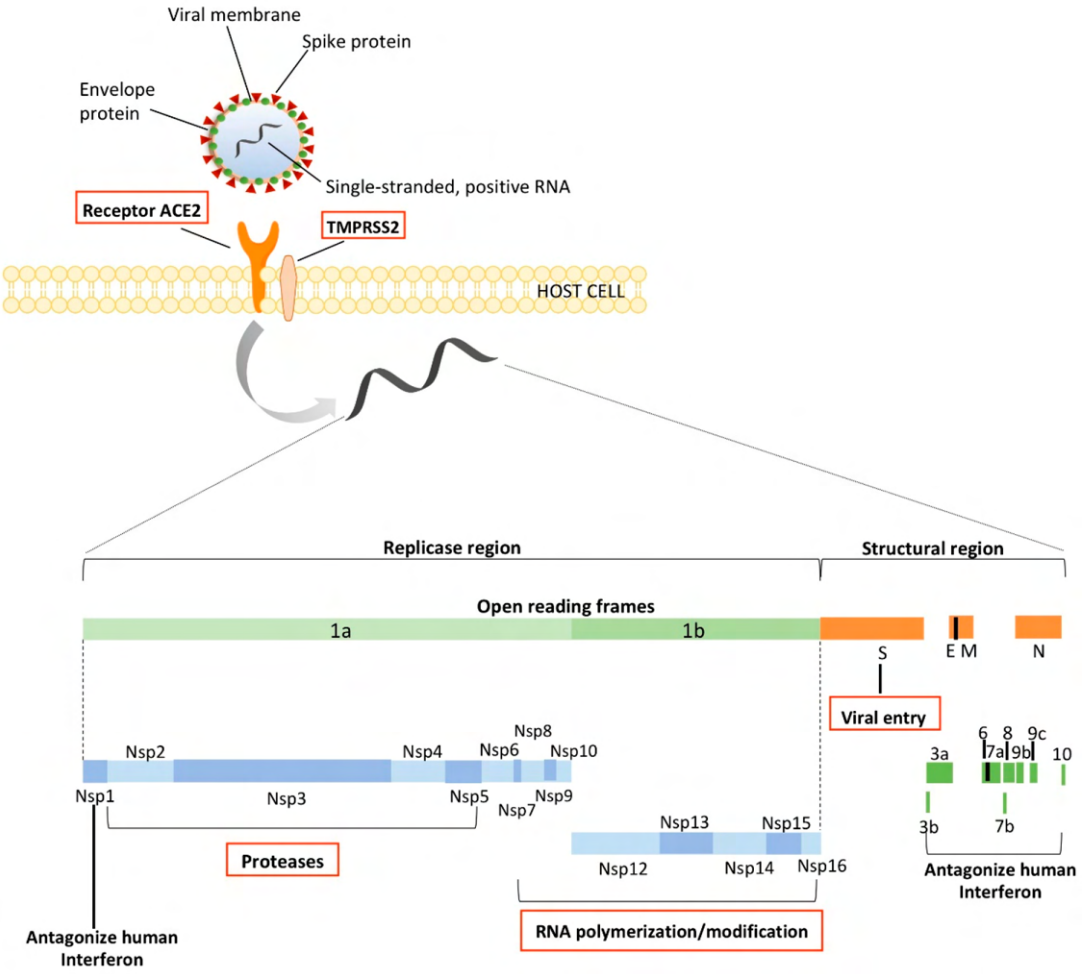

Figure 1. Schematic representation of SARS-CoV-2 virion, viral entry, genome translation, and polyprotein processing.

In this context, drug repurposing offers the opportunity to quickly identify a drug to prevent, control or, hopefully, eradicate the SARS-CoV-2 virus, although a serious clinical validation is required.[10] WHO has launched "Solidarity", one of the largest international clinical trials aimed at identifying successful treatments against COVID-19.[11] Among the drugs under investigation, Remdesivir was included. It is an intravenous (iv) monophosphoramidate nucleoside prodrug polymerase inhibitor with broad-spectrum activity against RNA viruses, originally under investigation as an Ebola virus disease (EVD) medication. On the basis of the clinical trials results, Remdesivir was granted an emergency use authorization (EUA) for the treatment of patients with severe COVID-19 symptoms being the only pathogen specific drug approved for treatment of the disease at the moment.[12] The authorization was granted in the U.S. first, and then in a growing number of countries, including Japan, India, EU, UK, Australia, and South Korea, based on the promising results from the National Institute of Allergy and Infectious Diseases (NIAID), the Gilead clinical trials, and from the compassionate use programs.[13−15] The FDA subsequently broadened the scope of the existing EUA to include treatment of all hospitalized adult and pediatric patients with suspected or laboratory-confirmed COVID-19, irrespective of their severity of disease. Remdesivir eventually received the approval from the FDA for the treatment of COVID-19 patients requiring hospitalization.

Besides drug repurposing, which can offer the great advantage to translate safe-in-man drugs quickly into clinic with just little experimental evidence of antiviral activity, the rational design of new chemical entities to specifically act against key steps of viral replication, supported by appropriate biological and DMPK screening cascade, represents the main strategy to discover new potent and selective antiviral drugs.[16,17] Immediately after the understanding of the potential pandemic spread of the SARS-CoV-2 infection, the whole scientific community collaborated to characterize the viral genome and viable therapeutic targets in order to rapidly identify provisional treatments and, as a longer-term goal, find a cure.[18] Many efforts have been made in molecular biology, biochemistry, and structural biology of SARS-CoV-2, thus biochemical assays and 3D-structures have been made public for different viral proteins, while it has been shown that different cell lines are permissive toward viral infection thus allowing easy phenotypic screenings to identify antiviral compounds. Moreover, anti-SARS-CoV-2 drug discovery can take advantage from the knowledge and the biology tools acquired on other human pathogenic CoVs such as SARS-CoV and MERS-CoV, to cite a few, that can be utilized as counter screenings to develop broad-spectrum CoV inhibitors to

https://dx.doi.org/10.1021/acs.jmedchem.0c01140
J. Med. Chem. 2022, 65, 2716−2746

potentially protect also from emerging infection caused by the same virus family.[18]

Researchers all around the world are exploiting different strategies targeting both viral and host factors essential for the pathogen replication to block one or more steps of its life cycles, and their efforts have already produced a great amount of data and studies. Thus, COVID-19 drug discovery is an emerging, rapidly evolving, and intriguing research field for medicinal chemists.[19]

This Perspective will aim to critically describe some of the most promising approaches toward the identification of anti-CoVs agents, especially focusing on the best characterized virus targets and the state-of-the-art on the antiviral agents identified, providing an unbiased point-of-view on the gaps to be filled. The inhibition of viral protease and polymerase functionalities represents a milestone in antiviral drug discovery field and provided most of the effective antiviral drugs for the treatment of HIV and hepatitis C virus (HCV) infections and also allowed for the development of antiviral agents acting against different virus families. Indeed, viral protease and polymerase inhibitors are included in the WHO list of essential drugs. Therefore, an exhaustive comparative analysis of SARS-CoV-2 proteases and RdRp with respect to other human pathogenic CoVs homologues is provided. Moreover, the most interesting compounds targeting the SARS-CoV-2, 3-chymotrypsin-like (3CL), or Main (M) protease (pro), and the nsp12 RNA-dependent RNA polymerase (RdRp), are analyzed in detail, discussing biological activity *in vitro*/*in vivo*, DMPK and clinical data, when available. Possible strategies for further development of the inhibitors are also discussed providing an unbiased point-of-view on the gaps to be filled. Additionally, potential strategies targeting the less explored papain-like (PL) pro will be described.

BIOCHEMISTRY AND REPLICATIVE CYCLE OF SARS-COV-2

Belonging to the subfamily *Coronavirinae*, family *Coronavirdiae*, order *Nidovirales*, CoVs are single-stranded positive-sense (ss-(+)) RNA viruses, further clustered into four classes designated as alpha, beta, gamma, and delta.[20] Bats and rodents are the gene sources of most α-CoVs and β-CoVs, while avian species are those for most γ- and δ-CoVs, indeed, CoVs are able to cross species barriers, sometimes emerging as important human pathogens.[21] Before December 2019, six CoVs were known to infect humans, including α-CoVs, *i.e.*, HCoV-229E and HCoV-NL63, and β-CoVs, such as HCoV-OC43, HCoV-HKU1, SARS-CoV, and MERS-CoV.[21] The β-CoV HCoV-OC43 and HCoV-HKU1 usually cause common cold disease, while SARS-CoV and MERS-CoV and the newly identified SARS-CoV-2, to different extents, may cause severe life-threatening conditions to lower respiratory tract such as pneumonia, but they may also affect the gastrointestinal system, heart, kidney, liver, and central nervous system, leading to multiple organ failure.[4] Moreover, SARS CoV-2, even if associated with a lower mortality rate, is more transmissible than SARS-CoV.[22] Genomic comparative analysis showed that SARS-CoV-2 sequence has identity of 79.5 and 96% to SARS-CoV and a bat CoV, SL-CoV-RaTG13, respectively; thus, its outbreak highlights the ability of viral spillover from animals to humans.[3]

CoVs share many morphological, biochemical, and functional aspects, which help in the understanding of SARS-CoV-2 biology and life cycle.[4,20] CoVs are relatively big (50−200 nm) enveloped viruses containing an encapsidated (ss-(+))-RNA, which is the largest viral genome found so far, with SARS-CoV-2 made-up by 30 kb (Figure 1).[23] Similar to other CoVs, the SARS-CoV-2 viral membrane is studded with glycoprotein spikes (S), that give CoVs their crown-like appearance in electron microscope imaging.[23] The virion contains other three structural proteins, known as envelope (E), membrane (M), which form the viral envelope together with S, and nucleocapsid (N), a basic RNA-binding protein that complexes and protects the genome.[24]

The S protein mediates the virus attachment to the host cell membrane through subunit S1 interaction with the human angiotensin-converting enzyme 2 (ACE2), acting as the receptor for viral entry (Figure 1).[25,26] The interactions between the two proteins have been fully elucidated with the support of several 3D structures of the S/ACE2 complex, highlighting the key residues involved in the recognitions process.[27−29]

The host proteins CatB/L, transmembrane protease serine 2 (TMPRSS2) have been shown to be involved in the entry process.[26] Thus, the identification of drugs targeting either the viral or the host factors could represent a valid strategy to inhibit viral entry.[30,31]

Upon the entry, the uncoating by nucleocapsid degradation allows the release into the cytoplasm of the viral RNA, ready for translation. The genome contains a 5′ cap structure with a leader sequence along with a 3′ poly(A) tail that allows it acting as mRNA. The 5′- and the 3′-ends contain highly stem loop structured untranslated regions (UTRs) required for RNA replication and transcription.[20] The 5′- and 3′-UTRs flank the coding region with the two-thirds of the genome from the 5′-end comprising two overlapping open reading frames (ORFs), ORF1a and ORF1b, that encode for polyproteins pp1a (4382 amino acids) and pp1ab (7073 amino acids), respectively. The autoproteolytically processing by $3CL^{pro}$ and PL^{pro} affords 16 nonstructural proteins (nsp1−16), which form the replicase/transcriptase complex (RTC) (Figure 1). The terminal 10 kb toward the 3′-poly(A) tail encodes instead for the structural S, E, M, and N, following this order (Figure 1).[24] Among the genes for structural proteins, there are those encoding for accessory proteins that show roles in viral pathogenesis and host immunity suppression, although they are not essential for *in vitro* replication, as found for other CoVs.[32] SARS-CoV-2 and SARS-CoV display very similar genetic composition, sharing the Orf1ab encoding for the 16 nsps and the four typical CoV structural proteins. They differ in some accessory proteins, with SARS-CoV-2 Orf3b and Orf10 showing low homology to SARS-CoV and an intact Orf8 instead of the two subunits, Orf8a and Orf8b, expressed by the latter virus.[20]

The RTC includes different enzymes and cofactors involved in post-translational polyprotein processing, RNA synthesis, maturation, and virions assembly and egress, which therefore can constitute ideal viral targets for drug discovery, being essential for the virus life cycle and devoid of a close host homologue.[24] The nsps that exert enzymatic activities are the nsp3 PL^{pro} that catalyzes cleavages at the nsp1/2, nsp2/3, and nsp3/4 sites of the polyprotein, and the nsp5 $3CL^{pro}$ (or M^{pro}), which performs the remaining 11 proteolytic events.[24] PL^{pro} additionally cleaves post-translational modified host proteins involved in innate immune response, thus contributing to immune escape. Predominantly PL^{pro} can recognize and hydrolyze the cellular proteins ubiquitin (Ub) and the Ub-

https://dx.doi.org/10.1021/acs.jmedchem.0c01140
J. Med. Chem. 2022, 65, 2716−2746

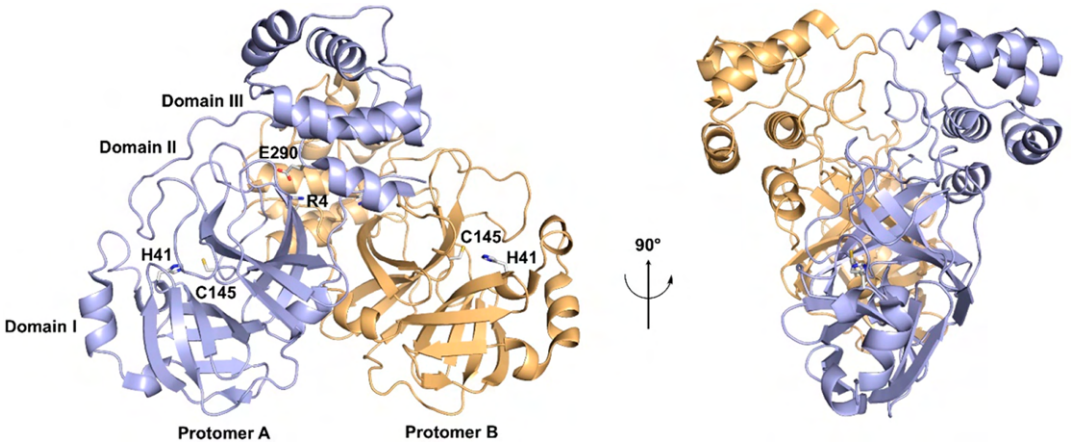

Figure 2. Overview of SARS-CoV-2 3CL^{pro} architecture. The X-ray structure of SARS-CoV-2 3CLpro (PDB 6Y2G) is shown as a ribbon model in two different orientations. For clarity, the bound inhibitor has been removed. Protomers A (light-blue) and B (light-orange) associate into a dimer stabilized by a salt bridge between Glu290 and Arg4, while the substrate binding site resides at the interface of domains I and II. The catalytic residues Cys145 and His41 are highlighted.

like protein ISG15 from interferon (IFN) responsive factor 3 (IRF3), blocking its nuclear translocation, thus reducing type I IFN response.[33] The nsp3, nsp4, and nsp6 have transmembrane domains and should serve as scaffold to anchor the RTC complex to intracellular membranes, a prerequisite for RNA virus replication. Then, the nsp7 nsp8 primase complex is able to synthesize short oligonucleotides, while the nsp12 RdRp is the elongating polymerase that, together with the nsp13 helicase/triphosphatase, the nsp14 exoribonuclease, the nsp15 endonuclease, and nsp10-N7- and nsp16−2′O-methyltransferases, assembles in the RTC, thus creating the suitable environment for RNA synthesis and maturation.[24] Moreover, nsp1, nsp3 deubiquitinase and nsp16−2′O-methyltransferase mediate suppression of the innate immune response.

Genomic ss-(+)-RNA transcription proceeds through (−)-strand intermediates that serve as templates for the production of both genomic and subgenomic RNAs, which are capped and polyadenylated as the full genomic RNA. The subgenomic RNAs are then translated into the four structural and some accessory proteins. Hence, discontinuous transcription may favor CoV genome recombination, as observed in the murine CoV experimental model.[34]

Assembly of new viral particles takes place on intracellular membranes, where N protein binds to genomic RNA and the nucleocapsid associates to M protein, which is thought to cause membrane curvature and drive budding into ER/Golgi membranes. During this process, S and E are also acquired. In particular, E protein by acting as viroporin alters cell secretory pathways and promotes virion egress by exocytosis.[24]

On the basis of the prominent roles in intracellular steps of viral life cycle, the amount of biochemical/structural data and the knowledge acquired on inhibitors of homologues proteins in other CoVs and other RNA viruses, the 3CL^{pro} and the nsp12 RdRp are at moment the most relevant viral targets to identify specific anti-CoVs agents.

THE 3CL^{PRO} (OR M^{PRO}): STRUCTURE AND FUNCTION

The 3CL^{pro}, known also as M^{pro}, is a 33.8 kDa cysteine protease able to process the polyprotein at no less than 11 conserved sites, starting with the autolytic cleavage from pp1a and pp1ab; thus, it is responsible for the release of most of the nsps CoV functional proteins. This pivotal role in the viral life cycle and the lack of homologous proteins in human cells make 3CL^{pro} a very attractive target for the identification of anti-SARS-CoV-2 agents.

A large number of crystal structures of 3CL^{pro} from SARS-CoV-2 and other CoVs have been solved either in their apo forms or in complex with inhibitors, providing very important information about the folding, the assembly, and the catalytic mechanism of these proteins. In around seven months, between the end of February and the end of September 2020, already 192 3D-structures of the SARS-CoV-2 3CL^{pro} have been released. Comparison of the apo structures of SARS-CoV-2 3CL^{pro} (PDB 6Y2E)[35] and SARS-CoV 3CL^{pro} (PDB 2BX4)[36] reveals analogous tridimensional features, consistent with the 96% sequence identity and the similar catalytic activity of the two enzymes. Indeed, similar to SARS-CoV 3CL^{pro},[37−39] the active form of SARS-CoV-2 3CL^{pro} is a dimer, with an estimated dissociation constant in the low μM range.[35] Each protomer is formed by three domains:[35,36] six antiparallel β-barrels form domains I and II (residues 10−99 and 100−182, respectively) and host the substrate-binding site, while domain III (residues 198−303) is a globular cluster of five helices that regulates protein dimerization. Arg4 and Glu290 from each protomer establish an ionic bond driving the formation of the dimer, which has contact interface between the perpendicularly oriented domain II of protomer A and domain III of protomer B (Figure 2). The N-terminal tail, called the "N-finger", of molecule B is squeezed in between domains II and III of the parent monomer and domain II of the other one. This peculiar arrangement is stabilized by some key hydrogen bonds, particularly those formed by Ser1 and Glu166 from each unit. In each monomer, the substrate binding site is located in a wide cleft between domains I and II, hosting the Cys145-His41 catalytic dyad. With respect to these residues, a number of subpockets can be identified, namely S4, S3, S2, S1, and S1′, which are occupied, respectively, by the substrate P4, P3, P2, P1, and P1′ amino acids. Notably, dimerization of 3CL^{pro} seems to help the shaping of the substrate-binding site, particularly of the S1 site, explaining why the enzyme is catalytically inactive in the monomeric form, as demonstrated for the SARS-CoV enzyme.[37−39] The

https://dx.doi.org/10.1021/acs.jmedchem.0c01140
J. Med. Chem. 2022, 65, 2716−2746

substrates of CoVs 3CL^{pro} display almost identical recognition motifs, which is consistent with the high structural similarity of the catalytic domains of these enzymes.[40] In particular, they all share the Leu-Gln-Ser (Ala, Gly) as preferred P2−P1−P1′ sequence, suggesting the possibility to identify very effective broad-spectrum inhibitors of the CoVs enzyme family. The substrate preferences of SARS-CoV and SARS-CoV-2 3CL proteases were recently compared by examining the hydrolytic rate of different peptides/peptidomimetics.[41] In particular, the catalytic performance of each enzyme was evaluated against a combinatorial library of fluorogenic substrates endowed with a glutamine at the P1 position, while displaying different natural and unnatural amino acids as P2, P3, and P4. Remarkably, this analysis showed that both SARS-CoV and SARS-CoV-2 3CL^{pro} have substrate specificity in S2 with Leu as the best P2 residue, although other hydrophobic replacers are tolerated, such as 2-Abz, Phe(4-NO_2), 3-Abz, β-Ala, Dht, hLeu, Met, and Ile. Several hydrophobic D and L but also basic amino acids are suitable as P3, but Tle, D-Phe, D-Tyr, Orn, hArg, Dab, Dht, Lys, D-Phg, D-Trp, Arg, and Met(O)$_2$ are mostly preferred.[40,41] Both enzymes have poor substrate specificity at the P4 position, with preference for small hydrophobic amino acids.

The SARS-CoVs 3CL^{pro} substrate affinity and specificity can be reasonably explained based on the shape and amino acid composition of the different subpockets of the cleavage site. In both SARS-CoVs 3CL^{pro}, the S1 pocket is formed by the side chains of residues Phe140, Asn142, His163, Glu166, and His172 and the main chains of Phe140 and Leu141. Interestingly, the imidazole of His163 is located at the very bottom of the cleft, suitably positioned to donate a H-bond to the side chain carbonyl of substrate/inhibitor P1 Gln. The S2 subsite of SARS-CoVs 3CL^{pro} is a buried hydrophobic pocket that can host bulky alkyl/aryl substituents as the substrate S1 Leu side chain. This cage is defined by a "lid" comprising the 3_{10} helix residues 46−51, particularly Met49, three walls defined by the main-chain of residues 186−188 and by the side chains of His41, Asp187, and Gln189 and a floor lined by Met165. Notably, the shape and the size of the S2 subsite of SARS-CoVs 3CL^{pro} is highly similar to that of the MERS-CoV homologue. Indeed, only two conservative mutations can be found, specifically the replacement of Met49 and Arg188 in SARS-CoVs with Leu49 and Lys191 in MERS-CoV, respectively. On the other hand, the volume of the S2 subsite in SARS-CoVs 3CL^{pro} (252 Å^3) is significantly larger than in other CoVs' homologues of the α-genus, such as the HCoV-NL63 3CL^{pro} (45 Å^3).[42] Actually, this knowledge might be exploited to guide the structure-based drug design (SBDD) of either specific or broad spectrum inhibitors of CoVs 3CL^{pro}. Compared to S1 and S2, the S4, S3, and the S1′ pockets of the SARS-CoVs 3CL^{pro} are more shallow and exposed to the solvent and could accommodate groups of various size and nature. In particular, S3 and S4 are defined by the flexible loops connecting residues 165−168 and 189−192, which can rearrange upon ligand binding, while the S1′ cleft is characterized by a number of threonine residues (Thr24, Thr25, and Thr26), which can potentially form either hydrogen bonds or lipophilic contacts with the substrate/inhibitor P1′ group.

The structure of CoVs 3CL^{pro} resembles that of the main proteases of enteroviruses (EVs), a family of small and naked (+)-*ss*-RNA viruses.[42,43] In fact, in EVs genome the M^{pro} is a cysteine protease encoded by the 3C region, hence the name 3C-like of CoVs protease. The EV 3C protein has a chymotrypsin-like fold with two catalytic domains similar in shape to domains I and II of CoVs 3CL. Contrary to CoVs 3CL^{pro}, the EV 3C protease lacks a dimerization domain, and it works as a monomer. Also, the EV 3C protease displays, in addition to the catalytic Cys-His, an acidic (Asp/Glu) residue to form a reactive triad. A very important similarity between CoVs and EVs M^{pro} is the peculiar almost absolute requirement for glutamine in the substrate P1. This represents an unknown specificity in human proteases that increases the appeal of these viral proteins as a target for safe and selective inhibitors. Indeed, Rupintrivir (Supporting Information, Figure S1), a potent peptidic inhibitor of EV 3C^{pro}, successfully completed phase II trials for human rhinovirus (HRV) infection in 1999 without showing toxicity in common cold patients.[44] This compound has inspired design of CoV 3CL^{pro} inhibitors, although it shows very weak activity when tested against the CoV protease.[45] A major difference between the 3C and the 3CL proteins is in the S2 subsite, which completely lacks the lid in the 3C protein. For instance, a comparison of SARS-CoV 3CL and EV Coxsackie B 3C highlighted that in EVs the S2 appears as an open hydrophobic channel lined by Arg39, Asn69, and Glu71, forming the back wall, residues 127−132 and His40 as the side walls, and Val162 constituting the floor.[42] Nonetheless, covalent peptidic inhibitors reported for both targets are able to broadly inhibit EVs and CoVs replication in cell cultures.[43,45]

TARGETING SARS-COV-2 3CL^{PRO}

The targeting of proteases represents a solid route for antiviral drug discovery as demonstrated by the therapeutic success of HIV and HCV proteases inhibitors. Inhibition of these enzymes can be achieved by different approaches; indeed, the design of reversible, covalent reversible, and irreversible binders has been exploited in different therapeutic areas including antivirals. The identification of potent noncovalent inhibitors generally requires much efforts and it is a time-consuming process, although it is the most favored strategy to obtain safe and efficacious drugs. On the other hand, the identification of irreversible inhibitors is an apparently simpler and attractive approach, but it suffers from a potential serious drawback due to lack of target selectivity that can lead to unpredictable severe toxicity. A similar but less risky approach is represented by the design of covalent reversible inhibitors that requires the knowledge of the catalytic mechanism and the substrate specificity, thus relying on natural substrate modifications. In general, such an approach consists of converting good substrates into good covalent reversible inhibitors. This can be achieved by replacing part of the protease substrate with a moiety, known as a "warhead", that is an electrophilic reactive group able to form the covalent reversible bond with the catalytic machinery. Indeed, this strategy has afforded the FDA approved α-ketoamide inhibitors of HCV NS3/4A serine protease, Telaprevir[46] and Boceprevir.[47] In fact, the reaction of these compounds with the enzyme affords stable hemiketals mimicking the tetrahedral transition state of the cleavage process. This approach also yielded human cysteine protease cathepsin K inhibitors, such as the clinical candidate Odanacatib,[48] which features a nitrile warhead, for the treatment of osteoporosis and bone metastasis, even if the phase III clinical trial was discontinued in 2016. Similar to irreversible binders, covalent reversible inhibitors might suffer of lack of high selectivity; furthermore, they have generally less favorable pharmacokinetic properties

https://dx.doi.org/10.1021/acs.jmedchem.0c01140
J. Med. Chem. 2022, 65, 2716−2746

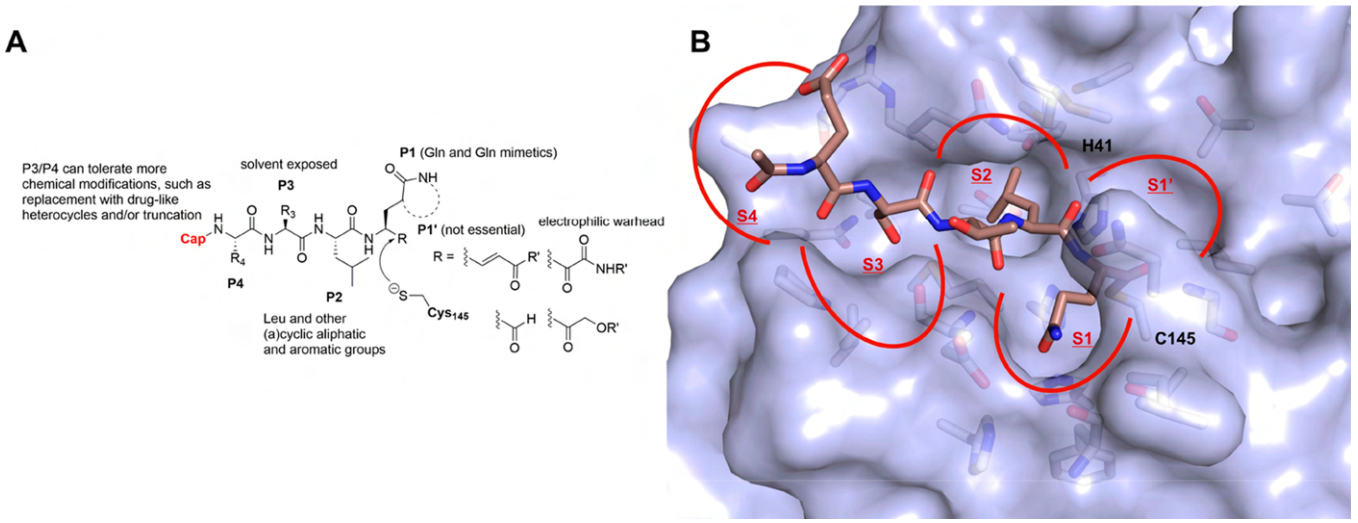

Figure 3. Schematization of the main features of 3CL^{pro} inhibitors and protease subsite specificity. (A) General representation of peptidic covalent reversible inhibitors of SARS-CoV-2 3CL^{pro} summarizing the chemical requirements and SAR of compounds so far reported in literature. (B) Surface representation of the active site pocket of SARS-CoV 3CL^{pro} bound to a peptide aldehyde inhibitor (dark salmon sticks, PDB 3SNE), chosen as a representative substrate-like inhibitor. The S1−S4 and S1′ subsites are indicated with red lines and labeled. The key residues forming the active site pocket are displayed as white sticks; the catalytic residues Cys145 and His41 are labeled.

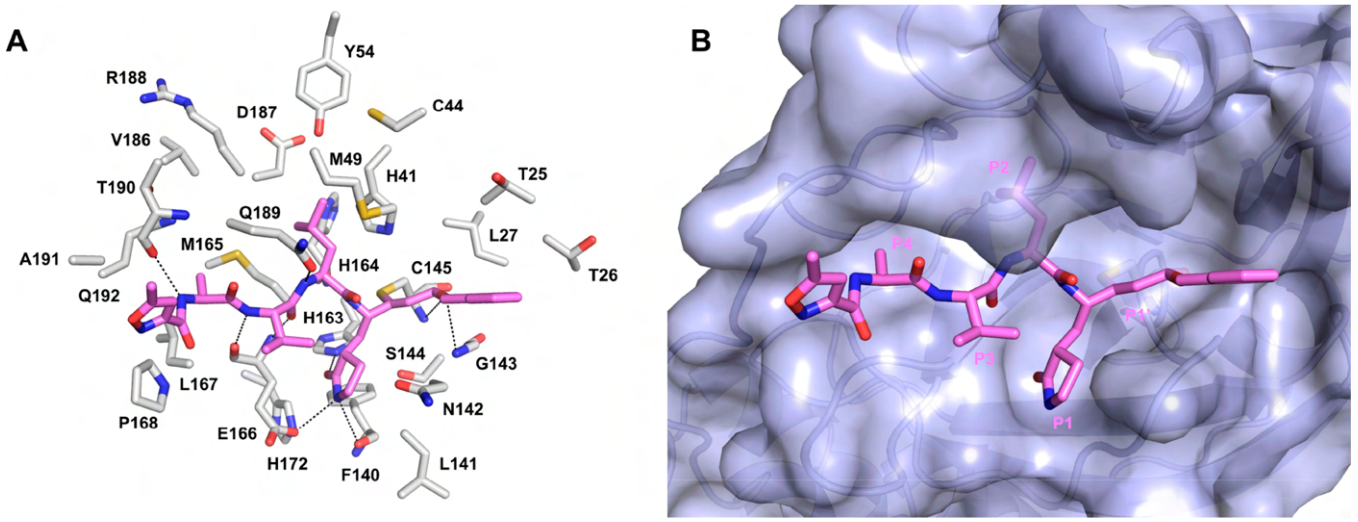

Figure 4. Co-crystallographic pose of compound **1** (violet sticks, PDB 7BQY) covalently bound to the active site of SARS-CoV-2 3CL^{pro}. (A) The key residues forming the active site pocket are displayed as white sticks and labeled. H-bonds are depicted as dashed black lines. (B) Surface representation of the active site pocket with bound N3. The P1−P4 and P1′ moieties are labeled.

that can lead to a suboptimal dosing regimen. However, because these drugs are designed based on the substrate sequences, they have higher specificity for target proteins, which reduces their potential side toxicity. In addition, considering that the length of COVID-19 patients treatment should be relatively short, this approach appears as a privileged route to discovery drugs targeting SARS-CoV-2 3CL^{pro} with limited side effects compared to the use of covalent binders for chronic treatments, and the suboptimal dosing regimen can be tolerated. Homologous proteins of related CoVs such as SARS- and MERS-CoVs have represented the main targets for the identification of potent and selective inhibitors of these viruses.[45,49,50] Indeed, several compounds targeting the 3CL^{pro} of different CoVs have been reported over the years, thus providing compounds and knowledge useful for the discovery of anti-SARS-CoV-2 agents.

As introduced in the previous section, several crystal structures of ligands bound to 3CL^{pro} have been released in the PDB, including complexes containing peptidic covalent reversible/irreversible inhibitors. These inhibitors act through a two-step mechanism: first, they bind to the active site, similar to a natural substrate, forming a noncovalent complex with the protease so that the C-terminal warhead comes in close proximity to the catalytic Cys145, to form, in the second step, a covalent bond with this residue by a nucleophilic attack. A number of academic groups have reported peptide covalent reversible inhibitors of SARS-CoV-2 3CL^{pro}, biological activities, and their cocrystal structures with the target protein; in these compounds, the explored chemical warheads include Michael acceptors, α-ketoamides, aldehydes, and ketones. To efficiently compete with the natural substrates at the catalytic site, most of the inhibitors span from P1−P4 to establish a considerable number of specific interactions with the binding

https://dx.doi.org/10.1021/acs.jmedchem.0c01140
J. Med. Chem. 2022, 65, 2716−2746

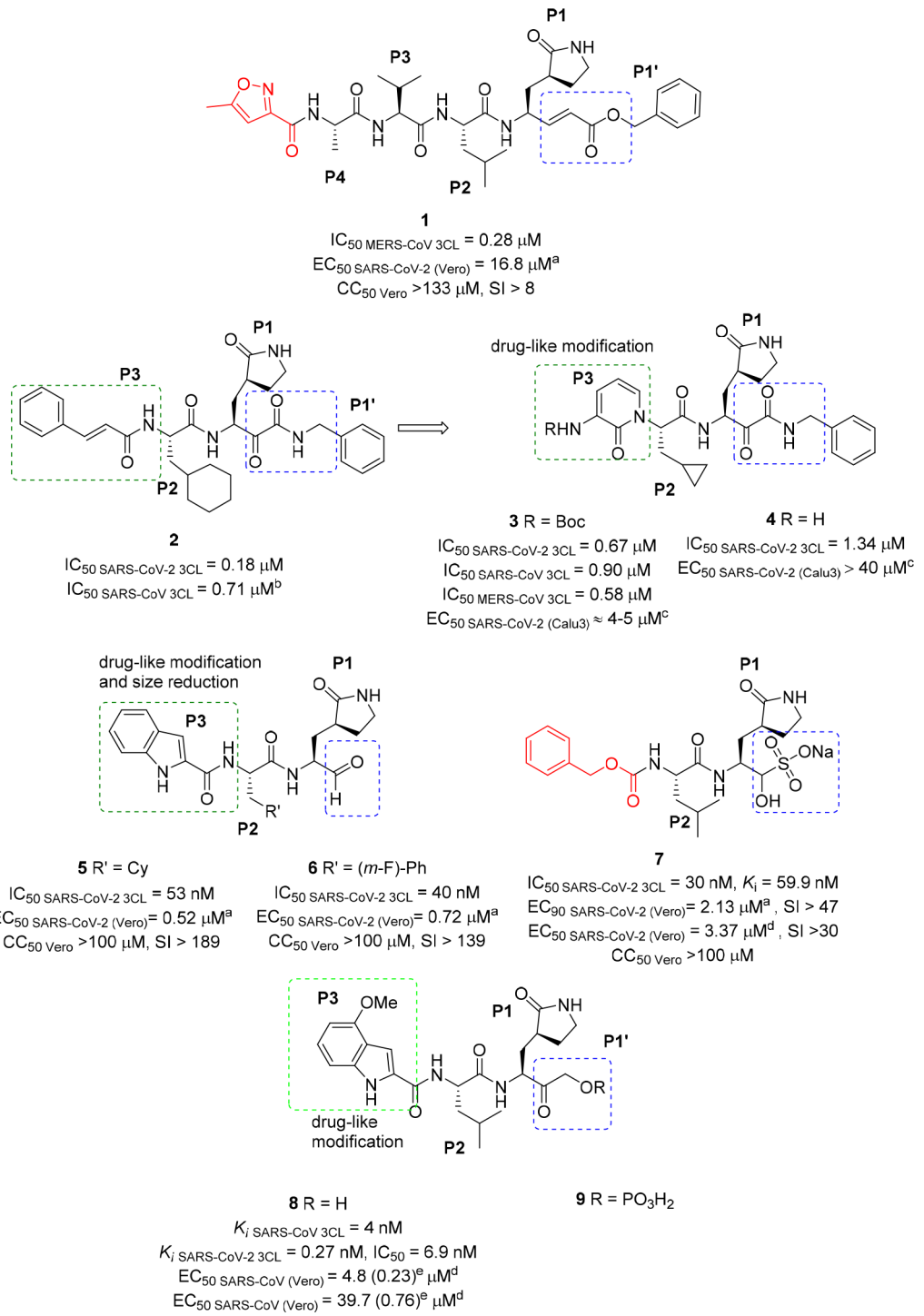

Figure 5. Compounds **1**–**9** with biological activities. [a]Antiviral activity evaluated by viral plaque assay. [b]Data from ref 42. [c]Antiviral activity evaluated by viral RNA qRT-PCR quantification. [d]Antiviral activity evaluated by CPE reduction. [e]Values in bracket have been obtained in the presence of a P-gp inhibitor. The main structural differences, significant modifications, and warheads are highlighted.

pockets (namely, the enzyme S1–S4 subsites), to facilitate the covalent reaction between the Cys145 and the warhead (Figure 3). This contributes not only to the affinity and potency, but, more importantly to the binding specificity, limiting the cross reactivity with other off targets that could lead to severe side effects. In addition, the reported inhibitors share similar peptide sequence organization in P1–P2 residues, while there are remarkable differences at P3/P4 positions and in the overall compound molecular size (Figure 3).

In the first released X-ray structure, SARS-CoV-2 $3CL^{pro}$ was in complex with the *N*-term isoxazole capped tetrapeptide **1** (PDB 6LU7, superseded by 7BQY; Figures 4 and 5).[40]

Compound **1** is endowed with a vinyl carboxyl ester acting as the Michael acceptor warhead that traps the catalytic Cys145 through its nucleophilic attack at the vinyl *β*-carbon. This compound was previously identified by SBDD as inhibitor of 3CL proteases of different CoVs,[51,52] including SARS- and MERS-CoVs, showing in enzymatic assay a K_i = 9

https://dx.doi.org/10.1021/acs.jmedchem.0c01140
J. Med. Chem. 2022, 65, 2716–2746

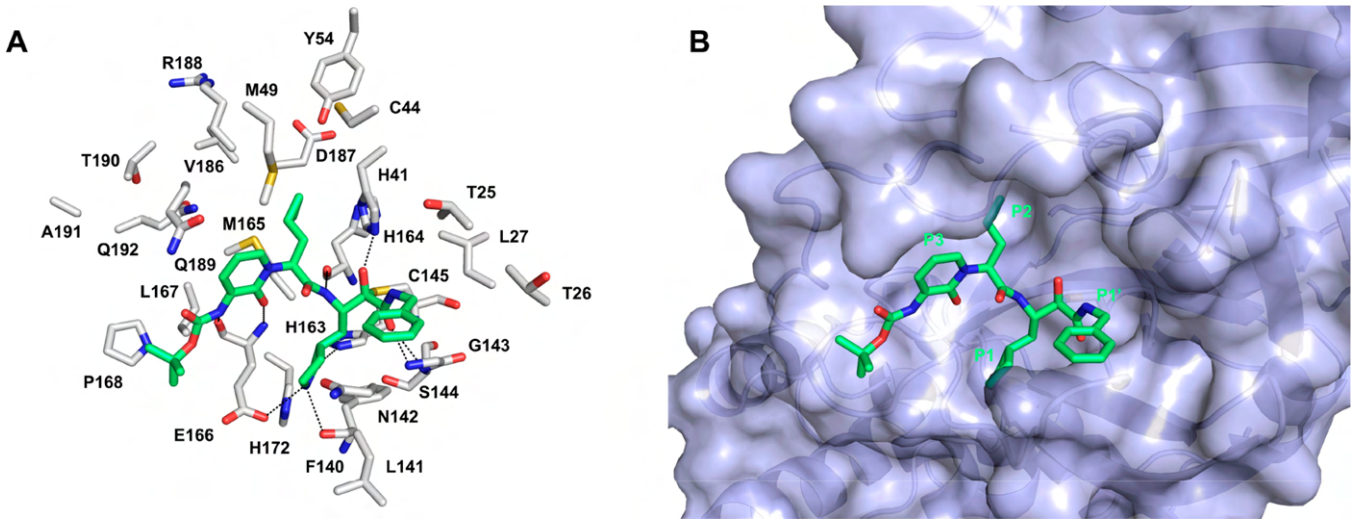

Figure 6. Co-crystallographic pose of compound **3** (green sticks, PDB 6Y2F) covalently bound to the active site of SARS-CoV-2 3CL^{pro}. (A) The key residues forming the active site pocket are displayed as white sticks. H-bonds are depicted as dashed black lines. (B) Surface representation of the active site pocket with bound compound **3**.

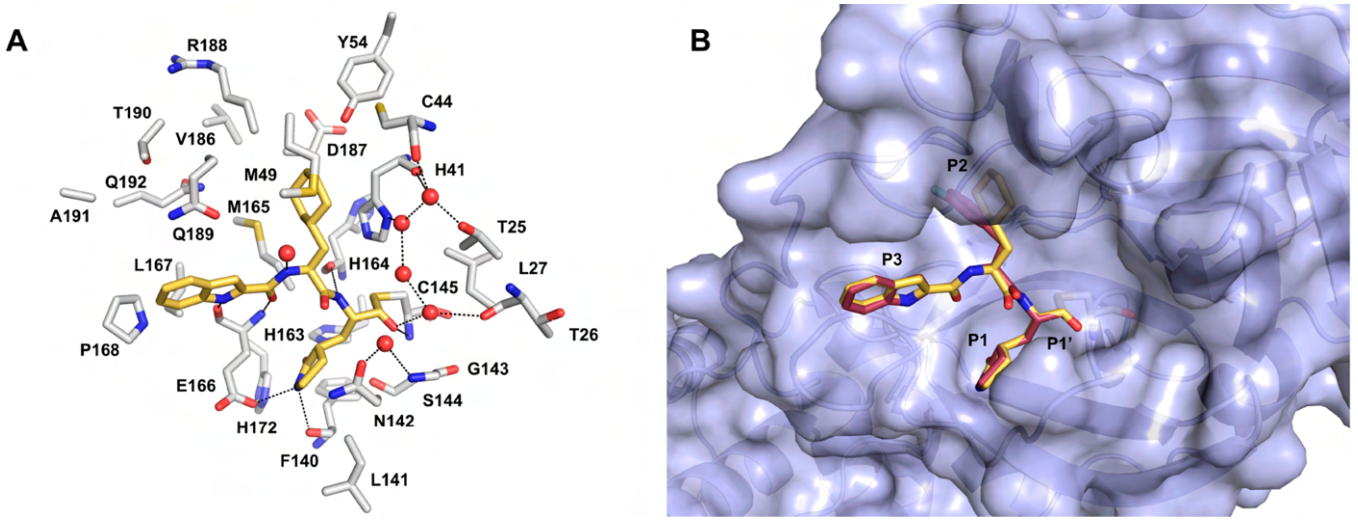

Figure 7. Co-crystallographic pose of compound **5** (yellow-orange sticks, PDB 6LZE) covalently bound to the active site of SARS-CoV-2 3CL^{pro}. (A) The key residues forming the binding pocket are displayed as white sticks; water molecules are shown as red spheres. H-bonds are depicted as dashed black lines. (B) Overlay of **5** and **6** (raspberry sticks, PDB 6M0K) co-crystallographic poses.

μM[53] and an IC$_{50}$ = 0.3 μM,[54] respectively, however no data in the same assay were reported against SARS-CoV-2 3CL^{pro}. Nonetheless, the high structure identity between this protein and its SARS-CoV homologue would suggest that **1** may reasonably inhibit also SARS-CoV-2 3CL^{pro} with similar potency. This hypothesis is supported by cell-based assay data showing that **1** inhibits SARS-CoV-2 replication with an EC$_{50}$ = 16.77 μM. As expected, **1** has modest selective index with respect to other CoVs (EC$_{50}$ = 4.0, 8.8, 2.7, and 3.4 μM against HCoV-229E, FIPV, MHV-A59, and MHV, respectively), and most likely the variability depends on subtle differences in amino acids sequences in the different CoVs proteases and cellular assay conditions.

Peptidomimetic α-ketoamides have been recently reported as broad-spectrum inhibitors of 3CL and 3C proteases active in cell-based assays against different CoVs and EVs, with derivative **2** showing the most promising activity.[42] Preliminary chemical optimization of **2** by SBDD led to derivatives **3** and **4**, the first SARS-CoV-2 3CL^{pro} inhibitors designed *ad hoc* (Figure 5).[35] The X-ray structure solved for the complex **3**/SARS-CoV-2 3CL^{pro} (PDB 6Y2F) (Figure 6) confirmed the formation of a thiohemiketal obtained by the nucleophilic attack of the Cys145 over the α-carbonyl of the ketoamide warhead.[35] The oxyanion group is stabilized by a H-bond with His41, while the amide oxygen of **3** accepts a H-bond from the main-chain amides of Gly143 and Cys145, which, together with Ser144, form the so-called "oxyanion hole" typical of cysteine proteases. Ketoamide derivative **3** inhibits SARS-CoV-2 3CL^{pro} in biochemical assay with an IC$_{50}$ = 0.67 μM, showing similar potency against SARS- and MERS-CoVs M^{pro}. **3** showed EC$_{50}$ ~ 4−5 μM against SARS-CoV-2 replication in human lung (Calu3) cells but, unfortunately, no data on cytotoxicity are provided (Figure 5).

In another study, a SBDD strategy led to the identification of dipeptides **5** and **6** having an aldehyde as warhead and exhibiting excellent inhibitory activity against SARS-CoV-2 3CL^{pro} in enzymatic assays, with IC$_{50}$ = 53 and 40 nM, respectively (Figures 5 and 7).[55] Notably, derivatives **5** and **6**

https://dx.doi.org/10.1021/acs.jmedchem.0c01140
J. Med. Chem. 2022, 65, 2716−2746

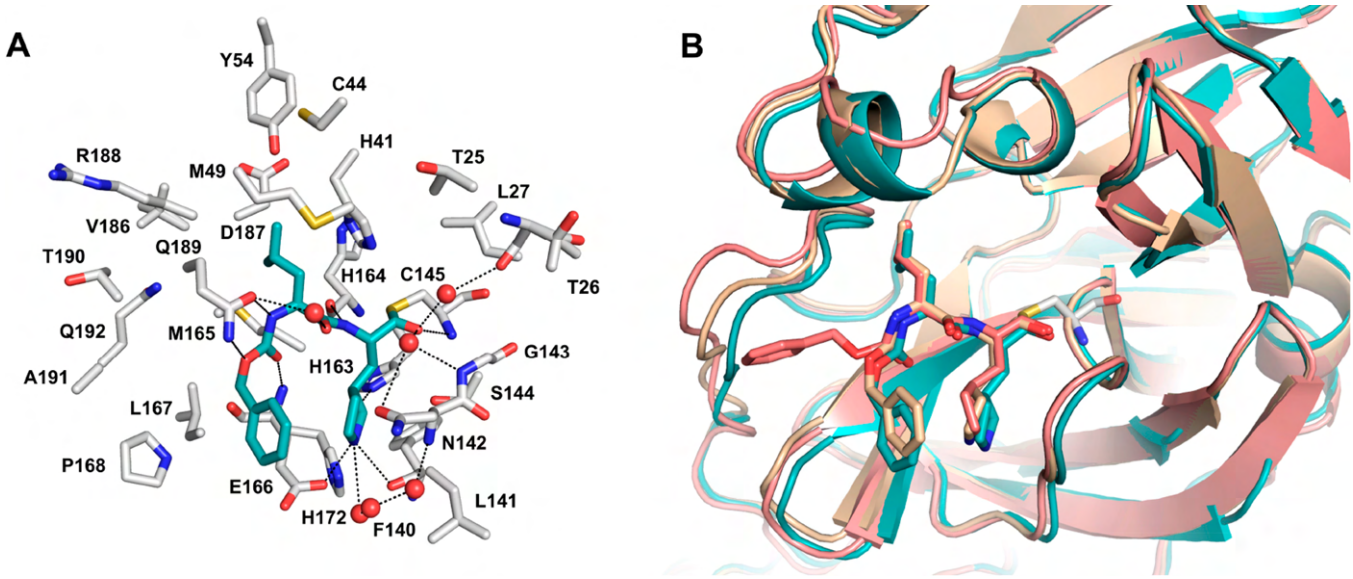

Figure 8. Co-crystallographic pose of compound 7 (teal sticks, PDB 7BRR) covalently bound to the active site of SARS-CoV-2 3CL^{pro}. (A) The key residues forming the active site pocket are displayed as white sticks; water molecules are shown as red spheres. H-bonds are depicted as dashed black lines. (B) Overlay of 7 bound to SARS-CoV-2 3CL^{pro} structures (PDBs: 7BRR, teal; 6WTJ, wheat; 6WTT, salmon), showing the different conformations of the benzyloxycarbonyl group.

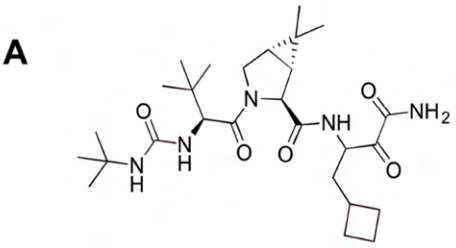

Boceprevir

$IC_{50\ SARS\text{-}CoV\text{-}2\ 3CL}$ = 4.13 μM, K_i = 1.18 μM
$EC_{50\ SARS\text{-}CoV\text{-}2\ (Vero)}$ = 1.95 μM[a], SI > 51.3
$EC_{50\ SARS\text{-}CoV\text{-}2\ (Vero)}$ = 1.31 μM[b], SI >76.3
$CC_{50\ Vero}$ >100 μM

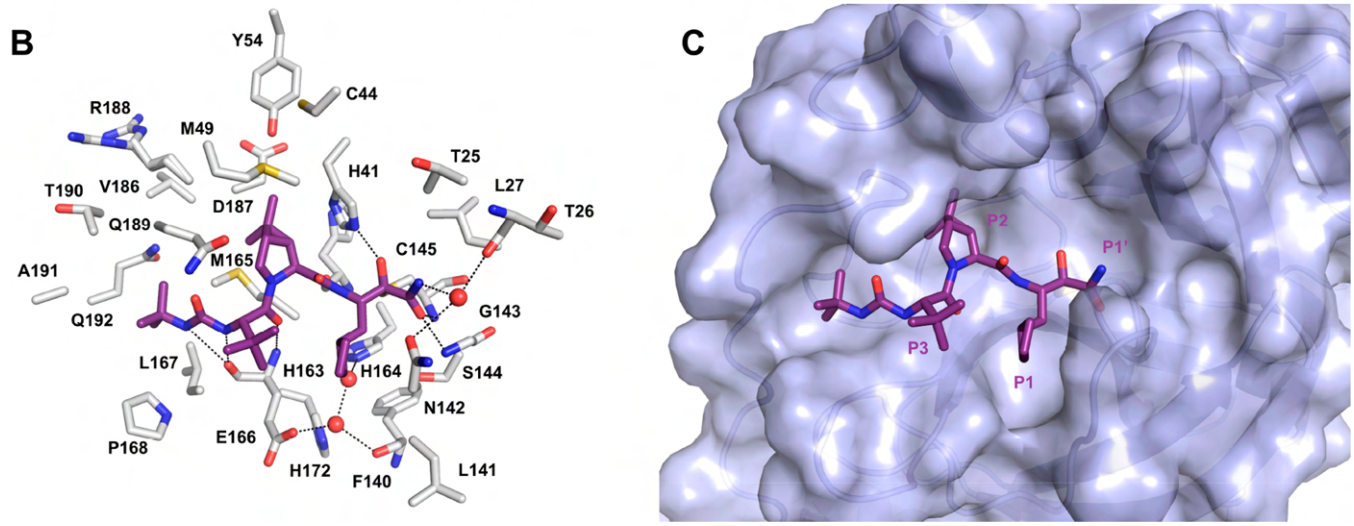

Figure 9. (A) Structure and biological activity of Boceprevir. [a]Antiviral activity evaluated by viral plaque assay. [b]Antiviral activity evaluated by CPE reduction. (B) Co-crystallographic pose of Boceprevir (purple sticks, PDB 6WNP) covalently bound to the active site of SARS-CoV-2 3CL^{pro}. The key residues forming the active site pocket are displayed as white sticks; water molecules are displayed as red spheres. H-bonds are depicted as dashed black lines. (C) Surface representation of the active site pocket with bound Boceprevir.

https://dx.doi.org/10.1021/acs.jmedchem.0c01140
J. Med. Chem. 2022, 65, 2716−2746

are the smallest and most potent SARS-CoV-2 3CL^{pro} inhibitors reported so far. More interestingly, both compounds potently inhibited SARS-CoV-2 infection in cell culture with sub-μM potencies (EC_{50} = 0.53 and 0.72 μM for **5** and **6**, respectively), coupled with low toxicity (CC_{50}s > 100 μM, SIs > 139) (Figure 5). As expected, both compounds bind to the protein with similar poses, as shown in cocrystal structures (PDBs: 6LZE for **5** and 6M0K for **6**), where the carbon of the aldehyde and the sulfur of Cys145 form the thiohemiacetal, the oxygen of the resulting tetrahedral adduct is stabilized by interaction with backbone of residue Cys145 and through a water bridge with the Thr26 side chain (Figure 7).[55]

Additional peptidic reversible covalent inhibitors have been identified through a biochemical screening based on enzymatic assay against SARS-CoV-2 3CL^{pro} using a focused library of 68 known protease inhibitors, including approved and investigational drugs.[56] An investigational veterinary drug (usually administered via a subcutaneous route) for feline infectious peritonitis (FIP),[57,58] compound **7** (GC376), is a α-hydroxybisulfite dipeptide able to potently inhibit SARS-CoV-2 3CL^{pro} (IC_{50} = 30 nM) and viral replication, even though with almost two orders lower potency (EC_{50} = 3.37 μM in CPE assay) and no cytotoxicity up to 100 μM (Figure 5). Thermal shift assay and kinetic enzymatic experiments supported specific binding and reversible covalent inhibition (K_i = 60 nM). This inhibitor is a prodrug, converted into the aldehyde form by the removal of the bisulfite group to alkylate the Cys145 of the 3CL^{pro}. Derivative **7** was originally designed to target 3CL of feline CoV and shares several chemical features with the inhibitors described for SARS-CoV-2 3CL^{pro}.[43,57] It shows activity against multiple 3CL proteases ($IC_{50\ FIPV\ 3CL}$ = 0.72 μM, $IC_{50\ TGEV\ 3CL}$ = 0.82 μM, $IC_{50\ SARS\text{-}CoV\ 3CL}$ = 4.35 μM, $IC_{50\ MERS\text{-}CoV\ 3CL}$ = 1.56 μM) and against CoVs (TGEV, FIPV, MHV, 229E, and BCV) in cell lines with high nM potency.[43,57,58] **7** and two close previously reported analogues, differing only in the electrophilic warhead (*i.e.*, an aldehyde or an α-ketoamide), resulted also in potent inhibition of EV 3C and norovirus 3CL cysteine proteases and of the replication of several of these viruses, including HRVs.[43] Notably, **7** has been crystallized in complex with SARS-CoV-2 3CL^{pro}, revealing an interaction mode similar to the aldehyde derivatives **5** and **6** (PDBs: 7BRR,[59] 6WTJ,[60] 6WTT,[56] 7C8U, 7C6U, and 7CBT) (Figure 8). Recently, a small set of new analogues of compound **7**, differing for the N-terminal capping moieties, has been reported as inhibitors of 3CL^{pro} from SARS-CoV-2, MERS-, and SARS-CoVs.[61] The new compounds showed biological activities in the same range of parent compound **7**.

Three further reversible covalent inhibitors of SARS-CoV-2 3CL^{pro} have been identified by applying the same biological screening protocol as for compound **7**. The anti-HCV drug Boceprevir[47] shows low μM potency against the isolated 3CL^{pro} and the viral replication with no host cell toxicity up to 100 μM. Note that Boceprevir, originally optimized as HCV NS3 serine protease inhibitor, was 100-fold more potent against this target in comparison to the activity against the 3CL^{pro}. Calpain cysteine protease inhibitors (Calpain inhibitor II: (2*S*)-2-acetamido-4-methyl-*N*-[(2*S*)-4-methyl-1-[[(2*S*)-4-methylsulfanyl-1-oxobutan-2-yl]amino]-1-oxopentan-2-yl]-pentanamide; Calpain inhibitor XII: benzyl *N*-[1-[[1,2-dioxo-1-(pyridin-2-ylmethylamino)hexan-3-yl]amino]-4-methyl-1-oxopentan-2-yl]carbamate) with aldehyde warheads are slightly more potent in enzymatic and antiviral assays. These three inhibitors are structurally unrelated and deviate from 3CL substrate sequence specificity. Nonetheless, Boceprevir has been recently cocrystallized with SARS-CoV-2 3CL^{pro} (PDBs: 7BRP,[59] 6WNP, 7C6S, and 6ZRU), providing hints to improve its enzyme inhibition (Figure 9). Noted that none of the HIV protease inhibitors, including Lopinavir, have shown activity in this study, thus providing an explanation to the difficult interpretation of the clinical results for the use of these drugs to treat COVID-19. Indeed, the results published for a clinical trial evaluating Lopinavir−Ritonavir in hospitalized adult patients with severe COVID-19 have shown no benefit.[62]

In spite of their different warheads, compounds **1**, **3**, and **5**−**7** share a Gln mimetic γ-lactam, replacing the substrate P1 Gln to specifically fill the S1 subsite of the SARS-CoV-2 3CL^{pro} catalytic pocket. Indeed, the γ-lactam here establishes key H-bonds with the Phe140 main chain and with the side chains of His163 and Glu166 (Figures 4, 6−8). Notably, Glu166 is involved not only in substrate recognition but also in the substrate-induced dimerization of SARS CoVs 3CL proteases through the interaction with Ser1 from the other monomer;[35,63] therefore, the interaction of the inhibitor γ-lactam with this residue could stabilize the monomeric and inactive form of the enzyme. Literature data on 3CL^{pro} inhibitors of related CoVs clearly indicate that the P1 γ-lactam enhances the inhibitory potency up to 10-fold, probably because the higher rigidity reduces the loss of entropy upon binding if compared to the flexible Gln.[45] In Boceprevir, the γ-lactam is replaced by a cyclobutyl ring that cannot form any hydrogen bond at the S1 subsite, and this is likely one of the reasons for the modest inhibitory 3CL^{pro} activity of this compound. Nevertheless, the presence of a modified proline at the P2 position would suggest the possibility to synthesize proline-based analogues with higher affinity and specificity toward the target enzyme. Indeed, the P2 amino acids of the other reported inhibitors show that this position tolerates a wide variety of residues characterized by similar lipophilicity and size to the substrate Leu and thus able to occupy the S2 subsite. In particular, leucine occupies the P2 position in **1** and **7**, while it is replaced by a cyclopropyl alanine in **3** or by cyclohexyl- and *m*-F-phenyl alanine residues in **5** and **6**, respectively. Compared to the other cocrystallized compounds, a difference in the binding mode of **6** is observed. In fact, the *m*-F-phenyl of this ligand undergoes a downward rotation so that the fluorine atom can form a H-bond with Gln189 (Figure 7). It is interesting to report that this residue can alternatively form a hydrogen bond with the backbone nitrogen of the inhibitor P2 residue, as observed in the case of **1**.

As described in the previous paragraph, the S3 and S4 pockets of SARS-CoVs 3CL^{pro} are less structured and indeed can rearrange upon the binding of distinct P3/P4 residues. Hence, these amino acids are generally modified to modulate both potency and drug-like properties of the inhibitors. For instance, in peptide **1** the P3 lipophilic Val is solvent exposed, although it can establish van der Waals contacts with P1 γ-lactam to stabilize the inhibitor binding conformation, while the P4 *N*-capped Ala can form some lipophilic contacts with residues Met165, Leu167, and Gln192 in S4 (Figure 4). Remarkably, the P3 backbone of the inhibitor establishes two key hydrogen bonds with the main chain of Glu166. These interactions can also be formed by derivative **3** (Figure 6), in which the P2−P3 amide bond is masked by a *N*-Boc-aminopyridone, likely to prevent cellular proteases cleavage. Indeed, the pyridone CO donates a H-bond to Glu166, which in turn accepts another H-bond from the NH of the ligand

https://dx.doi.org/10.1021/acs.jmedchem.0c01140
J. Med. Chem. 2022, 65, 2716−2746

carbamate. The analysis of the 3/3CL^{pro} complex shows that the terminal hydrophobic Boc group does not establish significant interactions at the S3/S4 enzyme subsites. However, this group is fundamental to gain cell activity, probably due to the improvement of membrane permeation; in fact, its deletion did not affect biochemical inhibition of the protease but completely abrogated antiviral activity in cell-based assay (compound **4** in Figure 5). Nonetheless, in the 3/3CL^{pro} cocrystal structure, a DMSO molecule is found between the Gln189 side chain and the pyridone moiety, suggesting that there is space for larger and more functionalized groups (Figure 6). Similar to **3**, in aldehydes **5** and **6**, the P3 is replaced by a more drug-like moiety, specifically a 2-indolic acid that caps the *N*-terminal of P2. In the enzyme-bound conformation, the indole ring is exposed to solvent and stabilized by H-bonds with the amide backbone Glu166 (Figure 7), as the pyridone of **3**. Also, in derivative **7**, the P2 Leu is capped by a benzyloxycarbonyl group which can alternatively extend toward the S3/S4 pockets or downward to form intramolecular contacts with the P1 γ-lactam; in both cases, however, this moiety can form only one hydrogen bond with Glu166 with respect to the two formed by inhibitors **1**, **3**, **5**, and **6**. To conclude, the crystallographic complexes of SARS-CoV-2 3CL^{pro} with **1** and **3** show that the P1′ benzyl group cannot form specific interactions at the S1′ site. In fact, the aldehydes **5** and **6**, which completely lack a P1′ moiety, display the highest inhibitory potency against the enzyme, indicating the role of this substituent needs to be further investigated. It is worth noting that some of the cocrystallized inhibitors, namely derivatives **1**, **7**, and Boceprevir, fold, bringing the P3 residue or the benzyloxycarbonyl cap close to the P1 γ-lactam, thus suggesting that P1−P3 macrocyclization could be explored as optimization strategy. Indeed, macrocyclization has been widely employed as strategy to preorganize HCV NS3 protease inhibitors in their bioactive conformation, leading to BILN-2061[64,65] and the approved pan-genotypic drug Grazoprevir.[66,67] Moreover, macrocyclization generally show additional advantages potentially leading to greater stability and improved PK properties.

Compounds **3**, **5**, and **6** have been also evaluated for their *in vivo* PK properties in mice, and even if dosages, parameters, and administration routes are not fully aligned, it is worth comparing the collected data. Pyridone **3** upon sc administration (3 mg/kg) showed modest half-life ($T_{1/2}$ < 2 h) and a rather low C_{max} (around 126 ng/mL), indicating a suboptimal PK profile and the need of further optimization.[35] More interestingly, indole derivatives **5** and **6** were dosed via iv (5 mg/kg), and ip (5 and 20 mg/kg) administrations (single dose), resulting in a reasonable profile with $T_{1/2}$ ranging from ∼2 to ∼5 h, depending on the administration route and the compounds, CL = 17 and 21 mL/min/kg, respectively, via iv, high C_{max} (>2390 ng/mL) and availability >85%.[55] Overall, by comparing PK profiles of both compounds after iv administration at 5 mg/kg, **5** resulted metabolically more stable than **6**, showing a $T_{1/2}$ = 4.4 h and CL = 17 mL/min/kg with respect to $T_{1/2}$ = 1.65 h and CL = 21 mL/min/kg, respectively. Compound **5** was further evaluated in rats (10 mg/kg, iv) and dogs (5 mg/kg, iv), showing good half-life values (rat, 7.6 h; dog, 5.5 h), low clearance (rat, 4.01 mL/min/kg; dogs, 5.8 mL/min/kg), and high AUCs (rat, 41 500 h·ng/mL and dog, 14900 h·ng/mL). The PK profile was considered good enough to proceed in acute and seven-day toxicity studies in rats and dogs. In particular, compound **5** was evaluated for acute toxicity in rats by iv administration at 24 mg/kg (1 rat), 40 mg/kg (10 rats), and 60 mg/kg (4 rats); one rat from the last group died. The seven-day studies were carried out in rats by administering via iv at 2, 6, 18 mg/kg of the compound to four rats per study; four dogs were dosed via iv at 10 mg/kg (the first day), 15 mg/kg (the second day), 20 mg/kg (the third day), 25 mg/kg (the fourth day), 25 mg/kg (the fifth to seventh days, randomly two dogs), 40 mg/kg (the fifth to seventh days, other two dogs). All animals were clinically observed during seven days for toxic signs, which include bodyweight, food intake, and hematology, and no anomalies were observed. Therefore, **5** was considered well tolerated after iv administration at different doses in rats and dogs. The plasma concentration and the concentration at trough unfortunately were not reported.

In summary, although there are slight differences in biochemical experimental conditions, in cell-based assays, and in the PK *in vivo* evaluation, that complicate a rigorous head-to-head comparison between the above mentioned inhibitors, some conclusions can be drawn. Compound **5**, having the indole as P2 capping group and aldehyde as the warhead, resulted in the most potent 3CL^{pro} inhibitor, with acceptable PK after iv administration and an acceptable safety profile in preclinical species. Remarkably, compound **5** is reminiscent of SARS-CoV 3CL^{pro} inhibitors disclosed in two patents by Pfizer, following the SARS outbreak in 2002−2003.[68,69] Moreover, the introduction of an indole or other heterocycles in P3 was already reported for peptidomimetic inhibitors of SARS-CoV 3CL^{pro}.[70] Similarly, these compounds having an indole as P2 drug-like cap and either a ketone-based warheads showed nM potency against the isolated target in biochemical assays. The COVID-19 pandemic prompted Pfizer to investigate the efficacy of these compounds and of newly developed analogues against SARS-CoV-2, and the obtained data have been recently reported.[71,72] One of the most potent derivatives is compound **8** (PF-00835231), which exhibits as P3−P1 substituents, respectively, a 6-methoxyindole capping group, a leucine, and the canonical Gln mimetic residue. Interestingly, the latter is functionalized with a hydroxymethylketone, enabling reversible covalent chemistry. Compound **8** exerts very potent inhibitory activity against a wide panel of 3CL^{pro} from α-, β-, and γ-CoVs, with K_i/IC_{50} ranging from the low-nM to pM range. Particularly, a K_i = 0.27 nM and an IC_{50} = 6.9 nM against SARS-CoV-2 3CL^{pro} and a K_i = 4 nM against SARS-CoV 3CL^{pro} have been reported. On the other hand, **8** resulted as being inactive on HIV and HCV proteases as well as against a panel of human proteases. Therefore, this molecule can be considered a selective 3CL^{pro} inhibitor with broad-spectrum activity against CoVs. The efficacy of **8** against SARS-CoV and SARS-CoV-2 was evaluated in Vero cells, showing EC_{50} values of 4.8 and 39.7 μM, respectively. However, **8** has been shown to be substrate of P-gp, which is indeed highly expressed in Vero cells. In fact, in the presence of a P-gp inhibitor, the antiviral activity of **8** was significantly increased, with EC_{50} values of 0.23 and 0.76 μM against SARS-CoV and SARS-CoV-2, respectively, coupled to low toxicity (CC_{50} > 100 μM). Interestingly, **8** exhibits additive/synergistic effect in combination with Remdesivir against SARS-CoV-2 in cell-based assays. X-ray structures of **8** bound to the 3CL^{pro} of either SARS-CoVs have been solved (PDBs: 6XHL and 6XHM, respectively). As expected, the crystal poses in both structures are almost identical and are very similar to those reported for **5** and **6**. DMPK profiling of **8** highlighted

https://dx.doi.org/10.1021/acs.jmedchem.0c01140
J. Med. Chem. 2022, 65, 2716−2746

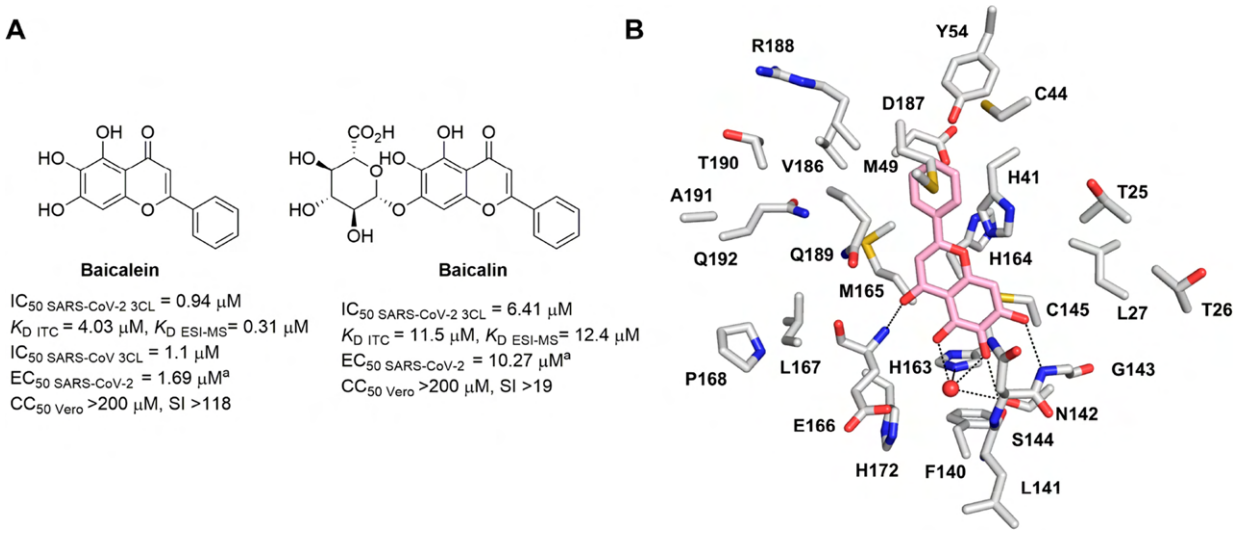

Figure 10. (A) Structures and biological activities of flavones Baicalein and Baicalin. [a]Antiviral activity evaluated by viral RNA measurement by qRT-PCR. (B) Co-crystallographic pose of Baicalein (light-pink sticks, PDB 6M2N) into the active site of SARS-CoV-2 3CL^{pro}. The key residues forming the binding pocket are displayed as white sticks. The buried water molecule is displayed as a red sphere. H-bonds are depicted as dashed black lines.

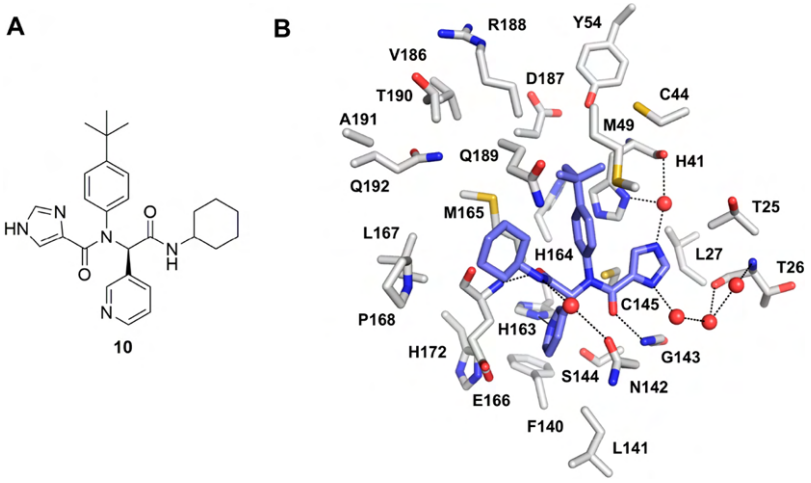

Figure 11. (A) Chemical structure of compound **10**. (B) Co-crystallographic pose of **10** (slate sticks, PDB 6W63) into the active site of SARS-CoV-2 3CL^{pro}. The key residues forming the binding pocket are displayed as white sticks; water molecules are displayed as red spheres. H-bonds are depicted as dashed black lines.

promising results but limited aqueous solubility to enable iv administration.[72] To increase the solubility, a prodrug strategy has been applied to compound **8** and its phosphate ester **9** (PF-07304814) has been reported as a suitable clinical candidate,[72] even though projected effective dose (500 mg/day) is high. On 15 September 2020, Pfizer announced the initiation of a double-blind, placebo-controlled phase Ib clinical trial (NCT04535167) to evaluate the safety, tolerability, and pharmacokinetics of **9**.[73]

Besides the X-ray structures of the 3CL^{pro} with the peptidic covalent inhibitors, some other strategies are currently underway to identify reversible inhibitors of the enzyme. Few results have been published and are available in preprint manuscripts, in press release on organization websites, and some crystal structure have been released in the PDB.

Baicalein, one of the main flavones of *Scutelarria baicalensis*, has been shown to inhibit the proteases of SARS-CoV-2 and SARS-CoV with IC_{50}s of 0.94 and 1.1 μM (Figure 10A), respectively; its glucuronide analogue Baicalin is still active but less potent ($IC_{50\ SARS\text{-}CoV\text{-}2\ 3CL}$ = 6.41 μM).[74] These data are partly consistent with those reported in another study, where Baicalein was found to be active against SARS-CoV-2 3CL^{pro} ($IC_{50\ SARS\text{-}CoV\text{-}2\ 3CL}$ = 0.34 μM), while Baicalin was only a weaker inhibitor (40% inhibition at 50 μM).[75] Perhaps the hydrolysis of the glucuronide moiety in one sample can explain the difference in activity. However, Baicalein was shown to be more potent in both studies. The specific binding of the flavones Baicalein and Baicalin to the protein target has been characterized by ITC showing K_Ds of 4.03 and 11.5 μM, respectively, and consistently with the compound structures the ITC profiles were typical of reversible binders.[76] In the same study, the X-ray structure of Baicalein noncovalently bound to the active site of the 3CL^{pro} (PDB 6M2N, Figure 10B) has been solved, revealing that Baicalein mainly occupies the S1 pocket, with the three phenolic hydroxyl groups forming multiple H-bonds with the main chain of Leu141 and Gly143 and the side chains of Ser144 and His163 by water bridges.[76] The catalytic Cys145 and His41 stabilize the flavone

https://dx.doi.org/10.1021/acs.jmedchem.0c01140
J. Med. Chem. 2022, 65, 2716−2746

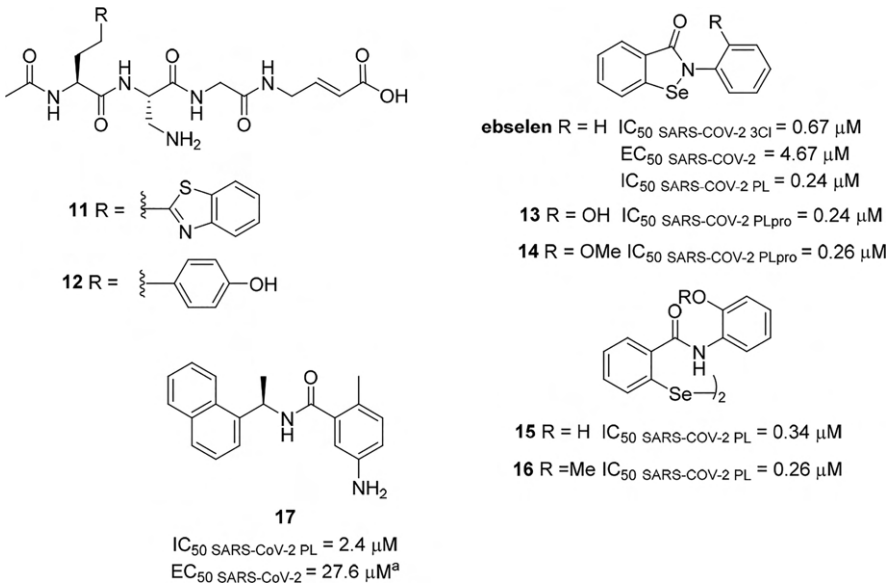

Figure 12. Chemical structures and biological activities of Ebselen and compounds **11**−**17**.

binding mode by S−π and π−π interactions, respectively, while the carbonyl accepts a H-bond by the Glu166 backbone amide. Finally, the C-2 phenyl ring extends toward the S2 subsite forming favorable contacts with residues such as His41, Met49, and Tyr54. Therefore, Baicalein fills the core of the substrate binding site including the catalytic dyad and the S1/S2 protein residues sharing several recognition elements with peptide substrates and inhibitors.

Interestingly, Baicalein also showed antiviral activity (EC_{50} = 1.69 μM) against SARS-CoV-2 in infected cells without toxicity (CC_{50} > 200 μM, SI > 118), while Baicalin was less potent in the same assay (Figure 10A).[76] It is worth noting that Baicalin tablets have been used as adjuvant therapy for the treatment of acute, chronic, or persistent hepatitis in China and were shown to be well tolerated up to the dose of 2.8 g.[77] Phase IIa clinical trials are currently ongoing to evaluate Baicalin in healthy adults with influenza fever (NCT03830684).

The 3D coordinates of SARS-CoV-2 $3CL^{pro}$ bound to another noncovalent ligand **10** (PDBs: 6W63, 6W79) have been recently released, showing that this compound can extend from S1′ to S3 establishing H-bonds with the backbone of Gly143 and Glu166 as well as with the His163 side chain (Figure 11). However, the data on the activity of **10** in enzymatic and antiviral cell-based assays are still unknown. Similar compounds belonging to a Ugi library were previously reported as SARS-CoV3CL^{pro} inhibitors, demonstrating μM inhibitory potency against the isolated target and poor activity in cell lines.[78]

Scientists from the Diamond Light Source, the UK's national synchrotron, solved a new apo-structure of the SARS-CoV-2 $3CL^{pro}$ (PDB 6YB7) and then carried out a large X-ray crystallographic fragment screening, which resulted in the identification of 22 noncovalent and 44 covalent active-site binders. The corresponding complexes were deposited in the PDB, providing opportunity for fragments growing and/or merging. Indeed, follow-up medicinal chemistry efforts are currently focusing on a group of fragments functionalized with chloroacetamide warheads, which were selected because they were not identified as hits in previous screens and could thus in principle be selective for $3CL^{pro}$.[79]

Additional approaches are based on drug repositioning through performing virtual screenings of approved and investigational drugs libraries, followed by experimental validation against the target protein in biochemical experiments and/or in cell-based SARS-CoV-2 replication assays. A large collection of about 10 000 drugs and clinical candidates has been screened through this approach. Among the compounds identified (see chemical structures in Supporting Information, Figure S2), Ebselen (Figure 12),[80] a synthetic organoselenium molecule endowed with anti-inflammatory, antioxidant, and cytoprotective properties, turned out as a covalent inhibitor of the SARS-CoV-2 $3CL^{pro}$ displaying antiviral activity in cell line, but the overall results are not particularly encouraging.[40]

THE PL^{PRO} AS ANTIVIRAL TARGET

The CoV nsp3 multidomain protein is the largest replicase subunit (1922 aa).[81] This macromolecule, having transmembrane domains, is likely to play an essential role during the formation of the replication complex by mediating intracellular membranes rearrangement and by multiple interactions with other nsps.[82] Several domains of nsp3 have been identified and are conserved in all CoVs.[83] Among these, the PL^{pro} domain (residues 1602−1855) is a cysteine protease that cleaves the viral polyprotein in the nsp1/2, nsp2/3 and nsp3/4 cleavage sites. Additionally, PL^{pro} can recognize and hydrolyze the cellular proteins Ub and UbL protein ISG15 from the lysine ε-amino group of ubiquitinated host proteins involved in innate antiviral response.[33,84,85] The PL^{pro} thus acts as a potent suppressor of Ub-dependent host immunity mechanisms, blocking the production of IFNβ and other cytokines as well as IRF3 and NF-κB pathways. By exerting proteolytic activity on part of the immature viral polyprotein and on Ub-modified host cell proteins, inhibitors of PL^{pro} can block CoV replication and potentiate antiviral host cell immunity. In contrast to SARS-CoV-2 $3CL^{pro}$, which is already well characterized and for which several inhibitors have been described, PL^{pro} has been not investigated in detail so far.

https://dx.doi.org/10.1021/acs.jmedchem.0c01140
J. Med. Chem. 2022, 65, 2716−2746

However, this protein is quite similar to the SARS-CoV homologue PL^{pro}, sharing 83−86% sequence identity while differing from MERS-CoV PL^{pro} (33% identity).[33] Thus, a description based on the structural and functional data on the SARS-CoV PL^{pro} is possible. SARS-CoV-2 PL^{pro} has the classic catalytic triad of cysteine proteases made by Cys111-His272-Asp286 (corresponding to Cys112-His273-Asp287 in SARS-CoV PL^{pro}) that specifically recognize the P1−P4 sequence GGXL conserved in all the nsp1/2, nsp2/3, and nsp3/4 cleavage sites of the viral polyprotein.[33,85] As anticipated above, PL^{pro} is also able to cleave Ub and the UbL protein ISG15, both showing the GGRL recognition motif at the C-term, from the ε-amino group of host proteins. Indeed, the PL^{pro} overall architecture resembles that of human deubiquitinating enzymes of the Ub-specific protease family. This comprises a three-dimensional right-hand structure that hosts the catalytic triad at the interface of the thumb and the palm subdomains, an Ub binding motif at the N-term, and a fingers region containing an essential structural zinc ion tetrahedrally coordinated by four cysteines.[86] The Trp106 residue (Trp107 in SARS-CoV PL) in the oxyanion hole of the PL^{pro} is required for the enzymatic activity because it stabilizes the hemithioacetal substrate intermediate through a single H-bond established by its indole nitrogen.[33,85] An additional key common feature between SARS-CoV and SARS-CoV-2 PL^{pro} is the presence of the flexible BL2 loop containing a Tyr residue (Tyr268). It is found in an open conformation in the unliganded PL^{pro}, while it is in the closed form upon inhibitor binding.

Like for SARS-CoV-2 3CL^{pro}, the substrate specificity profile of PL^{pro} was evaluated by determining the hydrolytic rate of different substrates from a combinatorial library, in comparison with the SARS-CoV enzyme.[87] This analysis has shown that both proteases are highly specific for Gly in P1−P2, while they can accept a wide panel of P3 residues, tolerating not only basic residues like Arg, Lys Orn Phe(guan), hArg Dap, Dab but also hydrophobic amino acids, such as hTyr, Phe(F5), Cha, Met, Met(O), and Met(O)$_2$. On the other hand, these pockets cannot recognize D-amino acids. The S4 subsite can host only hydrophobic residues, among natural amino acids, with a strong preference for Leu. Notably, SARS-CoV PL^{pro} can bind two P4 unnatural residues, namely hTyr and hTyr(Me), with higher affinity than leucine. On the basis of these specificities, two tetrapeptides, **11** and **12**, displaying a GG-Dap-X as P1−P4 sequence and functionalized with a vinyl ester warhead, were designed as covalent inhibitors of the SARS-CoV-2 and SARS-CoV PL PRs. Their IC$_{50}$s were not reported in the original manuscript but can be derived from the inhibition curve. Thus, IC$_{50}$ for both compounds can be approximately estimated to be around 10 μM, however their antiviral activity in cell-based assay was not reported (Figure 12). As expected, the compounds were inactive against MERS-CoV-PL^{pro}, significantly differing from the SARS homologues. The X-ray structures of compounds **11** or **12** covalently bound to SARS-CoV-2 PL^{pro} (PDBs: 6WUU and 6WX4, respectively) have been released.

Seleno-organic compounds have been described in two preprint papers as irreversible inhibitors of PL^{pro} of both SARS-CoV and SARS-CoV-2, with Ebselen (Figure 12) showing IC$_{50}$s of 8.35 and 2.26 μM, respectively, after incubation (60 min) with each enzyme, whereas no activity was detected without incubation.[88] Later on, benzisoselenazol-3(2*H*)-one derivatives, differing from Ebselen in the N substituent, and 2,2′-dicarbamoyldiaryl diselenides have been reported as inhibitors of PL^{pro} (Figure 12).[89] In particular, *o*-hydroxy (**13**) and *o*-methoxy (**14**) *N*-phenyl substituted benzisoselenazol-3(2*H*)-ones are 10-fold more potent against SARS-CoV-2 PL^{pro} than Ebselen, with IC$_{50}$s of 0.24 and 0.26 μM, respectively. Similarly, the corresponding 2,2′-dicarbamoyldiaryl diselenide analogues **15** and **16** show inhibitory potency in the same range (IC$_{50}$ = 0.34 and 0.26 μM). Antiviral activity in cell-based assays was not investigated for Ebselen and its analogues. However, Ebselen has been shown to covalently inhibit also SARS-CoV-2 3CL^{pro}[40] and a plethora of protein targets, while benzisoselenazol-3(2*H*)-one and 2,2′-dicarbamoyldiaryl diselenide derivatives have been shown to also irreversibly inhibit human methionine aminopeptidase 2,[90] thus hinting at a nonspecific effect on a wide panel of proteins due to the high reactivity of Se atom.

Noncovalent naphthalene-based SARS-CoV PL^{pro} inhibitors have been previously identified through HTS approaches showing high-nM/low-μM potency in biochemical assays and weak antiviral activity in cell lines, with the optimized derivative **17** (Figure 12) displaying the best performance (IC$_{50\ \text{SARS-CoV PL}}$ = 0.6 μM, EC$_{50\ \text{SARS-CoV}}$ = 14.5 μM, Figure 12).[91,92] As demonstrated by enzymatic kinetic experiments, **17** is a reversible competitive inhibitor that in the X-ray complex with SARS-CoV PL^{pro} (PDB 3E9S) is bound at the S3−S4 subsites in a cleft for the access to the active site.[93] Recent results show that **17** is able to inhibit SARS-CoV-2 PL^{pro} (IC$_{50}$ = 2.4 μM, EC$_{50\ \text{SARS-CoV}}$ = 27.6 μM Figure 12), while it is not able to inhibit MERS-CoV PL^{pro} due to the replacement with a threonine of Tyr268, in the BL2 loop, that is present in both the SARS-CoV and SARS-CoV-2 enzymes where the residue mediates interactions with the inhibitors.[33] However, compound **17** demonstrated weak antiviral activity in cell-based assays (EC$_{50\ \text{SARS-CoV-2}}$ = 27.6 μM in plaque assay, in Figure 12).[33]

In summary, targeting PL^{pro} may represent a promising approach to tackle SARS-CoV-2 replication and host immune escape. However, no potent and cell-based active covalent inhibitor is yet available, probably because the design of peptidic compounds, resembling the substrate sequence, is hampered by P1−P2 specificity for glycine. On the other hand, known reversible noncovalent inhibitors of SARS-CoV PL^{pro} show only moderate and narrow antiviral activity, being not active against the related MERS-CoV homologue. Therefore, much work is needed to validate PL^{pro} as a viral target for successful drug discovery.

SARS-COV-2 RDRP: STRUCTURE AND FUNCTION

CoVs rely on a multisubunit machinery for the replication and transcription of the viral genome. This macromolecular assembly is made up of nonstructural proteins (nsp), which are cleavage products of the ORF1a and ORF1ab viral polyproteins.[94] In particular, RdRp activity resides in nsp12 and catalyzes the formation of a phosphodiester bond between nucleoside triphosphates (NTPs) in a primer-dependent manner. The NTP substrates involved in this reaction are coordinated by two metal ions, which are bound by the conserved Asp residues. Consistent with this conserved mechanism, strong amino acid conservation can be observed in regions that are directly involved in nucleotide selection or catalysis.[95]

Upon the formation of a complex with nsp7 and nsp8, nsp12 acquires processivity for the synthesis of large RNAs, a

https://dx.doi.org/10.1021/acs.jmedchem.0c01140
J. Med. Chem. 2022, 65, 2716−2746

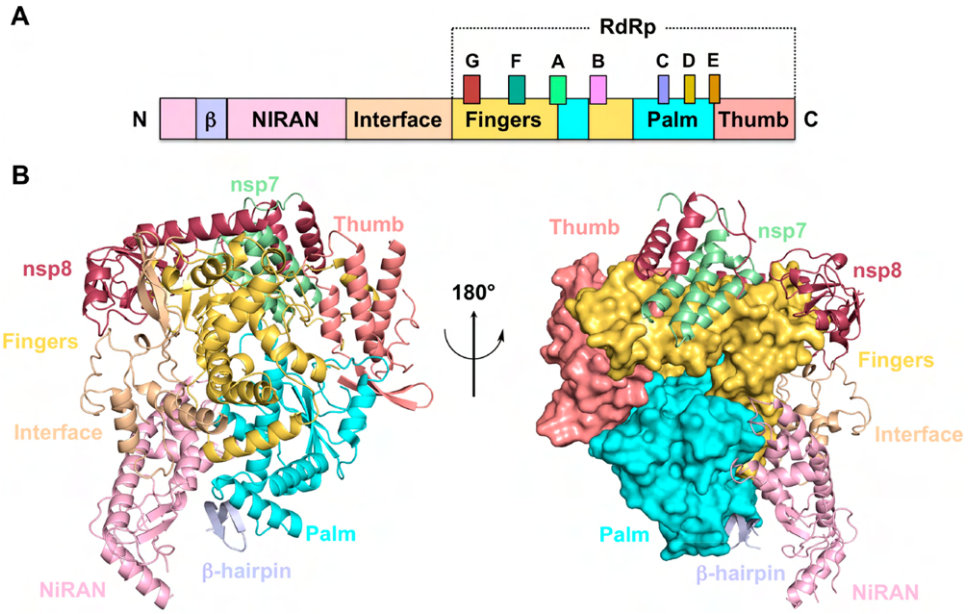

Figure 13. Architecture of SARS-CoV-2 nsp12. (A) Schematic diagram outlining the domain organization of SARS-CoV-2 nsp12. The domains are colored as: palm, cyan; fingers, yellow-orange; thumb, salmon. The N-terminal NiRAN domain, the interface and the β-hairpin are colored light-pink, wheat, and blue-white, respectively. The polymerase conserved motifs are colored as: motif A, lime green; motif B, violet; motif C, slate; motif D, olive; motif E, sand; motif F, deep-teal; motif G, ruby. (B) Structure of SARS-CoV-2 in two different orientations (PDB 6M71). (left) Ribbon diagram of nsp12 showing the arrangement of palm, fingers, and thumb domains. Domains are colored as in (A). Nsp7 and nsp8 cofactors are shown as pale-green and raspberry ribbon models, respectively. (right) The palm, fingers, and thumb domains are shown as a molecular surface.

mechanism that in CoVs has evolved to control the viral RNA synthesis during infection.[96] In addition, nsp8 has shown RNA primase activity, that is, the ability to synthesize an RNA primer,[97] enabling *de novo* RNA synthesis. The structural and functional features of the RdRps among CoV family are highly conserved; for example, the RdRp of SARS-CoV-2 has 96% amino acid identity to that of SARS-CoV.[98,99]

Recently, the structure of SARS-CoV-2 full-length RdRp, in complex with cofactors nsp7 and nsp8, was determined by cryoelectron microscopy (cryo-EM) at 2.90 Å resolution (PDB 6M71)[100] showing the typical right-hand architecture of the viral RdRps (Figure 13), constituted by the finger, palm, and thumb subdomains.[101] The nsp12 RdRp domain is connected through an interface to the N-terminal region possessing nucleotidyltransferase activity, named NiRAN, whose exact role in the viral life-cycle remains elusive.[102] SARS-CoV-2 RdRp cryo-EM structure revealed also an additional, unique N-terminal β-hairpin, which was previously not observed in SARS-CoV RdRp.[100]

The RdRp active site is composed by seven conserved motifs (A−G) lining a central cavity where the template-directed RNA synthesis takes place (Figure 14). In particular, the incoming NTP binds within motif F, whereas the RNA template enters the active site through a channel formed by motifs F and G; motif E and the thumb subdomain sustain the primer strand. The product of RNA synthesis leaves the active site through an RNA exit path, situated at the front side of the polymerase.[100]

Three other groups reported further cryo-EM structures of nsp12 catalytic subunit and nsp7-nsp8 cofactors. The nsp12-nsp7-nsp8 complex has been solved both in the apo form (PDB 7BV1) and bound to the template-primer RNA and Remdesivir monophosphate (PDB 7BV2);[103] this latter is described in more detail below. Subsequently, another apo structure was reported (PDB 7BW4).[104] By using circular

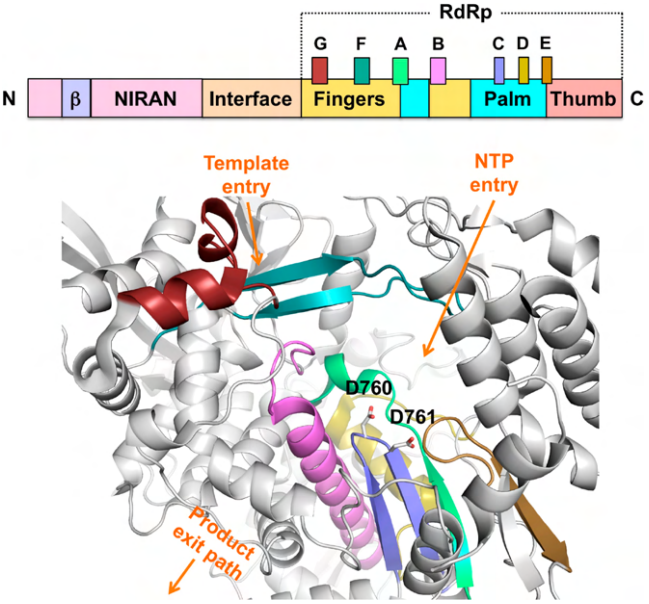

Figure 14. Overview of SARS-CoV-2 nsp12 active site. For clarity, the RdRp core region is shown as a white ribbon model, whereas the polymerase conserved motifs (A−G) are colored according to the upper schematic diagram. The catalytic residues Asp760 and Asp761 are shown as white sticks. The template entry, NTP entry, product hybrid exits paths are indicated by orange arrows.

dichroism (CD) experiments, the authors pointed out that both the nsp8 and nsp12 subunits of SARS-CoV-2 have shown lower melting temperature values, as compared to the corresponding subunits of SARS-CoV, suggesting the poorer thermostability of SARS-CoV-2 proteins and a possible adaptation of SARS-CoV-2 toward humans with relatively lower body temperatures than the natural bat hosts. Then, the

https://dx.doi.org/10.1021/acs.jmedchem.0c01140
J. Med. Chem. 2022, 65, 2716−2746

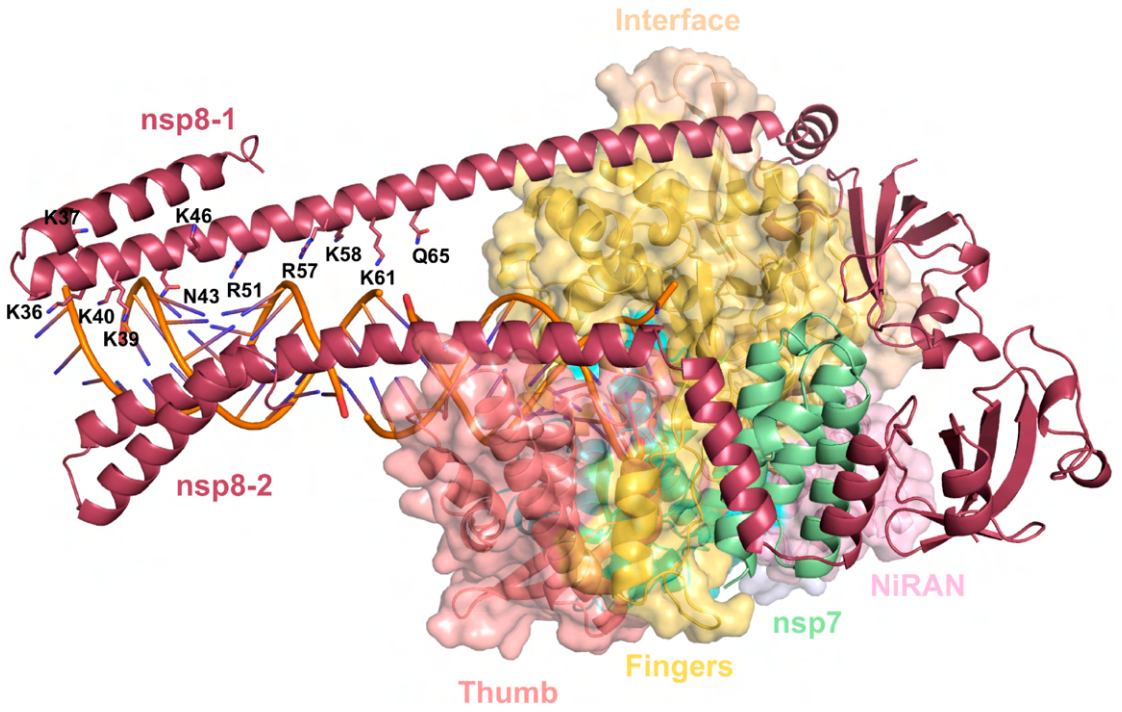

Figure 15. Structure of SARS-CoV-2 replicating RdRp-RNA complex (PDB 6YYT). Nsp12 is shown as a molecular surface (color code as in Figure 13), whereas the cofactors nsp7 and nsp8 (protomers 1 and 2) are shown as pale-green and raspberry ribbon models, respectively. RNA turns are shown as an orange ribbon model. The positively charged nsp8 residues, proposed to interact with RNA, are shown as sticks.

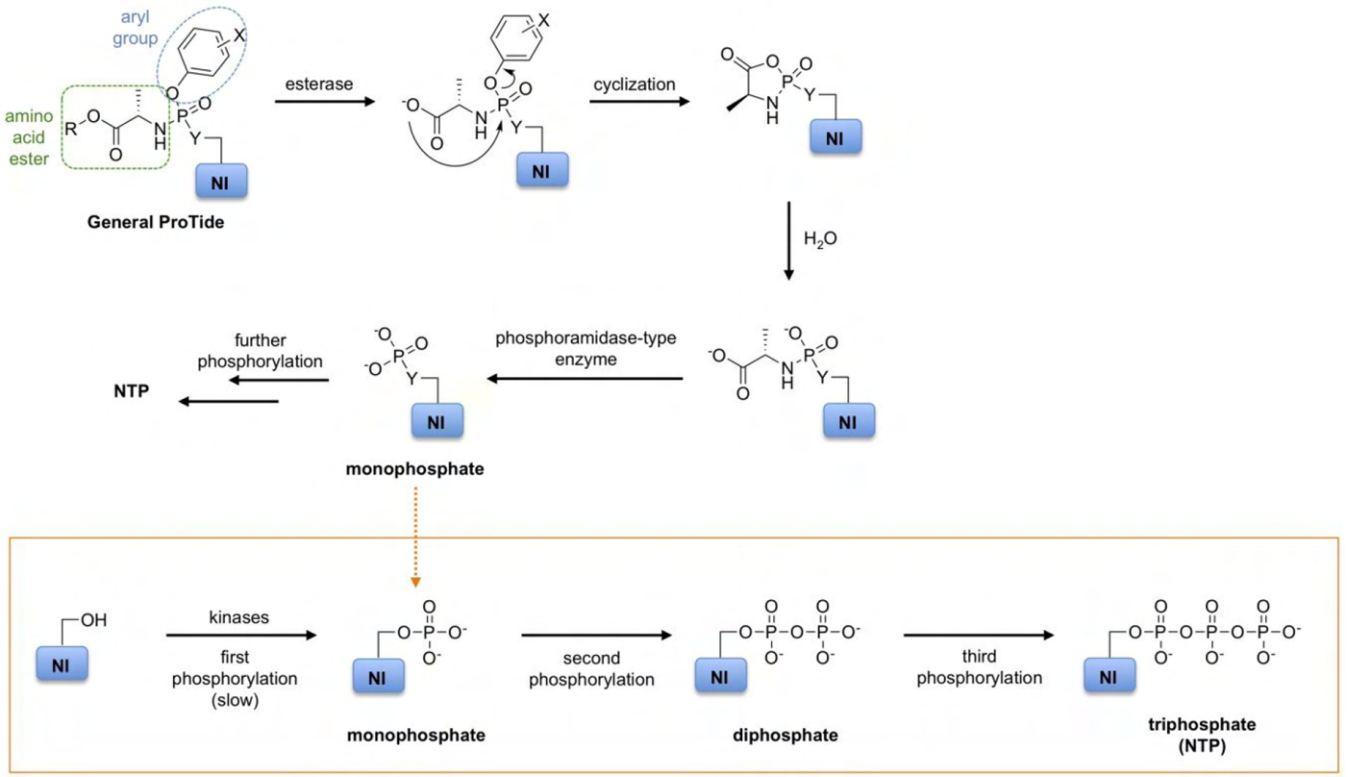

Figure 16. Putative mechanism of ProTides *in vivo* metabolism. Upon diffusion into the cell, the amino acid ester of the ProTide is cleaved by intracellular esterases, then a cyclization occurs onto the phosphorus, with the release of the phenoxide moiety. The unstable cyclic intermediate is then hydrolyzed by water to the alanine metabolite, whose P—N bond is hydrolyzed by phosphoramidase-type enzymes to unmask the NI monophosphate form. The NI monophosphate is routed to further phosphorylation steps, yielding the active triphosphate form (NTP) and thus circumventing the endogenous phosphorylation pathway (orange box). X, aromatic substituents; Y, O, or CH_2; R, ester substituents.

https://dx.doi.org/10.1021/acs.jmedchem.0c01140
J. Med. Chem. 2022, 65, 2716−2746

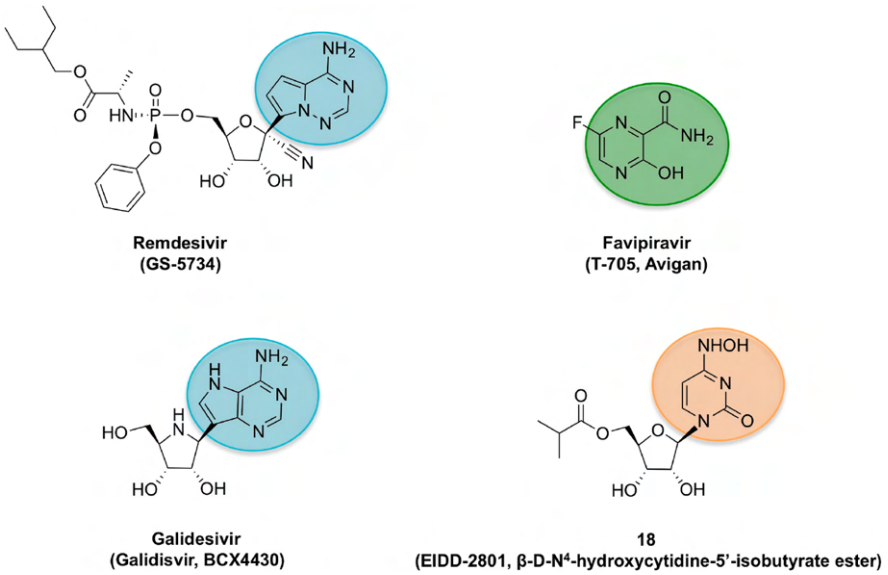

Figure 17. Chemical structures of antiviral nucleoside analogues in clinical development. The parent bases are highlighted in light-blue (adenine), green (guanine), and orange (cytosine).

cryo-EM structure of the replicating SARS-CoV-2 RdRp (PDB 6YYT), comprising nsp12, nsp8, and nsp7, and over two turns of RNA template-product duplex was reported, adding another piece of useful structural information (Figure 15).[105]

The active site cleft of nsp12 binds the first turn of RNA, whereas two subunits of nsp8 bind to opposite sides of the cleft, flanking the exiting RNA duplex with long α-helical extensions, called "sliding poles". These nsp8 extensions are rich in positively charged residues and form multiple RNA backbone interactions. Notably, this structure revealed large additional portions in nsp8 that become ordered upon RNA binding, while nsp8 nsp7 complexes are usually more flexible.[105] The mutation of one of these positively charged residues, namely Arg58, with Ala, was previously reported as lethal in SARS-CoV because of the strong decrease of polymerase activity, leading to a nonviable phenotype (as evaluated by immunofluorescence microscopy and plaque assays).[96]

TARGETING SARS-COV-2 RDRP

The SARS-CoV-2 RdRp represents an ideal drug target due to its critical role in virus replication and the absence of an enzymatic counterpart in the host cell. In fact, viral polymerases inhibitors represent the cornerstone of antiviral therapeutics; indeed, most of the approved drugs for the treatment of viral infections, including HIV and HCV, belong to this class.

Inhibitors of viral polymerases fall into two main categories, according to their mode of action and structure, with nucleoside inhibitors (NIs) acting at the substrate site and the non-nucleoside inhibitors (NNIs) interacting with allosteric binding sites.

Therefore, building on the experience and achievements obtained in the past, these approaches might lead to strategies that effectively control SARS-CoV-2 infection. NIs represent an attractive avenue toward disrupting viral RNA replication because of the high degree of conservation of active sites of RdRp and relatively low mutation rate in these regions, thus allowing for a broad antiviral activity and a high barrier to resistance. To compete with the natural substrates for incorporation into the viral RNA, NIs requires activation to the pharmacologically active triphosphate form (NTP) by a multistep process, carried out by host kinases (Figure 16, orange box). The first phosphorylation step is often the rate-limiting step in the activation.[106] To overcome this drawback, the application of the ProTide strategy, based on the synthesis of ester phosphoramidate prodrug of monophosphate nucleotides, has been extensively explored in NIs to bypass the initial phosphorylation step. After cellular uptake, ProTide ester hydrolysis is mediated by host esterases (Figure 16), followed by spontaneous cyclization, phenol release, and phosphoramidase cleavage to deliver the nucleotide monophosphate, which is then converted into the active NTP form.[106]

The viral RdRp binds the drug in the form of NTP; then, the hydrolysis and release of a pyrophosphate group provides the energy source for nucleotide monophosphate incorporation into the nascent RNA chain, with consequent inhibition of strand elongation and viral replication. Antiviral NIs fall into three categories: obligate chain terminators, nonobligate chain terminators, and mutagenic.[107] Obligate chain terminators do not possess the 3′-hydroxyl group at the riboside moiety of the molecule. Nonobligate chain terminators possess instead a natural base and a 3′-hydroxyl on the sugar, but they display an additional substituent at the C-1′ or the C-2′ positions of the ribose ring, blocking the formation of the phosphodiester linkage with the incoming NTP.[107] The mechanism of lethal mutagenesis involves the inability to recognize the nucleoside analogues as regular nucleobases, thus inducing a mismatch in base pairing and an increase in mutations, ultimately leading to nonviable genomes.

Despite the large amount of structural data produced for the SARS-CoV-2 RdRp, this protein may appear as a still underexplored antiviral target in comparison with the $3CL^{pro}$ of CoVs. Indeed, no focused medicinal chemistry programs, aimed at identifying specifically designed inhibitors of CoV RdRp, have been reported so far. On the other hand, the few inhibitors identified derive from a large repurposing campaign on known broad spectrum, well characterized NIs which can be readily used in the clinic. In fact, Remdesivir (GS-5734, developed by Gilead Sciences) was recently granted EUA[12] for

https://dx.doi.org/10.1021/acs.jmedchem.0c01140
J. Med. Chem. 2022, 65, 2716−2746

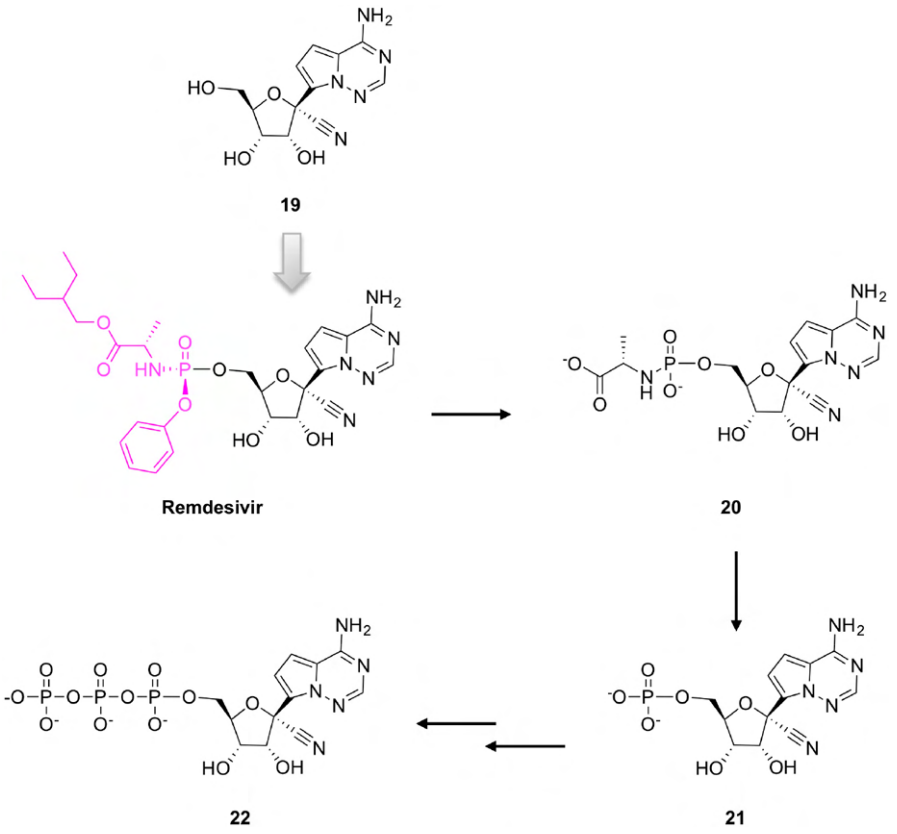

Figure 18. Schematization of Remdesivir metabolic conversion to the active triphosphate form. Remdesivir is first transformed into the intermediate alanine metabolite **20**, then to the monophosphate form **21** and finally to the triphosphate form **22**. The phosphoramidate prodrug moiety is shown in magenta. **19** (GS-441524) is the parent nucleoside of Remdesivir.

the treatment of SARS-CoV-2, following the encouraging results from the National Institute of Allergy and Infectious Diseases (NIAID) and Gilead clinical trials and from the compassionate use programs.[13−15] Other attractive candidates include Favipiravir (T-705, Avigan), which was granted emergency use approval in Russia and India, Galidesivir (Galidisvir, BCX4430), and the compound β-D-N^4-hydroxycytidine-5′-isobutyrate ester **18** (EIDD-2801). These compounds can be grouped in adenine (Remdesivir and Galidesivir), guanine (Favipiravir), and cytosine (**18**) analogues (Figure 17). Remdesivir and Galidesivir are C nucleosides obtained by introducing a C-glycosidic bond to link the sugar to the nucleobase, showing higher resistance to phosphorolysis mediated by intracellular phosphorylases.

Remdesivir is the Sp isomer ester monophosphoramidate prodrug of 1′-cyano-substituted adenine C-nucleoside ribose analogue **19** (GS-441524, Figure 18).[108] It was designed to deliver the nucleoside monophosphate **21** into the cell, circumventing the rate-limiting first phosphorylation step and allowing for efficient formation of the active triphosphate form (Figure 18).[109,110] This advantage is not present in Favipiravir, **18**, and Galidesivir. Structurally, the 1-cyano group of Remdesivir provides potency and selectivity toward viral RNA polymerases. The Sp isomer was selected because of the high potency across multiple cell lines and the crystalline nature of an Sp prodrug reagent that allowed rapid synthesis scale-up, a key element for the current request of active pharmaceutical ingredients (API).[110]

The cryo-EM structure of Remdesivir in complex with RdRp from SARS-CoV-2 and a 50-base template-primer RNA (PDB 7BV2) has been recently released.[103] This structure, generated using the drug's triphosphate metabolite **22**, shows the nucleotide analogue in its monophosphate form, covalently bound to the primer strand at the 3′-end (Figure 19) to terminate the chain elongation.

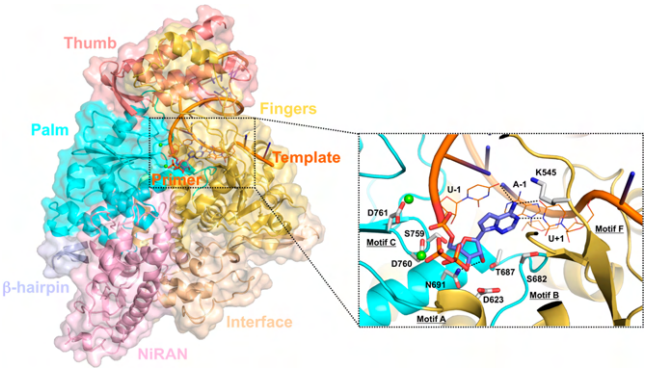

Figure 19. Binding mode of Remdesivir into the SARS-CoV-2 nsp12 active site (PDB 7BV2). (left) nsp12 is shown as a molecular surface, colored according to the schematic diagram in Figure 13. For clarity, nsp7 and nsp8 cofactor have been removed. The template and primer RNA are shown as ribbon models and labeled. (right) Zoom-in of the nsp12 active site. The covalently bound monophosphate form of Remdesivir (slate) and the pyrophosphate group are shown as sticks. Magnesium ions are shown as green spheres. The RNA bases interacting with Remdesivir are shown as orange thin sticks, while protein residues are shown as white thick sticks. Hydrogen bonds are shown as black dashed lines.

https://dx.doi.org/10.1021/acs.jmedchem.0c01140
J. Med. Chem. 2022, 65, 2716−2746

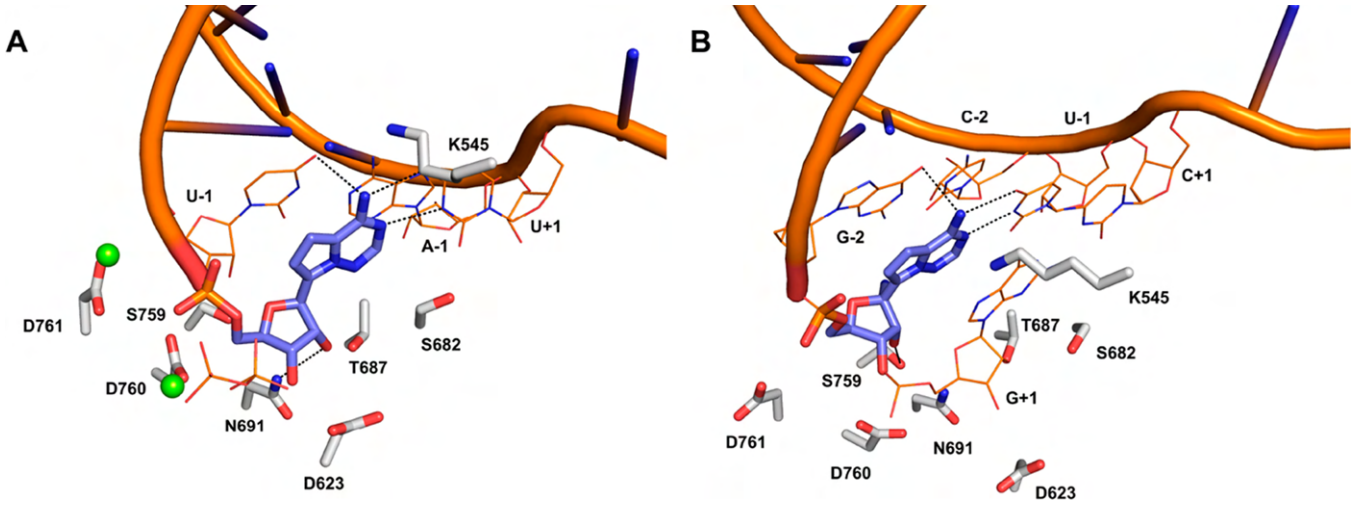

Figure 20. A close view of the covalently bound Remdesivir within the RdRp active site. (A) Remdesivir is incorporated into the primer strand and terminates chain elongation (PDB 7BV2). (B) Remdesivir incorporation induces a mechanism of delayed-chain termination (PDB 7C2K). RNA is shown as orange ribbon model. For clarity, only key residues (thick white sticks) and bases (orange thin sticks) that interact with Remdesivir are shown. Hydrogen bonds are shown as dashed lines.

Next to the covalently bound Remdesivir, there is the leaving pyrophosphate group; the two catalytic magnesium ions, coordinated by two aspartic acid residues Asp760 and Asp761, are also visible. Strikingly, nsp7 and nsp8 do not form interactions with RNA, although they are required for RNA binding by RdRp. Remdesivir is positioned at the center of the catalytic site, with the adenosine analogue forming stacking interactions with the upstream bases U-1 and A-1 of the primer and template strands. In addition, Remdesivir engages three strong H-bonds with the uridine bases U−1 and U+1, whereas the sugar 2′-OH group forms a further H-bond with Asn691 (Figure 20A). The Asp623, Ser682, and Asn691 residues are involved in the recognition of the ribose hydroxyl groups of the incoming NTP and are responsible for the proper positioning of the ribose moiety. Such residues represent a conserved feature among viral RdRps.[111] Among them, Ser682, located on motif B, is considered a "fidelity checkpoint" because it is sensitive to the conformational changes of motif B upon binding of the NTP, which, in turn, triggers the active site closure.[112] This structure shows for the first time a clear picture of how the template-primer RNA is recognized by the enzyme and how the covalently bound Remdesivir interacts with the active site residues.

A "delayed" chain termination has been proposed for Remdesivir, according to which the RNA synthesis is terminated after the addition of three more nucleotides (at position i+3, where i corresponds to the position of the first incorporated Remdesivir monophosphate);[113,114] this mechanism has been reported for SARS-CoV, MERS-CoV, and also SARS-CoV-2.[111,115] This hypothesis is consistent with a recently released cryo-EM structure of the SARS-CoV-2 RdRp in complex with RNA, before and after RNA translocation (PDBs: 7C2K and 7BZF, respectively).[116] In the pretranslocated catalytic complex structure, the incorporated Remdesivir has been translocated to the −1 position, whereas the 3′-guanosine occupies the +1 position (Figure 20B). Remdesivir engages four H-bonds, with the upstream G-2 base, the uridine base U-1, and with Ser759. The primer strand with the incorporated Remdesivir may translocate without obstruction to positions i+1, i+2, or i+3, allowing the incorporation of three subsequent nucleotides. However, at position i+4, a putative steric clash was postulated between the 1′-CN substituent of Remdesivir and Ser861 along the RNA exit tunnel.[111] Ser861 is highly conserved among CoV RdRps, and its important role in Remdesivir induced RdRp inhibition was ultimately supported by mutagenesis studies, revealing that the Ser861Ala RdRp mutant yields a smaller fraction of i+3 termination compared with the wild-type RdRp, possibly supporting the steric clash hypothesis.[116]

The analysis of the pretranslocated complex cryo-EM maps revealed the two bound nsp8 protomers in two distinct states, named conformations I and II;[116] this latter resembles the previously observed "sliding poles" (PDB 6YYT), whereas in conformation I, the nsp8 protomer, which lays on the fingers and interface domains, show an orientation change of about 45°. Taken together, the structural information reported so far suggest that, besides targeting nsp12, an alternative approach for RdRp inhibition would be the disruption of the polymerase complex integrity, for example, targeting the interaction between nsp8 and nsp12. Indeed, it would be interesting to explore the presence of "hot spots", which are small areas of the protein−protein interface providing most of the binding energy. In fact, protein−protein interactions (PPIs) are today a validated target for drug discovery, and in this perspective, the structure of the replicating RdRp (Figure 15) may offer hints for the development of peptidomimetics or small molecules capable of impairing the PPIs between nsp7-nsp8-nsp12. For instance, the recognition between the upper part of nsp8−1 and the fingers domain of nsp12 is mediated by a β sheet, suggesting the possibility to design small peptidomimetics capable of resembling a β-strand motif.

Remdesivir was originally developed within antiviral research program against HCV and respiratory syncytial virus (RSV) but has shown a broad antiviral activity against other different viruses, including Dengue, parainfluenza type 3 virus (hPIV3), Ebola virus, and SARS-CoV with EC_{50} in the sub-μM range.[108,117,118] Remdesivir showed efficacy in preclinical rhesus monkey models of Ebola virus infection;[109] it was evaluated in humans on a compassionate basis in some isolated cases of EVD[119,120] and in a large-scale clinical trial for EVD

https://dx.doi.org/10.1021/acs.jmedchem.0c01140
J. Med. Chem. 2022, 65, 2716−2746

conducted in Congo.[121] Although the efficacy of Remdesivir was lower than the antibodies treatments tested, the survival rate was significantly higher than in the EVD outbreak.

The efficacy of Remdesivir against CoVs was only recently reported.[122,123] In particular, it showed dose-dependent inhibition of SARS-CoV and MERS-CoV replication in primary human airway epithelial cell (HAE) cultures, with average EC_{50} = 0.069 μM (SARS-CoV) and 0.074 μM (MERS-CoV).[122] While typical chain terminators are excised by the viral exonuclease nsp14, Remdesivir seems to be able to escape the exonuclease activity. Two amino acid substitutions were found in the nsp12 polymerase providing low-level resistance to Remdesivir, corresponding to the SARS-CoV residues Phe480Leu and Val557Leu. Such residues are identical across CoVs and have been found to cause an impairing of fitness and virulence.[124]

The possible structural and function implications of such resistance mutations have been recently analyzed.[112] The two mutations do not have a direct impact on the catalytic site or substrate-binding pocket but rather cause minor structural alterations, which likely impact an NTP fidelity checkpoint performed by the polymerase before catalysis. Phe480 is located at the interface between the fingers and palm domains, facing a patch of hydrophobic residues that indirectly impact motif B. The mutation Phe480Leu likely reduces the interactions within the hydrophobic core, thereby reducing its structural rigidity. Therefore, one possible interpretation is that the phenylalanine to leucine mutation would have an impact on the positioning of the Ser682 of motif B, altering the fidelity checkpoint. On the other hand, Val557 is located at the end of motif F and forms a hydrophobic wall upon which the template base is stacked. The consequence of a valine to leucine mutation is a more extended hydrophobic side chain, possibly generating a steric hindrance with the template RNA. As a result, the RNA would be expected to be deviated from the groove, away from the serine of motif B. Remdesivir also showed potential to treat SARS-CoV-2 infections, with different studies reporting slightly different antiviral activities for this drug (Table 1).[125−128]

Table 1. Remdesivir Antiviral Activities against SARS-CoV-2 Measured in Different Cell Lines and Assays

	EC_{50} (μM)			
cell line	plaque assay	genome copy number	log_{10} $TCID_{50}$ (mL)	cytopathic effect (CPE)
Vero E6		0.77[a]		
		26.90[b]	23.15[b]	
				0.651[c]
	1.65[d]	1.49[d]		
Calu3 2B4	0.28[d]	0.60[d]		
HAE	0.010[d]			

[a]From ref 125, [b]From ref 126, [c]From ref 127, [d]From ref 128,

The potency of Remdesivir is highly dependent on the intracellular concentration of the pharmacologically active triphosphate metabolite, which can vary in different cell systems. Indeed, such concentration is markedly higher in primary HAE cultures compared to human lung cells (Calu3 195 2B4) and monkey kidney cells (Vero E6). Therefore, the differences in EC_{50} may be due to intrinsic differences of SARS-CoV-2 virus isolates, methods of quantification, and assay conditions. Because SARS-CoV-2 does not readily infect wild-type mice because of incompatibilities between virus spike and the murine orthologue of ACE2, which is needed for SARS-CoV-2 entry, a recombinant SARS-CoV-1 chimeric virus, encoding the SARS-CoV-2 RdRp, was engineered to rapidly assess the *in vivo* efficacy of Remdesivir in mice.[128] Remdesivir inhibited chimeric virus replication in a dose-dependent manner in human epatoma (Huh7) cells, with mean EC_{50} = 3 nM. Moreover, Remdesivir treatment significantly ameliorated loss of pulmonary function in female C57Bl/6 Ces1c−/− (carboxyl esterase 1c deficient) mice administered 25 mg/kg Remdesivir subcutaneously 1 day postinfection (dpi) and BID thereafter. The transgenic mice model better recapitulates the DMPK profile of Remdesivir in humans. Indeed, carboxyl esterase 1c is a serum esterase which dramatically reduces half-life of Remdesivir and is absent in humans.[122] For instance, the plasma stability of Remdesivir was significantly improved in Ces1c−/− mice ($T_{1/2}$ ∼ 25 min) with respect to wild-type mice ($T_{1/2}$ < 5 min). *In vivo* experiments in mice infected with MERS-CoV proved the higher efficacy of Remdesivir than a combination of Lopinavir/Ritonavir and IFN-β in improving lung function.[129] Remdesivir *in vivo* efficacy against SARS-CoV-2 was gauged in rhesus macaques: therapeutic treatment started 12 h after inoculation with SARS-CoV-2 and continued once daily through 6 days post inoculation (dpi).[130] One group of rhesus macaques was treated with a loading dose of 10 mg/kg Remdesivir, followed by a daily maintenance dose of 5 mg/kg, while the other group, serving as control, received a vehicle solution. Remdesivir was able to reduce virus titers in bronchoalveolar lavages already 12 h after the first treatment, also reducing clinical disease and damage to the lungs. The treatment resulted in reduced virus replication in the lower respiratory tract but not in the upper tract, suggesting the need to explore drug delivery strategies to improve Remdesivir distribution. Furthermore, the study suggested that treatment of patients with Remdesivir should be initiated early during infection.

Remdesivir received the approval from the FDA for the treatment of hospitalized patients diagnosed with COVID-19.[12]

The optimal duration of treatment is still under evaluation in clinical trials. Both 5-day and 10-day treatment durations are suggested, based on the severity of disease, with 200 mg iv on the first day, followed by 100 mg each day thereafter. The approval was granted on the basis of the available data from the Gilead's SIMPLE trials (NCT04292899), the Adaptive COVID-19 Treatment Trial (ACTT), sponsored by NIAID (NCT04280705), in patients with severe manifestations of COVID-19, and from the compassionate use program.

The two SIMPLE trials evaluated the safety and efficacy of 5-day and 10-day dosing duration of Remdesivir in hospitalized patients with severe (first study) and moderate manifestations (second study) of COVID-19. The results from the first study showed that patients receiving a 10-day treatment course had a distribution in clinical status similar to those taking a 5-day treatment course.[13] Thus, priority should be given to a 5-day regimen for patients at the early stages of severe disease (patients receiving supplemental oxygen but not yet been intubated).[14] During the trial, the side effects were mild and, however, the absence of a placebo control group and the open-label design of this study did not permit an overall assessment

https://dx.doi.org/10.1021/acs.jmedchem.0c01140
J. Med. Chem. 2022, 65, 2716−2746

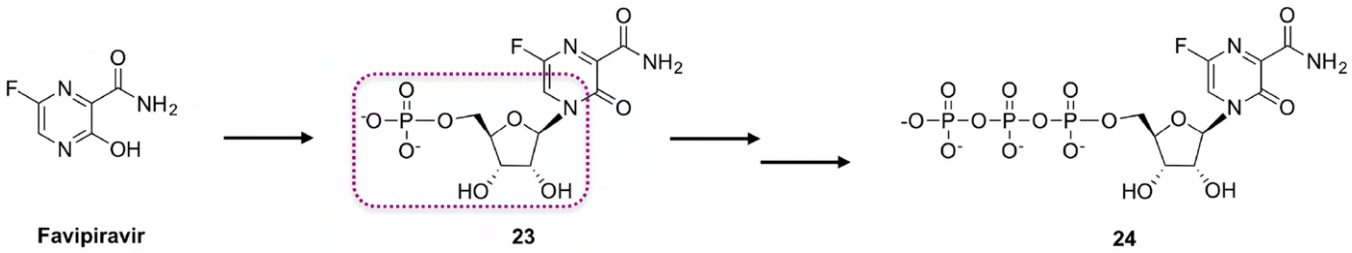

Figure 21. Schematization of Favipiravir metabolic conversion. Favipiravir is first converted to its ribofuranosyl monophosphate derivative **23** and subsequently to the triphosphate active form **24**.

of the benefit of Remdesivir. Another limitation is the lack of SARS-CoV-2 viral-load results during and after treatment due to the variability in local access to testing and practices across the global sites.

The recently published results of the second SIMPLE trial study showed that among patients with moderate COVID-19, those randomized to a 5-day course of Remdesivir plus standard of care had higher odds of having an improvement in clinical status compared to those randomized to standard of care alone. Patients randomized to a 10-day course of Remdesivir did not show a statistically significant difference in clinical status compared to standard care at 11 days after initiation of treatment.[131]

The ACTT trial is a randomized, double-blind, placebo-controlled multicenter trial conducted in around 100 sites globally, evaluating the time to recovery of hospitalized adults diagnosed with COVID-19 up to day 29. The recently published results indicate that Remdesivir was superior to placebo in shortening the time to recovery; mortality was numerically lower in the Remdesivir group than in the placebo group (11.4% with Remdesivir and 15.2% with placebo by day 29).[15] On the other hand, according to the published results of a trial carried out at 10 hospitals in Hubei, China, Remdesivir was not associated with statistically significant clinical benefits beyond those of standard of care treatment.[132] However, the trial was underpowered because the study terminated earlier, before attaining the prespecified sample size, as there were no further patients meeting eligibility criteria.[132,133]

It has to be noted how challenging it is provide robust findings when conducting trials during a pandemic: in this light, it is highly valuable to share results across multiple, even smaller, but high-quality studies. Some of the variation in results from the RCTs of Remdesivir could be due to differences in study design.[134] The overall results suggest that Remdesivir improves the recovery of patients hospitalized with COVID-19 and may prevent the progression to more severe respiratory disease.[15]

Moreover, there is room for further studies involving potential combination therapies with other antivirals and anti-inflammatory agents in appropriate regimen. In this regard, the ACTT3 trial (NCT04492475) will evaluate the combination of INF-β1a and Remdesivir compared to Remdesivir alone.

Significant efforts are devoted to find an alternative route of administration to the currently iv used. Because the upper respiratory tract is the most prevalent site of SARS-CoV-2 infection in early disease, an inhaled, nebulized formulation of Remdesivir is being seen as a valid noninvasive alternative. This should afford a more targeted administration with a lower systemic exposure, increasing the therapeutic index of the drug. Inhaled Remdesivir would be particularly suited for early stage COVID-19 patients who do not need to be hospitalized. Additional clinical trials (GS-US-553-9018 and NCT04539262) have thus been initiated to evaluate this inhaled formulation.

Favipiravir contains a carboxamide moiety, reminiscent of guanine; it is mainly incorporated in the salvage pathways for purine nucleotides through the purine phosphoribosyltransferases, then it needs to be converted to its ribofuranosyl monophosphate **23** and to be further processed to the active triphosphate form **24** (Figure 21).[135]

This drug possesses a broad-spectrum activity toward RNA viruses.[136] High concentrations (EC_{50} of 61.88 μM) were required to reduce viral infection in Vero E6 cells infected with SARS-CoV-2.[125] Conversely, no apparent antiviral effect against SARS-CoV-2 was observed *in vitro* at concentrations under 100 μM. Favipiravir is thought to act as chain terminator;[135] however, a putative mechanism of lethal mutagenesis has been proposed in the activity of this drug against influenza A (H1N1) viruses *in vitro*.[136,137] Thus, antiviral nucleoside mechanisms of action may well vary from one virus to another. Favipiravir received approval in Japan for restricted use in uncomplicated influenza virus infections. The established dose for influenza in Japan is 1600 mg twice a day on day 1 followed by 600 mg twice a day for four days.[135] An important feature of this drug is the apparent lack of resistant mutants in cell cultures, as well as in clinical trials. Some studies, however, found mutants of influenza A (H1N1)[138] and chikungunya virus[139] with reduced susceptibility to Favipiravir in cell cultures, suggesting the need to implement diagnostic approaches to control the emergence of Favipiravir resistance in clinical settings.

Regarding the use of Favipiravir against COVID-19, to date, the only published clinical results appeared in a preprint, describing an open-label randomized trial carried out in China, comparing the efficacy and safety of Favipiravir (1600 mg BID first day, followed by 600 mg BID) and Arbidol (200 mg TID) to treat COVID-19 patients.[140] The clinical recovery rate on day 7 did not significantly differ between the Favipiravir group and the Arbidol group; patients administered Favipiravir experienced faster resolution of fever and cough but similar rates of respiratory failure compared to the control group receiving Arbidol. On 1 June 2020, Russia's Ministry of Health temporarily approved a Favipiravir-based medication for use in patients with COVID-19. Favipiravir also received accelerated approval in India for the treatment of mild to moderate COVID-19 patients. Despite the quite fast approval, more robust data, coming from well-designed studies and possibly involving larger population, are needed to provide strong evidence about the clinical benefit of this drug.

Galidesivir's (Galidisvir, BCX4430) effect on the inhibition of RNA transcriptional activity was first assessed in a cell-free

https://dx.doi.org/10.1021/acs.jmedchem.0c01140
J. Med. Chem. 2022, 65, 2716−2746

isolated HCV RdRp assay.[141] Galidesivir acts as a nonobligate RNA chain terminator; the switch from furanose to an azasugar is thought to alter the electrostatic interaction of the ring so that the viral RdRp is unable to add more than one or two further nucleotides.[141,142] Galidesivir was shown to possess weak antiviral activities against many RNA viruses, also including SARS-CoV (EC_{50} = 57.7 μM, measured by NR uptake assay) and MERS-CoV (EC_{50} = 68.4 μM assessed by high-content image analysis) and to protect nonhuman primates from lethal filovirus challenge.[141] On the other hand, Galidesivir does not inhibit SARS-CoV-2 viral replication at concentrations below 100 μM.[126] Notably, Galidesivir can be administered by both parenteral (im and ip) and oral routes.[142] Galidesivir is efficiently taken up into cells and converted to the active triphosphate. In mouse, rat (both treated with 2 mg/kg), guinea pig (50 mg/kg), and cynomolgus macaque (20 mg/kg), Galidesivir DMPK is characterized by rapid clearance from the plasma with a $T_{1/2}$ < 5 min. Conversely, the $T_{1/2}$ of the active triphosphate form in the liver in rats (administered 30 mg/kg) is substantially longer at 6.2 h.[141] Despite the apparently weak anti-CoV activity, on 10 April 2020, the company BioCryst Pharmaceuticals, Inc. announced that a clinical trial will be conducted in Brazil to evaluate the antiviral efficacy of Galidesivir (administered (iv) in patients with SARS-CoV-2 infection (NCT03891420).

The isobutyrate ester derivative **18** is the orally available prodrug of the ribonucleoside analogue **25** (β-D-N^4-hydroxycytidine, NHC, EIDD-1931) (Figure 22).

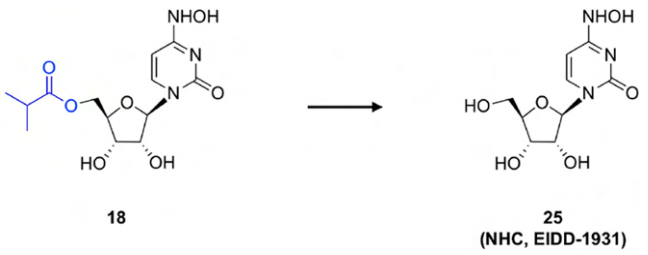

Figure 22. Chemical structures of the prodrug **18** and its parent compound **25**. The isobutyrate ester prodrug moiety is shown in blue.

Compound **25** is a broad-spectrum antiviral agent with *in vitro* activity against multiple unrelated viruses, including influenza, RSV, chikungunya virus, Ebola, Venezuelan equine encephalitis virus, and Eastern equine encephalitis virus.[98,143−146] In a recent study, **25** displayed potent antiviral activity in two cell lines infected with SARS-CoV-2, namely Vero cells, with EC_{50} = 0.3 μM and low toxicity (CC_{50} > 10 μM), as well as Calu3 cells, with EC_{50} = 0.08 μM (plaque assay). Moreover, **25** turned out to be active against SARS-CoV (average EC_{50} = 0.14 μM), MERS-CoV (average EC_{50} = 0.024 μM), and SARS-CoV-2 in HAE cultures[98] and shows remarkable potency against a model CoV mouse hepatitis virus (MHV) bearing resistance mutations to Remdesivir.[124] Thus, the lack of cross-resistance suggests that **25** and Remdesivir may select for exclusive and mutually sensitizing resistance pathways.[98] **25** was reported as a potent broad-spectrum inhibitor of respiratory viruses during a HTS campaign for influenza A virus (IAV) and RSV inhibitors. Derivative **25** was found to be active at concentrations in the nM to low-μM range and selectivity indices (SIs) of ≥89 against a broad panel of RSV, IAV, and IBV laboratory strains and isolates.[147] DMPK profiling for **25** demonstrated dose-dependent oral bioavailability of 56, 43, and 36% as well as $T_{1/2}$ of 5.2, 3.2, and 2.7 h following oral administration of 50, 150, and 500 mg/kg, respectively. The dose dependency of prodrug exposure was consistently observed in lung tissue, however, the peak of **25** triphosphate concentrations saturated above the oral dose levels of approximately 150 mg/kg, suggesting an anabolism bottleneck of **25** in mouse respiratory tissue at higher prodrug levels. Lung tissue distribution assessment revealed sustained levels of the active triphosphate anabolite of approximately 10 nmol/g for over 8 h after administration of 150 and 500 mg/kg. Compound **25** was also well tolerated after extended dosing at 800 mg/kg of body weight/day. While PK properties were good in rodents, oral bioavailability of **25** in cynomolgus macaques was limited. This liability led to the development of the prodrug **18**, a 5′-isobutyrate ester of **25**, which demonstrated good oral bioavailability in nonhuman primates. Upon intestinal absorption, **18** can be efficiently hydrolyzed to free **25**.[148]

Compound **18** has shown a significant reduction of the virus titer and ameliorated the pulmonary function in animal models of SARS-CoV and MERS-CoV infection.[98] In prophylactic efficacy studies, mice were administered **18** at doses of 50, 150, or 500 mg/kg by oral gavage 2 h before infection with SARS-CoV and MERS-CoV, and then every 12 h. At the dose of 500 mg/kg, the most complete protection from disease was observed, therefore the same dose was used for therapeutic efficacy studies for both viruses, with treatment starting 2 h before infection or 12, 24, or 48 h post infection (hpi). The overall results showed that early treatment with **18** provides higher clinical benefit, highlighting a window of 24 to 48 h within which to treat emerging CoV infection in mice before peak replication. The decrease of MERS-CoV yields both *in vitro* and *in vivo* were correlated with an increase of the frequency of mutation in the viral RNA but not in the host RNA, highlighting a putative mechanism of lethal mutagenesis. The interesting preclinical results, suggesting that **25**/**18** might be a promising clinical candidate, prompted the FDA and the UK Medicines and Healthcare Products Regulatory Agency to quickly give approval to initiate human safety testing. Inhibitor **18** has been evaluated in a phase I trial, recently completed (NCT04392219), whereas in late May, two phase II randomized, double-blind, placebo-controlled trials were activated to evaluate the antiviral efficacy of **18** in adults diagnosed with COVID-19 (NCT04405570, NCT04405739). To this aim, the Drug Innovation Ventures at Emory (DRIVE) LLC, which developed the drug, partnered with the biotech company Ridgeback Biotherapeutics LP and with Merck to advance **18** through clinical development and to optimize the drug's availability during the pandemic.

The structural information on CoV viral proteins available to date, evolving at unprecedented speed, has prompted a number of *in silico* studies attempting to provide new lead compounds or to repurpose known drugs as possible antiviral agents against SARS-CoV-2.[149,150] However, experimental validation of the findings from such studies is still missing.

So far, NIs reached the most advanced stages of development; even if the activity of the currently evaluated candidates could be improved by medicinal chemistry efforts, taking into account the wealth of structural information that become available. Conversely, NNIs have not yet been reported for SARS-CoV-2 and for other human pathogenic CoVs. NNIs generally show lower resistance barrier with respect to NI/

https://dx.doi.org/10.1021/acs.jmedchem.0c01140
J. Med. Chem. 2022, 65, 2716−2746

NTP and are characterized by drug-like heterocyclic scaffold; thus, the identification of such agents may offer the advantage to handle molecules with higher optimization potential. However, no allosteric sites have been mapped on the RdRp protein surface for CoVs. Because viral RdRp shows the typical 3D right-hand shape, organized in palm, thumb, and fingers subdomains, the knowledge acquired on other RNA virus polymerase may allow similar considerations also for CoVs RdRp. In this regard, the best characterized viral RdRp is HCV NS5B that, despite working in absence of a primer in cell environment, shows four distinct binding sites for different classes of NNIs that are able to allosterically modulate the enzyme.[151] A very large number of inhibitors, specifically binding one of these sites, have been reported, with some of them reaching late stages of clinical trials and also approval (for instance, Dasabuvir).

The integrated computational and experimental analysis of the nsp12 surface may point toward the discovery of potential allosteric sites. The functional replicase complex requires the tight association of nsp12 with cofactors nsp7 and nsp8, as shown by cryo-EM, therefore these interfaces could represent druggable sites to be explored.

CONCLUDING REMARKS

Concurrent to the pandemic outbreak of the SARS-CoV-2 infection, the scientific community in collaboration with private and public funding organizations, started an unprecedented task force to find effective antiviral agents to stop the COVID-19 crisis. Impressive efforts in molecular biology, biochemistry, and structural biology of SARS-CoV-2 have indeed provided in a very short time a huge amount of data. Both biochemical assays and 3D structures have been made public for several viral and host proteins, whereas newly developed phenotypic screenings might allow rapid identification of alternative molecular targets and antiviral compounds.

The knowledge acquired in the past years on other human pathogenic CoVs, such as SARS-CoV and MERS-CoV, to cite a few, can accelerate COVID-19 drug discovery. Considering the information available to date, $3CL^{pro}$ and nsp12 RdRp are among the most characterized SARS-CoV-2 targets, from both a structural and biochemical perspective, prompting the discovery of specific inhibitors as promising anti-CoV agents. Moreover, $3CL^{pro}$ and nsp12 RdRp show the highest degree of conservation across different CoVs, with 96% sequence identity between the SARS-CoV-2 and the SARS-CoV proteins, thus fostering the identification of broad-spectrum inhibitors.

At a glance, NIs targeting the nsp12 RdRp appear to be the most advanced candidates in the therapeutic arsenal for COVID-19 treatment. Indeed, the broad-spectrum viral RdRp inhibitor Remdesivir has received EUA for the treatment of patients diagnosed with COVID-19, being approved as the first specific antiviral drug. Remdesivir is iv administered, and this can be considered a main drawback limiting a fast large-scale production and forcing its use in hospital setting. To overcome this hurdle, an inhalation formulation is currently under evaluation in phase I clinical trials. The second most advanced NI is the orally available derivative **18**, namely the 5-isobutyrate ester of **25**, acting as a broad RdRp inhibitor that could be administered outside of a clinical setting. Both **18** and **25** showed interesting preclinical results against CoVs in *in vitro*/*in vivo* models; thus, a phase I trial started in mid-April and two phase II randomized, double-blind, placebo-controlled trials launched in late May are currently ongoing. The findings collected from both clinical and preclinical studies highlight that these drugs should be administered as early as possible after infection, as they might not be as effective in the later stages of the disease. Notably, these are the most advanced compounds coming from repurposing of molecules already profiled for other viruses, indicating that there is still room for the identification and development of further CoV RdRp inhibitors. In fact, on the basis of the experience with other viral polymerases, an alternative route to NIs would be represented by the discovery of NNIs. Such an approach would require the identification of allosteric pockets, which, however, have not been validated so far, although many efforts are ongoing in this direction. The NNIs have several advantages comparable to the NIs, particularly the higher chemical diversity and likely po administration. A major drawback of these compounds could be instead the low genetic barrier for resistance and narrow-spectrum activity, as previously found for NNIs targeting other viruses such as HIV-1 and HCV.

The second most studied essential viral target is the $3CL^{pro}$. This protease shows a unique substrate sequence specificity for Gln-Leu as P1−P2 and maintains an overall high degree of conservation across the CoV genus. Remarkably, the considerable amount of data generated on other human pathogenic CoVs together with the available structural data on SARS-CoV-2 $3CL^{pro}$ enable SBDD of novel inhibitors of this enzyme. In the initial effort to identify $3CL^{pro}$ inhibitors, several research groups are mainly focusing on the development of peptidic covalent and covalent reversible inhibitors. However, the inhibitors reported so far do not significantly deviate from the sequence specificity, showing only small differences in P3/P4. The most relevant examples are the indole dipeptide derivatives with an aldehyde and ketone-based warheads, with compounds **5** and **8** resulting in the leading SARS-CoV-2 $3CL^{pro}$ inhibitors. Interestingly, these molecules are endowed with nM potency against the isolated target and in cell-based assays that are coupled to promising *in vivo* DMPK and safety properties. However, the efficacy of derivatives **5** and **8** in animal models are still unknown. It is worth noting that the prodrug of compound **8**, *i.e.*, its phosphate ester **9**, has been reported as a suitable clinical candidate for iv administration, advanced into a phase Ib clinical trial. The additive/synergistic antiviral effect observed *in vitro* for the combination of **8** plus Remdesivir represents a promising result to plan possible multidrug regimen.

Nonetheless, so far, there is no report describing peptidic inhibitors of CoVs $3CL^{pro}$ that are orally available, an important feature required for the domestic management of a widespread infection such as COVID-19. Through additional approaches, such as fragment screenings and HTS of libraries of approved and investigational drugs, Bacalein, a flavone derivative widely employed in traditional Chinese medicine, has been described in a preprint as noncovalent active site inhibitor of $3CL^{pro}$, as shown by X-ray crystallography, able to selectively inhibit SARS-CoV-2 replication in cells. Due to the stage of the development of such molecules, it is, however, clear that current $3CL^{pro}$ inhibitors cannot be considered a near-term strategy to tackle COVID-19, although they represent a suitable starting point for lead optimization programs.

Finally, another putative emerging target is the PL^{pro}, which is nevertheless a more challenging and underexplored protein

https://dx.doi.org/10.1021/acs.jmedchem.0c01140
J. Med. Chem. 2022, 65, 2716−2746

Table 2. List of All the Compounds, Including Repurposed Drugs, Discussed in the Text

compd	target	phase	clinical trial ID	refs
1	$3CL^{pro}$	preclinical		40,51,52
2	$3CL^{pro}$	preclinical		42
3	$3CL^{pro}$	preclinical		35
4	$3CL^{pro}$	preclinical		35
5	$3CL^{pro}$	preclinical		55
6	$3CL^{pro}$	preclinical		55
7 (GC376)	$3CL^{pro}$	preclinical		43,56,57,59,60
8	$3CL^{pro}$	preclinical		71
9	$3CL^{pro}$	Ib	NCT04535167	72
Boceprevir	$3CL^{pro}$	preclinical[a]		47,59
Baicalein	$3CL^{pro}$	preclinical[b]		76
Baicalin	$3CL^{pro}$	preclinical[c]		76
10	$3CL^{pro}$	preclinical		
11	PL^{pro}	preclinical		87
12	PL^{pro}	preclinical		87
Ebselen	$3CL^{pro}$ PL^{pro}	preclinical[d]		40,88
13	PL^{pro}	preclinical		89
14	PL^{pro}	preclinical		89
15	PL^{pro}	preclinical		89
16	PL^{pro}	preclinical		89
17	PL^{pro}	preclinical		91,92
Remdesivir	RdRp	FDA approved[12]	NCT04292899, NCT04280705	109,110
Favipiravir	RdRp	III[e]	ChiCTR2000030254	135
Galidesivir	RdRp	I	NCT03891420	141,142
18 (EIDD-2801)	RdRp	II	NCT04405570, NCT04405739	98,143−146

[a]Marketed for HCV. [b]Phase II for influenza fever (NCT03830684). [c]Phase I as an ingredient of Moist Exposed Burn Ointment (MEBO) for the treatment of pain and re-epithelization (NCT03728244, NCT02737943). [d]Phase II for brain disorders. [e]Marketed for influenza virus infections.

for the identification of inhibitors. Furthermore, this protease is less conserved across the CoVs family, and for this reason it may be less attractive in view of possible future CoV outbreaks.

A summary table reporting all inhibitors for each of the three targets, with references and the current stage of development, is provided (Table 2).

The current scenario has emphasized that CoV infection coming from the spillover such as MERS, SARS-CoV, and SARS-CoV-2 could benefit from broad-spectrum antivirals, which today is still an unmet necessity. Therefore, stimulating research efforts toward this direction is of pivotal importance in order to face potential future pandemics.

Looking at the current panorama, the drug repurposing approach identified one approved drug, Remdesivir, and a covalent inhibitor with the hydroxyl methylketone prodrug, which entered in phase I. Other compounds are under investigation but lagging behind in their development, and there is no certainty that they will conclude the process. Instead, the structural information acquired on the targets will be of great inspiration for the medicinal chemists that will design *ad hoc* molecules, especially for the proteases where this approach has been successful for other viral infections. The antiviral approach put in place for this emergency will also be very important for future pandemics.

■ ASSOCIATED CONTENT

Supporting Information

The Supporting Information is available free of charge at https://pubs.acs.org/doi/10.1021/acs.jmedchem.0c01140.

Chemical structure of Rupintrivir; additional repurposed $3CL^{pro}$ inhibitors reported in ref 40 of main text (PDF)

■ AUTHOR INFORMATION

Corresponding Author

Vincenzo Summa − *Department of Pharmacy, University of Naples "Federico II", 80131 Napoli, Italy;* orcid.org/0000-0002-6288-2681; Phone: +39 081-678656; Email: vincenzo.summa@unina.it

Authors

Rolando Cannalire − *Department of Pharmacy, University of Naples "Federico II", 80131 Napoli, Italy*

Carmen Cerchia − *Department of Pharmacy, University of Naples "Federico II", 80131 Napoli, Italy*

Andrea R. Beccari − *Dompé Farmaceutici SpA, 67100 L'Aquila, Italy*

Francesco Saverio Di Leva − *Department of Pharmacy, University of Naples "Federico II", 80131 Napoli, Italy*

Complete contact information is available at: https://pubs.acs.org/10.1021/acs.jmedchem.0c01140

Author Contributions

R.C. and C.C. contributed equally. The manuscript was written through contributions of all authors. All authors have given approval to the final version of the manuscript.

Notes

The authors declare no competing financial interest.

Biographies

Rolando Cannalire received his Ph.D. in Chemistry and Technology of Drug (curriculum Medicinal Chemistry) at the University of Perugia in 2016, under the supervision of Prof. V. Cecchetti. During his Ph.D. course, he spent research periods in the laboratories of Prof. M. Viveiros at Universidade Nova de Lisboa (Portugal) and of Prof. S.

https://dx.doi.org/10.1021/acs.jmedchem.0c01140
J. Med. Chem. 2022, 65, 2716−2746

Otto at University of Groningen (Netherlands). From 2016 to mid-2019, he held Postdoctoral Fellowships at the Department of Pharmaceutical Sciences of the University of Perugia. Since May 2019, he has been appointed Assistant Professor at the Department of Pharmacy of the University of Naples Federico II. His main research interests concern the design and synthesis of antiviral (mainly RNA viruses) and antibacterial small molecules, antitumor agents, kinase inhibitors, and development of innovative synthetic methodologies.

Carmen Cerchia obtained the Ph.D. in Pharmaceutical Sciences in 2016 at the Department of Pharmacy, University of Naples Federico II, under the supervision of Prof. Antonio Lavecchia. She then joined the group of Prof. Jürgen Bajorath at the Department of Life Science Informatics, B-IT, Rheinische Friedrich-Wilhelms-Universität, Bonn, for one year, as visiting researcher. She is currently a Postdoctoral Fellow at the Department of Pharmacy, University of Naples Federico II. Her research interests are in the field of drug discovery and computational chemistry, in particular, large-scale compound data mining and virtual screening methodologies applied to biological targets involved in cancer and metabolic diseases.

Andrea Beccari is currently responsible for the Business Unit EXSCALATE. He started his career as drug designer in a pharmaceutical company in The Netherlands. Back in Italy, first, he led the drug discovery programs and then also became responsible of the technological platform. He has developed, in the last 10 years, proprietary computational tools now all integrated in the EXSCALATE platform. He was promoter and coordinator of the Italian Drug Discovery Network and cofounder and member of the board of the Avicenna Alliance (Brussel). He was originator and chairman of the Computational Driven Drug Discovery series of meetings. He has co-organized several initiatives with the European commission and parliament promoting the use of in silico simulations to increase the awareness towards the potentiality of high performance computing in healthcare.

Francesco Saverio Di Leva received his Ph.D. in Drug Discovery from the Italian Institute of Technology in Genoa (Italy) under the Supervision of Prof. Andrea Cavalli. During his Ph.D. course, he spent 18 months in the laboratories of Prof. Michele Parrinello at USI Lugano (Switzerland). From 2014 to 2017, he held a Postdoctoral Fellowship at the Department of Pharmacy of the University of Naples Federico II, where he is Assistant Professor since December 2017. He has been awarded with the Medicinal Chemistry Division Prize 2020 of the Italian Chemical Society. His research interests focus on the identification, through bioinformatic methodologies and biosimulations, of either therapeutic or diagnostic agents for cancer and for the treatment of infectious and metabolic diseases.

Vincenzo Summa obtained the Ph.D. in Organic Chemistry from the University of Wuppertal. In 1996, he joined Merck Research Laboratory—Italy (IRBM). He served as Director in the Medicinal Chemistry Department, leading the team that discovered Isentress, the first-in-class HIV integrase inhibitor (Galien Prize USA and Italy for the best pharmaceutical agent—2008), and Grazoprevir, a pangenotype HCV protease inhibitor. For the discovery of Isentress and Grazoprevir, he was awarded as Hero of Chemistry from ACS in 2013 and 2017, respectively. In 2009, he became a cofounder of IRBM Science Park, the spinoff of Merck Research Laboratory—Italy, and Vice President of Drug Discovery. Since 2019, he is full Professor of Medicinal Chemistry at the Department of Pharmacy, University of Naples Federico II. His research interests focus on identification of anti-infectious and anticancer agents.

■ ACKNOWLEDGMENTS

R.C. acknowledges MIUR-Ministero dell'Istruzione, dell'Università e della Ricerca (Italian Ministry of Education, University and Research), PON R&I 2014-2020-AIM (Attraction and International Mobility), project AIM1873131, Num. Attività 2, Linea 2.1. This research was conducted under the project "EXaSCale smArt pLatform Against paThogEns for Corona Virus—Exscalate4CoV" founded by the EU's H2020-SC1-PHE-CORONAVIRUS-2020 call, grant no. 101003551.

■ ABBREVIATIONS USED

3CL^{pro}, 3-chymotrypsin-like protease; ACE2, angiotensin-converting enzyme II; CatB/L, cathepsinsB/L; CD, circular dichroism; CoV, coronavirus; COVID-19, coronavirus disease 2019; CPE, cytopathic effect; E, envelope protein; EVD, Ebola virus disease; EVs, enteroviruses; FIP, feline infectious peritonitis; HAE, human airway epithelial cells; HCoV, human coronavirus; HCV, hepatitis C virus; HIV, human immune deficiency virus; hpi, hours post infection; hPIV3, parainfluenza type 3 virus; HRV, human rhinovirus; HTS, high-throughput screen; IAV, influenza A virus; MERS, Middle East respiratory syndrome; SARS, severe acute respiratory syndrome; MERS-CoV, Middle East respiratory syndrome coronavirus; MHV, mouse hepatitis virus; N, nucleocapsid protein; NIAID, National Institute of Allergy and Infectious Diseases; Nsp, nonstructural proteins; ORF, open reading frame; PL^{pro}, papain-like protease; PPIs, protein−protein interactions; RBD, receptor-binding domain; RdRp, RNA-dependent RNA polymerase; RSV, respiratory syncytial virus; RTC, replicase/transcriptase complex; S, spike protein; SARS-CoV, severe acute respiratory syndrome coronavirus; SARS-CoV-2, severe acute respiratory syndrome coronavirus 2; SBDD, structure-based drug design; SPR, surface plasmon resonance; TM, transmembrane domain; TMPRSS2, transmembrane protease serine 2; UTR, untranslated regions; WHO, World Health Organization

■ REFERENCES

(1) *Ten Threats to Global Health in 2019*; World Health Organization, 2019; https://www.who.int/emergencies/ten-threats-to-global-health-in-2019 (accessed 2020-09-28).
(2) *Prioritizing Diseases for Research and Development in Emergency Contexts*; World Health Organization, 2020; https://www.who.int/activities/prioritizing-diseases-for-research-and-development-in-emergency-context (accessed 2020-09-28).
(3) Wu, F.; Zhao, S.; Yu, B.; Chen, Y. M.; Wang, W.; Song, Z. G.; Hu, Y.; Tao, Z. W.; Tian, J. H.; Pei, Y. Y.; Yuan, M. L.; Zhang, Y. L.; Dai, F. H.; Liu, Y.; Wang, Q. M.; Zheng, J. J.; Xu, L.; Holmes, E. C.; Zhang, Y. Z. A New Coronavirus Associated with Human Respiratory Disease in China. *Nature* **2020**, *579*, 265−269.
(4) Zhu, N.; Zhang, D.; Wang, W.; Li, X.; Yang, B.; Song, J.; Zhao, X.; Huang, B.; Shi, W.; Lu, R.; Niu, P.; Zhan, F.; Ma, X.; Wang, D.; Xu, W.; Wu, G.; Gao, G. F.; Tan, W. A Novel Coronavirus from Patients with Pneumonia in China, 2019. *N. Engl. J. Med.* **2020**, *382*, 727−733.
(5) *Coronavirus (COVID-19) Events As They Happen*; World Health Organisation, 2019; https://www.who.int/emergencies/diseases/novel-coronavirus-2019/events-as-they-happen (accessed 2020-09-28).
(6) Riddle, M. S.; Connor, B. A.; Beeching, N. J.; DuPont, H. L.; Hamer, D. H.; Kozarsky, P.; Libman, M.; Steffen, R.; Taylor, D.; Tribble, D. R.; Vila, J.; Zanger, P.; Ericsson, C. D. 2020 Hubei Lockdowns. *J. Travel Med.* **2020**, *24*, S63.

https://dx.doi.org/10.1021/acs.jmedchem.0c01140
J. Med. Chem. 2022, 65, 2716−2746

(7) Saglietto, A.; D'Ascenzo, F.; Zoccai, G. B.; De Ferrari, G. M. COVID-19 in Europe: The Italian Lesson. *Lancet* **2020**, *395*, 1110−1111.
(8) Remuzzi, A.; Remuzzi, G. COVID-19 and Italy: What Next? *Lancet* **2020**, *395*, 1225−1228.
(9) Lewnard, J. A.; Lo, N. C. Scientific and Ethical Basis for Social-Distancing Interventions against COVID-19. *Lancet Infect. Dis.* **2020**, *20*, 631−633.
(10) Pushpakom, S.; Iorio, F.; Eyers, P. A.; Escott, K. J.; Hopper, S.; Wells, A.; Doig, A.; Guilliams, T.; Latimer, J.; McNamee, C.; Norris, A.; Sanseau, P.; Cavalla, D.; Pirmohamed, M. Drug Repurposing: Progress, Challenges and Recommendations. *Nat. Rev. Drug Discovery* **2019**, *18*, 41−58.
(11) Alpern, J. D.; Gertner, E. Off-Label Therapies for COVID-19—Are We All In This Together? *Clin. Pharmacol. Ther.* **2020**, *108*, 182−184.
(12) *Remdesivir Emergency Use Authorization*; Gilead Sciences, Inc., 2020; https://www.gilead.com/-/media/files/pdfs/remdesivir/eua-fda-authorization-letter_01may2020-old.pdf?la=en&hash=2AE25800C7C9612D2F67F28D3F3B9921 (accessed 2020-08-09).
(13) Goldman, J. D.; Lye, D. C. B.; Hui, D. S.; Marks, K. M.; Bruno, R.; Montejano, R.; Spinner, C. D.; Galli, M.; Ahn, M.-Y.; Nahass, R. G.; Chen, Y.-S.; SenGupta, D.; Hyland, R. H.; Osinusi, A. O.; Cao, H.; Blair, C.; Wei, X.; Gaggar, A.; Brainard, D. M.; Towner, W. J.; Muñoz, J.; Mullane, K. M.; Marty, F. M.; Tashima, K. T.; Diaz, G.; Subramanian, A. Remdesivir for 5 or 10 Days in Patients with Severe Covid-19. *N. Engl. J. Med.* **2020**, DOI: 10.1056/NEJMoa2015301.
(14) Dolin, R.; Hirsch, M. S. Remdesivir — An Important First Step. *N. Engl. J. Med.* **2020**, DOI: 10.1056/NEJMe2018715.
(15) Beigel, J. H.; Tomashek, K. M.; Dodd, L. E.; Mehta, A. K.; Zingman, B. S.; Kalil, A. C.; Hohmann, E.; Chu, H. Y.; Luetkemeyer, A.; Kline, S.; Lopez de Castilla, D.; Finberg, R. W.; Dierberg, K.; Tapson, V.; Hsieh, L.; Patterson, T. F.; Paredes, R.; Sweeney, D. A.; Short, W. R.; Touloumi, G.; Lye, D. C.; Ohmagari, N.; Oh, M.; Ruiz-Palacios, G. M.; Benfield, T.; Fätkenheuer, G.; Kortepeter, M. G.; Atmar, R. L.; Creech, C. B.; Lundgren, J.; Babiker, A. G.; Pett, S.; Neaton, J. D.; Burgess, T. H.; Bonnett, T.; Green, M.; Makowski, M.; Osinusi, A.; Nayak, S.; Lane, H. C. Remdesivir for the Treatment of Covid-19 — Final Report. *N. Engl. J. Med.* **2020**, DOI: 10.1056/NEJMoa2007764.
(16) Vacca, J. Antiviral Drug Discovery and Development. *Nat. Rev. Drug Discovery* **2007**, *6*, 1019−1019.
(17) Everts, M.; Cihlar, T.; Bostwick, J. R.; Whitley, R. J. Accelerating Drug Development: Antiviral Therapies for Emerging Viruses as a Model. *Annu. Rev. Pharmacol. Toxicol.* **2017**, *57*, 155−169.
(18) Liu, C.; Zhou, Q.; Li, Y.; Garner, L. V.; Watkins, S. P.; Carter, L. J.; Smoot, J.; Gregg, A. C.; Daniels, A. D.; Jervey, S.; Albaiu, D. Research and Development on Therapeutic Agents and Vaccines for COVID-19 and Related Human Coronavirus Diseases. *ACS Cent. Sci.* **2020**, *6*, 315−331.
(19) Gil, C.; Ginex, T.; Maestro, I.; Nozal, V.; Barrado-Gil, L.; Cuesta-Geijo, M. Á.; Urquiza, J.; Ramírez, D.; Alonso, C.; Campillo, N. E.; Martinez, A. COVID-19: Drug Targets and Potential Treatments. *J. Med. Chem.* **2020**, DOI: 10.1021/acs.jmedchem.0c00606.
(20) Chan, J. F. W.; Kok, K. H.; Zhu, Z.; Chu, H.; To, K. K. W.; Yuan, S.; Yuen, K. Y. Genomic Characterization of the 2019 Novel Human-Pathogenic Coronavirus Isolated from a Patient with Atypical Pneumonia after Visiting Wuhan. *Emerging Microbes Infect.* **2020**, *9*, 221−236.
(21) Cui, J.; Li, F.; Shi, Z. L. Origin and Evolution of Pathogenic Coronaviruses. *Nat. Rev. Microbiol.* **2019**, *17*, 181−192.
(22) Sanche, S.; Lin, Y. T.; Xu, C.; Romero-Severson, E.; Hengartner, N.; Ke, R. RESEARCH High Contagiousness and Rapid Spread of Severe Acute Respiratory Syndrome Coronavirus 2. *Emerging Infect. Dis.* **2020**, *26*, 1470−1477.
(23) Shereen, M. A.; Khan, S.; Kazmi, A.; Bashir, N.; Siddique, R. COVID-19 Infection: Origin, Transmission, and Characteristics of Human Coronaviruses. *J. Adv. Res.* **2020**, *24*, 91−98.
(24) Fehr, A. R.; Perlman, S. Coronaviruses: An Overview of Their Replication and Pathogenesis. In *Coronaviruses: Methods and Protocols*; Springer: New York, 2015; Vol. *1282*, pp 1−23.
(25) Loganathan, S. K.; Schleicher, K.; Malik, A.; Quevedo, R.; Langille, E.; Teng, K.; Oh, R. H.; Rathod, B.; Tsai, R.; Samavarchi-Tehrani, P.; Pugh, T. J.; Gingras, A. C.; Schramek, D. Rare Driver Mutations in Head and Neck Squamous Cell Carcinomas Converge on NOTCH Signaling. *Science* **2020**, *367*, 1264−1269.
(26) Hoffmann, M.; Kleine-Weber, H.; Schroeder, S.; Krüger, N.; Herrler, T.; Erichsen, S.; Schiergens, T. S.; Herrler, G.; Wu, N. H.; Nitsche, A.; Müller, M. A.; Drosten, C.; Pöhlmann, S. SARS-CoV-2 Cell Entry Depends on ACE2 and TMPRSS2 and Is Blocked by a Clinically Proven Protease Inhibitor. *Cell* **2020**, *181*, 271−280. e8.
(27) Wrapp, D.; Wang, N.; Corbett, K. S.; Goldsmith, J. A.; Hsieh, C. L.; Abiona, O.; Graham, B. S.; McLellan, J. S. Cryo-EM Structure of the 2019-NCoV Spike in the Prefusion Conformation. *Science* **2020**, *367*, 1260−1263.
(28) Wang, Q.; Zhang, Y.; Wu, L.; Niu, S.; Song, C.; Zhang, Z.; Lu, G.; Qiao, C.; Hu, Y.; Yuen, K. Y.; Wang, Q.; Zhou, H.; Yan, J.; Qi, J. Structural and Functional Basis of SARS-CoV-2 Entry by Using Human ACE2. *Cell* **2020**, *181*, 894−904. e9.
(29) Lan, J.; Ge, J.; Yu, J.; Shan, S.; Zhou, H.; Fan, S.; Zhang, Q.; Shi, X.; Wang, Q.; Zhang, L.; Wang, X. Structure of the SARS-CoV-2 Spike Receptor-Binding Domain Bound to the ACE2 Receptor. *Nature* **2020**, *581*, 215−220.
(30) Xiu, S.; Dick, A.; Ju, H.; Mirzaie, S.; Abdi, F.; Cocklin, S.; Zhan, P.; Liu, X. Inhibitors of SARS-CoV-2 Entry: Current and Future Opportunities. *J. Med. Chem.* **2020**, DOI: 10.1021/acs.jmedchem.0c00502.
(31) Cannalire, R.; Stefanelli, I.; Cerchia, C.; Beccari, A. R.; Pelliccia, S.; Summa, V. Sars-Cov-2 Entry Inhibitors: Small Molecules and Peptides Targeting Virus or Host Cells. *Int. J. Mol. Sci.* **2020**, *21*, 5707.
(32) Zhao, L.; Jha, B. K.; Wu, A.; Elliott, R.; Ziebuhr, J.; Gorbalenya, A. E.; Silverman, R. H.; Weiss, S. R. Antagonism of the Interferon-Induced OAS-RNase L Pathway by Murine Coronavirus Ns2 Protein Is Required for Virus Replication and Liver Pathology. *Cell Host Microbe* **2012**, *11*, 607−616.
(33) Freitas, B. T.; Durie, I. A.; Murray, J.; Longo, J. E.; Miller, H. C.; Crich, D.; Hogan, R. J.; Tripp, R. A.; Pegan, S. D. Characterization and Noncovalent Inhibition of the Deubiquitinase and DeISGylase Activity of SARS-CoV-2 Papain-Like Protease. *ACS Infect. Dis.* **2020**, *6*, 2099−2109.
(34) Nakagawa, K.; Lokugamage, K. G.; Makino, S. Viral and Cellular MRNA Translation in Coronavirus-Infected Cells. In *Advances in Virus Research*; Academic Press, 2016; Vol. *96*, pp 165−192.
(35) Zhang, L.; Lin, D.; Sun, X.; Curth, U.; Drosten, C.; Sauerhering, L.; Becker, S.; Rox, K.; Hilgenfeld, R. Crystal Structure of SARS-CoV-2 Main Protease Provides a Basis for Design of Improved a-Ketoamide Inhibitors. *Science* **2020**, *368*, 409−412.
(36) Tan, J.; Verschueren, K. H. G.; Anand, K.; Shen, J.; Yang, M.; Xu, Y.; Rao, Z.; Bigalke, J.; Heisen, B.; Mesters, J. R.; Chen, K.; Shen, X.; Jiang, H.; Hilgenfeld, R. PH-Dependent Conformational Flexibility of the SARS-CoV Main Proteinase (Mpro) Dimer: Molecular Dynamics Simulations and Multiple X-Ray Structure Analyses. *J. Mol. Biol.* **2005**, *354*, 25−40.
(37) Fan, K.; Wei, P.; Feng, Q.; Chen, S.; Huang, C.; Ma, L.; Lai, B.; Pei, J.; Liu, Y.; Chen, J.; Lai, L. Biosynthesis, Purification, and Substrate Specificity of Severe Acute Respiratory Syndrome Coronavirus 3C-like Proteinase. *J. Biol. Chem.* **2004**, *279*, 1637−1642.
(38) Shi, J.; Wei, Z.; Song, J. Dissection Study on the Severe Acute Respiratory Syndrome 3C-like Protease Reveals the Critical Role of the Extra Domain in Dimerization of the Enzyme. Defining the Extra Domain as a New Target for Design of Highly Specific Protease Inhibitors. *J. Biol. Chem.* **2004**, *279*, 24765−24773.

(39) Chen, C. N.; Lin, C. P. C.; Huang, K. K.; Chen, W. C.; Hsieh, H. P.; Liang, P. H.; Hsu, J. T. A. Inhibition of SARS-CoV 3C-like Protease Activity by Theaflavin-3,3′- Digallate (TF3). *Evidence-based Complement. Altern. Med.* **2005**, *2*, 209−215.
(40) Jin, Z.; Du, X.; Xu, Y.; Deng, Y.; Liu, M.; Zhao, Y.; Zhang, B.; Li, X.; Zhang, L.; Peng, C.; Duan, Y.; Yu, J.; Wang, L.; Yang, K.; Liu, F.; Jiang, R.; Yang, X.; You, T.; Liu, X.; Yang, X.; Bai, F.; Liu, H.; Liu, X.; Guddat, L. W.; Xu, W.; Xiao, G.; Qin, C.; Shi, Z.; Jiang, H.; Rao, Z.; Yang, H. Structure of Mpro from SARS-CoV-2 and Discovery of Its Inhibitors. *Nature* **2020**, *582*, 289−293.
(41) Rut, W.; Groborz, K.; Zhang, L.; Sun, X.; Zmudzinski, M.; Hilgenfeld, R.; Drag, M. Substrate Specificity Profiling of SARS-CoV-2 Mpro Protease Provides Basis for Anti-COVID-19 Drug Design. *bioRxiv* **2020**, DOI: 10.1101/2020.03.07.981928.
(42) Zhang, L.; Lin, D.; Kusov, Y.; Nian, Y.; Ma, Q.; Wang, J.; Von Brunn, A.; Leyssen, P.; Lanko, K.; Neyts, J.; De Wilde, A.; Snijder, E. J.; Liu, H.; Hilgenfeld, R. α-Ketoamides as Broad-Spectrum Inhibitors of Coronavirus and Enterovirus Replication: Structure-Based Design, Synthesis, and Activity Assessment. *J. Med. Chem.* **2020**, *63*, 4562−4578.
(43) Kim, Y.; Lovell, S.; Tiew, K.-C.; Mandadapu, S. R.; Alliston, K. R.; Battaile, K. P.; Groutas, W. C.; Chang, K.-O. Broad-Spectrum Antivirals against 3C or 3C-Like Proteases of Picornaviruses, Noroviruses, and Coronaviruses. *J. Virol.* **2012**, *86*, 11754−11762.
(44) Hayden, F. G.; Turner, R. B.; Gwaltney, J. M.; Chi-Burris, K.; Gersten, M.; Hsyu, P.; Patick, A. K.; Smith, G. J.; Zalman, L. S. Phase II, Randomized, Double-Blind, Placebo-Controlled Studies of Ruprintrivir Nasal Spray 2-Percent Suspension for Prevention and Treatment of Experimentally Induced Rhinovirus Colds in Healthy Volunteers. *Antimicrob. Agents Chemother.* **2003**, *47*, 3907−3916.
(45) Pillaiyar, T.; Manickam, M.; Namasivayam, V.; Hayashi, Y.; Jung, S. H. An Overview of Severe Acute Respiratory Syndrome-Coronavirus (SARS-CoV) 3CL Protease Inhibitors: Peptidomimetics and Small Molecule Chemotherapy. *J. Med. Chem.* **2016**, *59*, 6595−6628.
(46) Kwong, A. D.; Kauffman, R. S.; Hurter, P.; Mueller, P. Discovery and Development of Telaprevir: An NS3−4A Protease Inhibitor for Treating Genotype 1 Chronic Hepatitis C Virus. *Nat. Biotechnol.* **2011**, *29*, 993−1003.
(47) Venkatraman, S.; Bogen, S. L.; Arasappan, A.; Bennett, F.; Chen, K.; Jao, E.; Liu, Y. T.; Lovey, R.; Hendrata, S.; Huang, Y.; Pan, W.; Parekh, T.; Pinto, P.; Popov, V.; Pike, R.; Ruan, S.; Santhanam, B.; Vibulbhan, B.; Wu, W.; Yang, W.; Kong, J.; Liang, X.; Wong, J.; Liu, R.; Butkiewicz, N.; Chase, R.; Hart, A.; Agrawal, S.; Ingravallo, P.; Pichardo, J.; Kong, R.; Baroudy, B.; Malcolm, B.; Guo, Z.; Prongay, A.; Madison, V.; Broske, L.; Cui, X.; Cheng, K. C.; Hsieh, Y.; Brisson, J. M.; Prelusky, D.; Korfmacher, W.; White, R.; Bogdanowich-Knipp, S.; Pavlovsky, A.; Bradley, P.; Saksena, A. K.; Ganguly, A.; Piwinski, J.; Girijavallabhan, V.; Njoroge, F. G. Discovery of (1R,5S)-N-[3-Amino-1-(Cyclobutylmethyl)-2,3-Dioxopropyl]-3- [2(S)-[[[(1,1-Dimethylethyl)Amino]Carbonyl]Amino]-3,3-Dimethyl-1-Oxobutyl]-6, 6-Dimethyl-3-Azabicyclo[3.1.0]Hexan-2(S)-Carboxamide (SCH 503034), a Selective, Potent, Orally Bioavaila. *J. Med. Chem.* **2006**, *49*, 6074−6086.
(48) Boggild, M. K.; Gajic-Veljanoski, O.; McDonald-Blumer, H.; Ridout, R.; Tile, L.; Josse, R.; Cheung, A. M. Odanacatib for the Treatment of Osteoporosis. *Expert Opin. Pharmacother.* **2015**, *16*, 1717−1726.
(49) Liang, R.; Wang, L.; Zhang, N.; Deng, X.; Su, M.; Su, Y.; Hu, L.; He, C.; Ying, T.; Jiang, S.; Yu, F. Development of Small-Molecule MERS-CoV Inhibitors. *Viruses* **2018**, *10*, 721.
(50) Hilgenfeld, R. From SARS to MERS: Crystallographic Studies on Coronaviral Proteases Enable Antiviral Drug Design. *FEBS J.* **2014**, *281*, 4085−4096.
(51) Wang, F.; Chen, C.; Tan, W.; Yang, K.; Yang, H. Structure of Main Protease from Human Coronavirus NL63: Insights for Wide Spectrum Anti-Coronavirus Drug Design. *Sci. Rep.* **2016**, *6*, 22677.
(52) Ren, Z.; Yan, L.; Zhang, N.; Guo, Y.; Yang, C.; Lou, Z.; Rao, Z. The Newly Emerged SARS-Like Coronavirus HCoV-EMC Also Has an "Achilles" Heel": Current Effective Inhibitor Targeting a 3C-like Protease. *Protein Cell* **2013**, *4*, 248−250.
(53) Xue, X.; Yu, H.; Yang, H.; Xue, F.; Wu, Z.; Shen, W.; Li, J.; Zhou, Z.; Ding, Y.; Zhao, Q.; Zhang, X. C.; Liao, M.; Bartlam, M.; Rao, Z. Structures of Two Coronavirus Main Proteases: Implications for Substrate Binding and Antiviral Drug Design. *J. Virol.* **2008**, *82*, 2515−2527.
(54) Yang, H.; Xie, W.; Xue, X.; Yang, K.; Ma, J.; Liang, W.; Zhao, Q.; Zhou, Z.; Pei, D.; Ziebuhr, J.; Hilgenfeld, R.; Yuen, K. Y.; Wong, L.; Gao, G.; Chen, S.; Chen, Z.; Ma, D.; Bartlam, M.; Rao, Z. Design of Wide-Spectrum Inhibitors Targeting Coronavirus Main Proteases. *PLoS Biol.* **2005**, *3*, e324.
(55) Dai, W.; Zhang, B.; Jiang, X. M.; Su, H.; Li, J.; Zhao, Y.; Xie, X.; Jin, Z.; Peng, J.; Liu, F.; Li, C.; Li, Y.; Bai, F.; Wang, H.; Cheng, X.; Cen, X.; Hu, S.; Yang, X.; Wang, J.; Liu, X.; Xiao, G.; Jiang, H.; Rao, Z.; Zhang, L. K.; Xu, Y.; Yang, H.; Liu, H. Structure-Based Design of Antiviral Drug Candidates Targeting the SARS-CoV-2 Main Protease. *Science* **2020**, *368*, 1331−1335.
(56) Ma, C.; Sacco, M. D.; Hurst, B.; Townsend, J. A.; Hu, Y.; Szeto, T.; Zhang, X.; Tarbet, B.; Marty, M. T.; Chen, Y.; Wang, J. Boceprevir, GC-376, and Calpain Inhibitors II, XII Inhibit SARS-CoV-2 Viral Replication by Targeting the Viral Main Protease. *Cell Res.* **2020**, *30*, 678−692.
(57) Kim, Y.; Liu, H.; Galasiti Kankanamalage, A. C.; Weerasekara, S.; Hua, D. H.; Groutas, W. C.; Chang, K. O.; Pedersen, N. C. Reversal of the Progression of Fatal Coronavirus Infection in Cats by a Broad-Spectrum Coronavirus Protease Inhibitor. *PLoS Pathog.* **2016**, *12*, 1005531.
(58) Pedersen, N. C.; Kim, Y.; Liu, H.; Galasiti Kankanamalage, A. C.; Eckstrand, C.; Groutas, W. C.; Bannasch, M.; Meadows, J. M.; Chang, K. O. Efficacy of a 3C-like Protease Inhibitor in Treating Various Forms of Acquired Feline Infectious Peritonitis. *J. Feline Med. Surg.* **2018**, *20*, 378−392.
(59) Fu, L.; Ye, F.; Feng, Y.; Yu, F.; Wang, Q.; Wu, Y.; Zhao, C.; Sun, H.; Huang, B.; Niu, P.; Song, H.; Shi, Y.; Li, X.; Tan, W.; Qi, J.; Gao, G. F. Both Boceprevir and GC376 Efficaciously Inhibit SARS-CoV-2 by Targeting Its Main Protease. *Nat. Commun.* **2020**, *11*, 4417.
(60) Vuong, W.; Khan, M. B.; Fischer, C.; Arutyunova, E.; Lamer, T.; Shields, J.; Saffran, H. A.; McKay, R. T.; van Belkum, M. J.; Joyce, M. A.; Young, H. S.; Tyrrell, D. L.; Vederas, J. C.; Lemieux, M. J. Feline Coronavirus Drug Inhibits the Main Protease of SARS-CoV-2 and Blocks Virus Replication. *Nat. Commun.* **2020**, *11*, 4282.
(61) Rathnayake, A. D.; Zheng, J.; Kim, Y.; Perera, K. D.; Mackin, S.; Meyerholz, D. K.; Kashipathy, M. M.; Battaile, K. P.; Lovell, S.; Perlman, S.; Groutas, W. C.; Chang, K.-O. 3C-like Protease Inhibitors Block Coronavirus Replication in Vitro and Improve Survival in MERS-CoV−Infected Mice. *Sci. Transl. Med.* **2020**, *12*, eabc5332.
(62) Cao, B.; Wang, Y.; Wen, D.; Liu, W.; Wang, J.; Fan, G.; Ruan, L.; Song, B.; Cai, Y.; Wei, M.; Li, X.; Xia, J.; Chen, N.; Xiang, J.; Yu, T.; Bai, T.; Xie, X.; Zhang, L.; Li, C.; Yuan, Y.; Chen, H.; Li, H.; Huang, H.; Tu, S.; Gong, F.; Liu, Y.; Wei, Y.; Dong, C.; Zhou, F.; Gu, X.; Xu, J.; Liu, Z.; Zhang, Y.; Li, H.; Shang, L.; Wang, K.; Li, K.; Zhou, X.; Dong, X.; Qu, Z.; Lu, S.; Hu, X.; Ruan, S.; Luo, S.; Wu, J.; Peng, L.; Cheng, F.; Pan, L.; Zou, J.; Jia, C.; Wang, J.; Liu, X.; Wang, S.; Wu, X.; Ge, Q.; He, J.; Zhan, H.; Qiu, F.; Guo, L.; Huang, C.; Jaki, T.; Hayden, F. G.; Horby, P. W.; Zhang, D.; Wang, C. A Trial of Lopinavir−Ritonavir in Adults Hospitalized with Severe Covid-19. *N. Engl. J. Med.* **2020**, *382*, 1787−1799.
(63) Cheng, S. C.; Chang, G. G.; Chou, C. Y. Mutation of Glu-166 Blocks the Substrate-Induced Dimerization of SARS Coronavirus Main Protease. *Biophys. J.* **2010**, *98*, 1327−1336.
(64) Lamarre, D.; Anderson, P. C.; Bailey, M.; Beaulieu, P.; Bolger, G.; Bonneau, P.; Bös, M.; Cameron, D. R.; Cartier, M.; Cordingley, M. G.; Faucher, A. M.; Goudreau, N.; Kawai, S. H.; Kukolj, G.; Lagacé, L.; LaPlante, S. R.; Narjes, H.; Poupart, M. A.; Rancourt, J.; Sentjens, R. E.; St George, R.; Simoneau, B.; Steinmann, G.; Thibeault, D.; Tsantrizos, Y. S.; Weldon, S. M.; Yong, C. L.; Llinàs-Brunet, M. An NS3 Protease Inhibitor with Antiviral Effects in Humans Infected with Hepatitis C Virus. *Nature* **2003**, *426*, 186−189.

(65) Llinàs-Brunet, M.; Bailey, M. D.; Bolger, G.; Brochu, C.; Faucher, A. M.; Ferland, J. M.; Garneau, M.; Ghiro, E.; Gorys, V.; Grand-Maître, C.; Halmos, T.; Lapeyre-Paquette, N.; Liard, F.; Poirier, M.; Rhéaume, M.; Tsantrizos, Y. S.; Lamarre, D. Structure-Activity Study on a Novel Series of Macrocyclic Inhibitors of the Hepatitis C Virus NS3 Protease Leading to the Discovery of BILN 2061. *J. Med. Chem.* **2004**, *47*, 1605−1608.
(66) Summa, V.; Ludmerer, S. W.; McCauley, J. A.; Fandozzi, C.; Burlein, C.; Claudio, G.; Coleman, P. J.; DiMuzio, J. M.; Ferrara, M.; Di Filippo, M.; Gates, A. T.; Graham, D. J.; Harper, S.; Hazuda, D. J.; McHale, C.; Monteagudo, E.; Pucci, V.; Rowley, M.; Rudd, M. T.; Soriano, A.; Stahlhut, M. W.; Vacca, J. P.; Olsen, D. B.; Liverton, N. J.; Carroll, S. S. MK-5172, a Selective Inhibitor of Hepatitis C Virus NS3/4a Protease with Broad Activity across Genotypes and Resistant Variants. *Antimicrob. Agents Chemother.* **2012**, *56*, 4161−4167.
(67) Harper, S.; McCauley, J. A.; Rudd, M. T.; Ferrara, M.; DiFilippo, M.; Crescenzi, B.; Koch, U.; Petrocchi, A.; Holloway, M. K.; Butcher, J. W.; Romano, J. J.; Bush, K. J.; Gilbert, K. F.; McIntyre, C. J.; Nguyen, K. T.; Nizi, E.; Carroll, S. S.; Ludmerer, S. W.; Burlein, C.; Dimuzio, J. M.; Graham, D. J.; McHale, C. M.; Stahlhut, M. W.; Olsen, D. B.; Monteagudo, E.; Cianetti, S.; Giuliano, C.; Pucci, V.; Trainor, N.; Fandozzi, C. M.; Rowley, M.; Coleman, P. J.; Vacca, J. P.; Summa, V.; Liverton, N. J. Discovery of MK-5172, a Macrocyclic Hepatitis C Virus NS3/4a Protease Inhibitor. *ACS Med. Chem. Lett.* **2012**, *3*, 332−336.
(68) Kania, R. S.; Mitchell, L. J., Jr.; Nieman, J. A. Anticoronaviral Compounds and Compositions, Their Pharmaceutical Uses and Materials for Their Synthesis. WO2005113580A1, 2006.
(69) Kania, R. S.; Mitchell, L. J., Jr.; Nieman, J. A. Anticoronaviral Compounds and Compositions, Their Pharmaceutical Uses and Materials for Their Synthesis. WO2006061714A2, 2006.
(70) Thanigaimalai, P.; Konno, S.; Yamamoto, T.; Koiwai, Y.; Taguchi, A.; Takayama, K.; Yakushiji, F.; Akaji, K.; Chen, S. E.; Naser-Tavakolian, A.; Schön, A.; Freire, E.; Hayashi, Y. Development of Potent Dipeptide-Type SARS-CoV 3CL Protease Inhibitors with Novel P3 Scaffolds: Design, Synthesis, Biological Evaluation, and Docking Studies. *Eur. J. Med. Chem.* **2013**, *68*, 372−384.
(71) Hoffman, R. L.; Kania, R. S.; Brothers, M. A.; Davies, J. F.; Ferre, R. A.; Gajiwala, K. S.; He, M.; Hogan, R. J.; Kozminski, K.; Li, L. Y.; Lockner, J. W.; Lou, J.; Marra, M. T.; Mitchell, L. J.; Murray, B. W.; Nieman, J. A.; Noell, S.; Planken, S. P.; Rowe, T.; Ryan, K.; Smith, G. J.; Solowiej, J. E.; Steppan, C. M.; Taggart, B. Discovery of Ketone-Based Covalent Inhibitors of Coronavirus 3CL Proteases for the Potential Therapeutic Treatment of COVID-19. *J. Med. Chem.* **2020**, DOI: 10.1021/acs.jmedchem.0c01063.
(72) Boras, B.; Jones, R. M.; Anson, B. J.; Arenson, D.; Aschenbrenner, L.; Bakowski, M. A.; Beutler, N.; Binder, J.; Chen, E.; Eng, H.; Hammond, J.; Hoffman, R.; Kadar, E. P.; Kania, R.; Kimoto, E.; Kirkpatrick, M. G.; Lanyon, L.; Lendy, E. K.; Lillis, J. R.; Luthra, S. A.; Ma, C.; Noell, S.; Obach, R. S.; O' Brien, M. N.; O'Connor, R.; Ogilvie, K.; Owen, D.; Pettersson, M.; Reese, M. R.; Rogers, T. F.; Rossulek, M. I.; Sathish, J. G.; Steppan, C.; Ticehurst, M.; Updyke, L. W.; Zhu, Y.; Wang, J.; Chatterjee, A. K.; Mesecar, A. D.; Anderson, A. S.; Allerton, C. Discovery of a Novel Inhibitor of Coronavirus 3CL Protease as a Clinical Candidate for the Potential Treatment of COVID-19. *bioRxiv* **2020**, DOI: 10.1101/2020.09.12.293498.
(73) *Pfizer Investor Day Features Significant Number of Pipeline Advances for COVID-19 Programs and Across Numerous Therapeutic Areas*; Pfizer, 2020;https://www.pfizer.com/news/press-release/press-release-detail/pfizer-investor-day-features-significant-number-pipeline (accessed 2020-09-25).
(74) Su, H.-x.; Yao, S.; Zhao, W.-f.; Li, M.-j.; Liu, J.; Shang, W.-j.; Xie, H.; Ke, C.-q.; Hu, H.-c.; Gao, M.-n.; Yu, K.-q.; Liu, H.; Shen, J.-s.; Tang, W.; Zhang, L.-k.; Xiao, G.-f.; Ni, L.; Wang, D.-w.; Zuo, J.-p.; Jiang, H.-l.; Bai, F.; Wu, Y.; Ye, Y.; Xu, Y.-c. Anti-SARS-CoV-2 Activities in Vitro of Shuanghuanglian Preparations and Bioactive Ingredients. *Acta Pharmacol. Sin.* **2020**, *41*, 1167−1177.
(75) Liu, H.; Ye, F.; Sun, Q.; Liang, H.; Li, C.; Lu, R.; Huang, B.; Tan, W.; Lai, L. Scutellaria Baicalensis Extract and Baicalein Inhibit Replication of SARS-CoV-2 and Its 3C-like Protease in Vitro. *bioRxiv* **2020**, DOI: 10.1101/2020.04.10.035824.
(76) Su, H.; Yao, S.; Zhao, W.; Li, M.; Liu, J.; Shang, W.; Xie, H.; Ke, C.; Gao, M.; Yu, K.; Liu, H.; Shen, J.; Tang, W.; Zhang, L.; Zuo, J.; Jiang, H.; Bai, F.; Wu, Y.; Ye, Y.; Xu, Y. Discovery of Baicalin and Baicalein as Novel, Natural Product Inhibitors of SARS-CoV-2 3CL Protease in Vitro. *bioRxiv* **2020**, DOI: 10.1101/2020.04.13.038687.
(77) Li, M.; Shi, A.; Pang, H.; Xue, W.; Li, Y.; Cao, G.; Yan, B.; Dong, F.; Li, K.; Xiao, W.; He, G.; Du, G.; Hu, X. Safety, Tolerability, and Pharmacokinetics of a Single Ascending Dose of Baicalein Chewable Tablets in Healthy Subjects. *J. Ethnopharmacol.* **2014**, *156*, 210−215.
(78) Jacobs, J.; Grum-Tokars, V.; Zhou, Y.; Turlington, M.; Saldanha, S. A.; Chase, P.; Eggler, A.; Dawson, E. S.; Baez-Santos, Y. M.; Tomar, S.; Mielech, A. M.; Baker, S. C.; Lindsley, C. W.; Hodder, P.; Mesecar, A.; Stauffer, S. R. Discovery, Synthesis, and Structure-Based Optimization of a Series of N -(Tert -Butyl)-2-(N -Arylamido)-2-(Pyridin-3-Yl) Acetamides (ML188) as Potent Non-covalent Small Molecule Inhibitors of the Severe Acute Respiratory Syndrome Coronavirus (SARS-CoV) 3CL. *J. Med. Chem.* **2013**, *56*, 534−546.
(79) *COVID-19, Main Protease Structure and XChem Fragment Screen*; Diamond Light Source, 2020; hhttps://www.diamond.ac.uk/covid-19/for-scientists/Main-protease-structure-and-XChem.html (accessed 2020-06-).
(80) Parnham, M.; Sies, H. Ebselen: Prospective Therapy for Cerebral Ischaemia. *Expert Opin. Invest. Drugs* **2000**, *9*, 607−619.
(81) Snijder, E. J.; Bredenbeek, P. J.; Dobbe, J. C.; Thiel, V.; Ziebuhr, J.; Poon, L. L. M.; Guan, Y.; Rozanov, M.; Spaan, W. J. M.; Gorbalenya, A. E. Unique and Conserved Features of Genome and Proteome of SARS-Coronavirus, an Early Split-off from the Coronavirus Group 2 Lineage. *J. Mol. Biol.* **2003**, *331*, 991−1004.
(82) Imbert, I.; Snijder, E. J.; Dimitrova, M.; Guillemot, J. C.; Lécine, P.; Canard, B. The SARS-Coronavirus PLnc Domain of Nsp3 as a Replication/Transcription Scaffolding Protein. *Virus Res.* **2008**, *133*, 136−148.
(83) Neuman, B. W.; Joseph, J. S.; Saikatendu, K. S.; Serrano, P.; Chatterjee, A.; Johnson, M. A.; Liao, L.; Klaus, J. P.; Yates, J. R.; Wüthrich, K.; Stevens, R. C.; Buchmeier, M. J.; Kuhn, P. Proteomics Analysis Unravels the Functional Repertoire of Coronavirus Nonstructural Protein 3. *J. Virol.* **2008**, *82*, 5279−5294.
(84) Lindner, H. A.; Fotouhi-Ardakani, N.; Lytvyn, V.; Lachance, P.; Sulea, T.; Ménard, R. The Papain-Like Protease from the Severe Acute Respiratory Syndrome Coronavirus Is a Deubiquitinating Enzyme. *J. Virol.* **2005**, *79*, 15199−15208.
(85) Báez-Santos, Y. M.; St John, S. E.; Mesecar, A. D. The SARS-Coronavirus Papain-like Protease: Structure, Function and Inhibition by Designed Antiviral Compounds. *Antiviral Res.* **2015**, *115*, 21−38.
(86) Ratia, K.; Saikatendu, K. S.; Santarsiero, B. D.; Barretto, N.; Baker, S. C.; Stevens, R. C.; Mesecar, A. D. Severe Acute Respiratory Syndrome Coronavirus Papain-like-Protease: Structure of a Viral Deubiquitinating Enzyme. *Proc. Natl. Acad. Sci. U. S. A.* **2006**, *103*, 5717−5722.
(87) Rut, W.; Lv, Z.; Zmudzinski, M.; Patchett, S.; Nayak, D.; Snipas, S. J.; El Oualid, F.; Huang, T. T.; Bekes, M.; Drag, M.; Olsen, S. K. Activity Profiling and Structures of Inhibitor-Bound SARS-CoV-2-PLpro Protease Provides a Framework for Anti-COVID-19 Drug Design. *bioRxiv* **2020**, DOI: 10.1101/2020.04.29.068890.
(88) Węglarz-Tomczak, E.; Tomczak, J. M.; Talma, M.; Brul, S. Ebselen as a Highly Active Inhibitor of PLProCoV2. *bioRxiv* **2020**, DOI: 10.1101/2020.05.17.100768.
(89) Weglarz-Tomczak, E.; Tomczak, J. M.; Giurg, M.; Burda-Grabowska, M.; Brul, S. Discovery of Potent Inhibitors of PLproCoV2 by Screening Libraries of Selenium-Containing Compounds. *bioRxiv* **2020**, DOI: 10.1101/2020.05.20.107052.
(90) Węglarz-Tomczak, E.; Burda-Grabowska, M.; Giurg, M.; Mucha, A. Identification of Methionine Aminopeptidase 2 as a

Molecular Target of the Organoselenium Drug Ebselen and Its Derivatives/Analogues: Synthesis, Inhibitory Activity and Molecular Modeling Study. *Bioorg. Med. Chem. Lett.* **2016**, *26*, 5254−5259.
(91) Ratia, K.; Pegan, S.; Takayama, J.; Sleeman, K.; Coughlin, M.; Baliji, S.; Chaudhuri, R.; Fu, W.; Prabhakar, B. S.; Johnson, M. E.; Baker, S. C.; Ghosh, A. K.; Mesecar, A. D. A Noncovalent Class of Papain-like Protease/Deubiquitinase Inhibitors Blocks SARS Virus Replication. *Proc. Natl. Acad. Sci. U. S. A.* **2008**, *105*, 16119−16124.
(92) Ghosh, A. K.; Takayama, J.; Aubin, Y.; Ratia, K.; Chaudhuri, R.; Baez, Y.; Sleeman, K.; Coughlin, M.; Nichols, D. B.; Mulhearn, D. C.; Prabhakar, B. S.; Baker, S. C.; Johnson, M. E.; Mesecar, A. D. Structure-Based Design, Synthesis, and Biological Evaluation of a Series of Novel and Reversible Inhibitors for the Severe Acute Respiratory Syndrome - Coronavirus Papain-like Protease. *J. Med. Chem.* **2009**, *52*, 5228−5240.
(93) Báez-Santos, Y. M.; Barraza, S. J.; Wilson, M. W.; Agius, M. P.; Mielech, A. M.; Davis, N. M.; Baker, S. C.; Larsen, S. D.; Mesecar, A. D. X-Ray Structural and Biological Evaluation of a Series of Potent and Highly Selective Inhibitors of Human Coronavirus Papain-like Proteases. *J. Med. Chem.* **2014**, *57*, 2393−2412.
(94) Ziebuhr, J. The Coronavirus Replicase. In *Current Topics in Microbiology and Immunology*; Enjuanes, L., Ed.; Springer: Berlin, Heidelberg, 2005; Vol. *287*, pp 57−94.
(95) Te Velthuis, A. J. W. Common and Unique Features of Viral RNA-Dependent Polymerases. *Cell. Mol. Life Sci.* **2014**, *71*, 4403−4420.
(96) Subissi, L.; Posthuma, C. C.; Collet, A.; Zevenhoven-Dobbe, J. C.; Gorbalenya, A. E.; Decroly, E.; Snijder, E. J.; Canard, B.; Imbert, I. One Severe Acute Respiratory Syndrome Coronavirus Protein Complex Integrates Processive RNA Polymerase and Exonuclease Activities. *Proc. Natl. Acad. Sci. U. S. A.* **2014**, *111*, E3900−E3909.
(97) Imbert, I.; Guillemot, J. C.; Bourhis, J. M.; Bussetta, C.; Coutard, B.; Egloff, M. P.; Ferron, F.; Gorbalenya, A. E.; Canard, B. A Second, Non-Canonical RNA-Dependent RNA Polymerase in SARS Coronavirus. *EMBO J.* **2006**, *25*, 4933−4942.
(98) Sheahan, T. P.; Sims, A. C.; Zhou, S.; Graham, R. L.; Pruijssers, A. J.; Agostini, M. L.; Leist, S. R.; Schäfer, A.; Dinnon, K. H.; Stevens, L. J.; Chappell, J. D.; Lu, X.; Hughes, T. M.; George, A. S.; Hill, C. S.; Montgomery, S. A.; Brown, A. J.; Bluemling, G. R.; Natchus, M. G.; Saindane, M.; Kolykhalov, A. A.; Painter, G.; Harcourt, J.; Tamin, A.; Thornburg, N. J.; Swanstrom, R.; Denison, M. R.; Baric, R. S. An Orally Bioavailable Broad-Spectrum Antiviral Inhibits SARS-CoV-2 in Human Airway Epithelial Cell Cultures and Multiple Coronaviruses in Mice. *Sci. Transl. Med.* **2020**, *12*, eabb5883.
(99) Kirchdoerfer, R. N.; Ward, A. B. Structure of the SARS-CoV Nsp12 Polymerase Bound to Nsp7 and Nsp8 Co-Factors. *Nat. Commun.* **2019**, *10*, 2342.
(100) Gao, Y.; Yan, L.; Huang, Y.; Liu, F.; Zhao, Y.; Cao, L.; Wang, T.; Sun, Q.; Ming, Z.; Zhang, L.; Ge, J.; Zheng, L.; Zhang, Y.; Wang, H.; Zhu, Y.; Zhu, C.; Hu, T.; Hua, T.; Zhang, B.; Yang, X.; Li, J.; Yang, H.; Liu, Z.; Xu, W.; Guddat, L. W.; Wang, Q.; Lou, Z.; Rao, Z. Structure of the RNA-Dependent RNA Polymerase from COVID-19 Virus. *Science* **2020**, *368*, 779−782.
(101) Mcdonald, S. M. RNA Synthetic Mechanisms Employed by Diverse Families of RNA Viruses. *Wiley Interdiscip. Rev. RNA* **2013**, *4*, 351−367.
(102) Lehmann, K. C.; Gulyaeva, A.; Zevenhoven-Dobbe, J. C.; Janssen, G. M. C.; Ruben, M.; Overkleeft, H. S.; Van Veelen, P. A.; Samborskiy, D. V.; Kravchenko, A. A.; Leontovich, A. M.; Sidorov, I. A.; Snijder, E. J.; Posthuma, C. C.; Gorbalenya, A. E. Discovery of an Essential Nucleotidylating Activity Associated with a Newly Delineated Conserved Domain in the RNA Polymerase-Containing Protein of All Nidoviruses. *Nucleic Acids Res.* **2015**, *43*, 8416−8434.
(103) Yin, W.; Mao, C.; Luan, X.; Shen, D.-D.; Shen, Q.; Su, H.; Wang, X.; Zhou, F.; Zhao, W.; Gao, M.; Chang, S.; Xie, Y.-C.; Tian, G.; Jiang, H.-W.; Tao, S.-C.; Shen, J.; Jiang, Y.; Jiang, H.; Xu, Y.; Zhang, S.; Zhang, Y.; Xu, H. E. Structural Basis for the Inhibition of the RNA-Dependent RNA Polymerase from SARS-CoV-2 by Remdesivir. *Science* **2020**, *368*, 1499−1504.
(104) Peng, Q.; Peng, R.; Yuan, B.; Zhao, J.; Wang, M.; Wang, X.; Wang, Q.; Sun, Y.; Fan, Z.; Qi, J.; Gao, G. F.; Shi, Y. Structural and Biochemical Characterization of the Nsp12-Nsp7-Nsp8 Core Polymerase Complex from SARS-CoV-2. *Cell Rep.* **2020**, *31*, 107774.
(105) Hillen, H. S.; Kokic, G.; Farnung, L.; Dienemann, C.; Tegunov, D.; Cramer, P. Structure of Replicating SARS-CoV-2 Polymerase. *Nature* **2020**, *584*, 154−156.
(106) Mehellou, Y.; Rattan, H. S.; Balzarini, J. The ProTide Prodrug Technology: From the Concept to the Clinic. *J. Med. Chem.* **2018**, *61*, 2211−2226.
(107) De Clercq, E.; Neyts, J. Antiviral Agents Acting as DNA or RNA Chain Terminators. In *Handbook of Experimental Pharmacology*; Kräusslich, H.-G., Bartenschlager, R., Eds.; Springer: Berlin, Heidelberg, 2009; Vol. *189*, pp 53−84.
(108) Cho, A.; Saunders, O. L.; Butler, T.; Zhang, L.; Xu, J.; Vela, J. E.; Feng, J. Y.; Ray, A. S.; Kim, C. U. Synthesis and Antiviral Activity of a Series of 1′-Substituted 4-Aza-7,9-Dideazaadenosine C-Nucleosides. *Bioorg. Med. Chem. Lett.* **2012**, *22*, 2705−2707.
(109) Warren, T. K.; Jordan, R.; Lo, M. K.; Ray, A. S.; Mackman, R. L.; Soloveva, V.; Siegel, D.; Perron, M.; Bannister, R.; Hui, H. C.; Larson, N.; Strickley, R.; Wells, J.; Stuthman, K. S.; Van Tongeren, S. A.; Garza, N. L.; Donnelly, G.; Shurtleff, A. C.; Retterer, C. J.; Gharaibeh, D.; Zamani, R.; Kenny, T.; Eaton, B. P.; Grimes, E.; Welch, L. S.; Gomba, L.; Wilhelmsen, C. L.; Nichols, D. K.; Nuss, J. E.; Nagle, E. R.; Kugelman, J. R.; Palacios, G.; Doerffler, E.; Neville, S.; Carra, E.; Clarke, M. O.; Zhang, L.; Lew, W.; Ross, B.; Wang, Q.; Chun, K.; Wolfe, L.; Babusis, D.; Park, Y.; Stray, K. M.; Trancheva, I.; Feng, J. Y.; Barauskas, O.; Xu, Y.; Wong, P.; Braun, M. R.; Flint, M.; McMullan, L. K.; Chen, S. S.; Fearns, R.; Swaminathan, S.; Mayers, D. L.; Spiropoulou, C. F.; Lee, W. A.; Nichol, S. T.; Cihlar, T.; Bavari, S. Therapeutic Efficacy of the Small Molecule GS-5734 against Ebola Virus in Rhesus Monkeys. *Nature* **2016**, *531*, 381−385.
(110) Siegel, D.; Hui, H. C.; Doerffler, E.; Clarke, M. O.; Chun, K.; Zhang, L.; Neville, S.; Carra, E.; Lew, W.; Ross, B.; Wang, Q.; Wolfe, L.; Jordan, R.; Soloveva, V.; Knox, J.; Perry, J.; Perron, M.; Stray, K. M.; Barauskas, O.; Feng, J. Y.; Xu, Y.; Lee, G.; Rheingold, A. L.; Ray, A. S.; Bannister, R.; Strickley, R.; Swaminathan, S.; Lee, W. A.; Bavari, S.; Cihlar, T.; Lo, M. K.; Warren, T. K.; Mackman, R. L. Discovery and Synthesis of a Phosphoramidate Prodrug of a Pyrrolo[2,1-f][Triazin-4-Amino] Adenine C-Nucleoside (GS-5734) for the Treatment of Ebola and Emerging Viruses. *J. Med. Chem.* **2017**, *60*, 1648−1661.
(111) Gordon, C. J.; Tchesnokov, E. P.; Woolner, E.; Perry, J. K.; Feng, J. Y.; Porter, D. P.; Götte, M. Remdesivir Is a Direct-Acting Antiviral That Inhibits RNA-Dependent RNA Polymerase from Severe Acute Respiratory Syndrome Coronavirus 2 with High Potency. *J. Biol. Chem.* **2020**, *295*, 6785−6797.
(112) Shannon, A.; Le, N. T. T.; Selisko, B.; Eydoux, C.; Alvarez, K.; Guillemot, J. C.; Decroly, E.; Peersen, O.; Ferron, F.; Canard, B. Remdesivir and SARS-CoV-2: Structural Requirements at Both Nsp12 RdRp and Nsp14 Exonuclease Active-Sites. *Antiviral Res.* **2020**, *178*, 104793.
(113) Tchesnokov, E. P.; Feng, J. Y.; Porter, D. P.; Götte, M. Mechanism of Inhibition of Ebola Virus RNA-Dependent RNA Polymerase by Remdesivir. *Viruses* **2019**, *11*, 326.
(114) Jordan, P. C.; Liu, C.; Raynaud, P.; Lo, M. K.; Spiropoulou, C. F.; Symons, J. A.; Beigelman, L.; Deval, J. Initiation, Extension, and Termination of RNA Synthesis by a Paramyxovirus Polymerase. *PLoS Pathog.* **2018**, *14*, e1006889.
(115) Gordon, C. J.; Tchesnokov, E. P.; Feng, J. Y.; Porter, D. P.; Götte, M. The Antiviral Compound Remdesivir Potently Inhibits RNAdependent RNA Polymerase from Middle East Respiratory Syndrome Coronavirus. *J. Biol. Chem.* **2020**, *295*, 4773−4779.
(116) Wang, Q.; Wu, J.; Wang, H.; Gao, Y.; Liu, Q.; Mu, A.; Ji, W.; Yan, L.; Zhu, Y.; Zhu, C.; Fang, X.; Yang, X.; Huang, Y.; Gao, H.; Liu, F.; Ge, J.; Sun, Q.; Yang, X.; Xu, W.; Liu, Z.; Yang, H.; Lou, Z.; Jiang, B.; Guddat, L. W.; Gong, P.; Rao, Z. Structural Basis for RNA Replication by the SARS-CoV-2 Polymerase. *Cell* **2020**, *182*, 417−428. e13.

https://dx.doi.org/10.1021/acs.jmedchem.0c01140
J. Med. Chem. 2022, 65, 2716−2746

(117) Lo, M. K.; Jordan, R.; Arvey, A.; Sudhamsu, J.; Shrivastava-Ranjan, P.; Hotard, A. L.; Flint, M.; McMullan, L. K.; Siegel, D.; Clarke, M. O.; Mackman, R. L.; Hui, H. C.; Perron, M.; Ray, A. S.; Cihlar, T.; Nichol, S. T.; Spiropoulou, C. F. GS-5734 and Its Parent Nucleoside Analog Inhibit Filo-, Pneumo-, and Paramyxoviruses. *Sci. Rep.* **2017**, *7*, 43395.
(118) Lo, M. K.; Feldmann, F.; Gary, J. M.; Jordan, R.; Bannister, R.; Cronin, J.; Patel, N. R.; Klena, J. D.; Nichol, S. T.; Cihlar, T.; Zaki, S. R.; Feldmann, H.; Spiropoulou, C. F.; de Wit, E. Remdesivir (GS-5734) Protects African Green Monkeys from Nipah Virus Challenge. *Sci. Transl. Med.* **2019**, *11*, eaau9242.
(119) Dörnemann, J.; Burzio, C.; Ronsse, A.; Sprecher, A.; De Clerck, H.; Van Herp, M.; Kolié, M.-C.; Yosifiva, V.; Caluwaerts, S.; McElroy, A. K.; Antierens, A. First Newborn Baby to Receive Experimental Therapies Survives Ebola Virus Disease. *J. Infect. Dis.* **2017**, *215*, 171−174.
(120) Jacobs, M.; Rodger, A.; Bell, D. J.; Bhagani, S.; Cropley, I.; Filipe, A.; Gifford, R. J.; Hopkins, S.; Hughes, J.; Jabeen, F.; Johannessen, I.; Karageorgopoulos, D.; Lackenby, A.; Lester, R.; Liu, R. S. N.; MacConnachie, A.; Mahungu, T.; Martin, D.; Marshall, N.; Mepham, S.; Orton, R.; Palmarini, M.; Patel, M.; Perry, C.; Peters, S. E.; Porter, D.; Ritchie, D.; Ritchie, N. D.; Seaton, R. A.; Sreenu, V. B.; Templeton, K.; Warren, S.; Wilkie, G. S.; Zambon, M.; Gopal, R.; Thomson, E. C. Late Ebola Virus Relapse Causing Meningoencephalitis: A Case Report. *Lancet* **2016**, *388*, 498−503.
(121) Mulangu, S.; Dodd, L. E.; Davey, R. T.; Tshiani Mbaya, O.; Proschan, M.; Mukadi, D.; Lusakibanza Manzo, M.; Nzolo, D.; Tshomba Oloma, A.; Ibanda, A.; Ali, R.; Coulibaly, S.; Levine, A. C.; Grais, R.; Diaz, J.; Lane, H. C.; Muyembe-Tamfum, J.-J. A Randomized, Controlled Trial of Ebola Virus Disease Therapeutics. *N. Engl. J. Med.* **2019**, *381*, 2293−2303.
(122) Sheahan, T. P.; Sims, A. C.; Graham, R. L.; Menachery, V. D.; Gralinski, L. E.; Case, J. B.; Leist, S. R.; Pyrc, K.; Feng, J. Y.; Trantcheva, I.; Bannister, R.; Park, Y.; Babusis, D.; Clarke, M. O.; MacKman, R. L.; Spahn, J. E.; Palmiotti, C. A.; Siegel, D.; Ray, A. S.; Cihlar, T.; Jordan, R.; Denison, M. R.; Baric, R. S. Broad-Spectrum Antiviral GS-5734 Inhibits Both Epidemic and Zoonotic Coronaviruses. *Sci. Transl. Med.* **2017**, *9*, eaal3653.
(123) Brown, A. J.; Won, J. J.; Graham, R. L.; Dinnon, K. H.; Sims, A. C.; Feng, J. Y.; Cihlar, T.; Denison, M. R.; Baric, R. S.; Sheahan, T. P. Broad Spectrum Antiviral Remdesivir Inhibits Human Endemic and Zoonotic Deltacoronaviruses with a Highly Divergent RNA Dependent RNA Polymerase. *Antiviral Res.* **2019**, *169*, 104541.
(124) Agostini, M. L.; Andres, E. L.; Sims, A. C.; Graham, R. L.; Sheahan, T. P.; Lu, X.; Smith, E. C.; Case, J. B.; Feng, J. Y.; Jordan, R.; Ray, A. S.; Cihlar, T.; Siegel, D.; Mackman, R. L.; Clarke, M. O.; Baric, R. S.; Denison, M. R. Coronavirus Susceptibility to the Antiviral Remdesivir (GS-5734) Is Mediated by the Viral Polymerase and the Proofreading Exoribonuclease. *mBio* **2018**, *9*, e00221.
(125) Wang, M.; Cao, R.; Zhang, L.; Yang, X.; Liu, J.; Xu, M.; Shi, Z.; Hu, Z.; Zhong, W.; Xiao, G. Remdesivir and Chloroquine Effectively Inhibit the Recently Emerged Novel Coronavirus (2019-NCoV) in Vitro. *Cell Res.* **2020**, *30*, 269−271.
(126) Choy, K. T.; Wong, A. Y. L.; Kaewpreedee, P.; Sia, S. F.; Chen, D.; Hui, K. P. Y.; Chu, D. K. W.; Chan, M. C. W.; Cheung, P. P. H.; Huang, X.; Peiris, M.; Yen, H. L. Remdesivir, Lopinavir, Emetine, and Homoharringtonine Inhibit SARS-CoV-2 Replication in Vitro. *Antiviral Res.* **2020**, *178*, 104786.
(127) Runfeng, L.; Yunlong, H.; Jicheng, H.; Weiqi, P.; Qinhai, M.; Yongxia, S.; Chufang, L.; Jin, Z.; Zhenhua, J.; Haiming, J.; Kui, Z.; Shuxiang, H.; Jun, D.; Xiaobo, L.; Xiaotao, H.; Lin, W.; Nanshan, Z.; Zifeng, Y. Lianhuaqingwen Exerts Anti-Viral and Anti-Inflammatory Activity against Novel Coronavirus (SARS-CoV-2). *Pharmacol. Res.* **2020**, *156*, 104761.
(128) Pruijssers, A. J.; George, A. S.; Schäfer, A.; Leist, S. R.; Gralinksi, L. E.; Dinnon, K. H.; Yount, B. L.; Agostini, M. L.; Stevens, L. J.; Chappell, J. D.; Lu, X.; Hughes, T. M.; Gully, K.; Martinez, D. R.; Brown, A. J.; Graham, R. L.; Perry, J. K.; Du Pont, V.; Pitts, J.; Ma, B.; Babusis, D.; Murakami, E.; Feng, J. Y.; Bilello, J. P.; Porter, D. P.; Cihlar, T.; Baric, R. S.; Denison, M. R.; Sheahan, T. P. Remdesivir Inhibits SARS-CoV-2 in Human Lung Cells and Chimeric SARS-CoV Expressing the SARS-CoV-2 RNA Polymerase in Mice. *Cell Rep.* **2020**, *32*, 107940.
(129) Sheahan, T. P.; Sims, A. C.; Leist, S. R.; Schäfer, A.; Won, J.; Brown, A. J.; Montgomery, S. A.; Hogg, A.; Babusis, D.; Clarke, M. O.; Spahn, J. E.; Bauer, L.; Sellers, S.; Porter, D.; Feng, J. Y.; Cihlar, T.; Jordan, R.; Denison, M. R.; Baric, R. S. Comparative Therapeutic Efficacy of Remdesivir and Combination Lopinavir, Ritonavir, and Interferon Beta against MERS-CoV. *Nat. Commun.* **2020**, *11*, 222.
(130) Williamson, B. N.; Feldmann, F.; Schwarz, B.; Meade-White, K.; Porter, D. P.; Schulz, J.; van Doremalen, N.; Leighton, I.; Yinda, C. K.; Pérez-Pérez, L.; Okumura, A.; Lovaglio, J.; Hanley, P. W.; Saturday, G.; Bosio, C. M.; Anzick, S.; Barbian, K.; Cihlar, T.; Martens, C.; Scott, D. P.; Munster, V. J.; de Wit, E. Clinical Benefit of Remdesivir in Rhesus Macaques Infected with SARS-CoV-2. *Nature* **2020**, *585*, 273−276.
(131) Spinner, C. D.; Gottlieb, R. L.; Criner, G. J.; Arribas López, J. R.; Cattelan, A. M.; Soriano Viladomiu, A.; Ogbuagu, O.; Malhotra, P.; Mullane, K. M.; Castagna, A.; Chai, L. Y. A.; Roestenberg, M.; Tsang, O. T. Y.; Bernasconi, E.; Le Turnier, P.; Chang, S. C.; Sengupta, D.; Hyland, R. H.; Osinusi, A. O.; Cao, H.; Blair, C.; Wang, H.; Gaggar, A.; Brainard, D. M.; McPhail, M. J.; Bhagani, S.; Ahn, M. Y.; Sanyal, A. J.; Huhn, G.; Marty, F. M. Effect of Remdesivir vs Standard Care on Clinical Status at 11 Days in Patients with Moderate COVID-19: A Randomized Clinical Trial. *JAMA - J. Am. Med. Assoc.* **2020**, *324*, 1048−1057.
(132) Wang, Y.; Zhang, D.; Du, G.; Du, R.; Zhao, J.; Jin, Y.; Fu, S.; Gao, L.; Cheng, Z.; Lu, Q.; Hu, Y.; Luo, G.; Wang, K.; Lu, Y.; Li, H.; Wang, S.; Ruan, S.; Yang, C.; Mei, C.; Wang, Y.; Ding, D.; Wu, F.; Tang, X.; Ye, X.; Ye, Y.; Liu, B.; Yang, J.; Yin, W.; Wang, A.; Fan, G.; Zhou, F.; Liu, Z.; Gu, X.; Xu, J.; Shang, L.; Zhang, Y.; Cao, L.; Guo, T.; Wan, Y.; Qin, H.; Jiang, Y.; Jaki, T.; Hayden, F. G.; Horby, P. W.; Cao, B.; Wang, C. Remdesivir in Adults with Severe COVID-19: A Randomised, Double-Blind, Placebo-Controlled, Multicentre Trial. *Lancet* **2020**, *395*, 1569−1578.
(133) Norrie, J. D. Remdesivir for COVID-19: Challenges of Underpowered Studies. *Lancet* **2020**, *395*, 1525−1527.
(134) McCreary, E. K.; Angus, D. C. Efficacy of Remdesivir in COVID-19. *JAMA - J. Am. Med. Assoc.* **2020**, *324*, 1041−1042.
(135) Shiraki, K.; Daikoku, T. Favipiravir, an Anti-Influenza Drug against Life-Threatening RNA Virus Infections. *Pharmacol. Ther.* **2020**, *209*, 107512.
(136) De Clercq, E. New Nucleoside Analogues for the Treatment of Hemorrhagic Fever Virus Infections. *Chem. - Asian J.* **2019**, *14*, 3962−3968.
(137) Baranovich, T.; Wong, S.-S.; Armstrong, J.; Marjuki, H.; Webby, R. J.; Webster, R. G.; Govorkova, E. A. T-705 (Favipiravir) Induces Lethal Mutagenesis in Influenza A H1N1 Viruses In Vitro. *J. Virol.* **2013**, *87*, 3741−3751.
(138) Goldhill, D. H.; Te Velthuis, A. J. W.; Fletcher, R. A.; Langat, P.; Zambon, M.; Lackenby, A.; Barclay, W. S. The Mechanism of Resistance to Favipiravir in Influenza. *Proc. Natl. Acad. Sci. U. S. A.* **2018**, *115*, 11613−11618.
(139) Delang, L.; Segura Guerrero, N.; Tas, A.; Quérat, G.; Pastorino, B.; Froeyen, M.; Dallmeier, K.; Jochmans, D.; Herdewijn, P.; Bello, F.; Snijder, E. J.; de Lamballerie, X.; Martina, B.; Neyts, J.; van Hemert, M. J.; Leyssen, P. Mutations in the Chikungunya Virus Non-Structural Proteins Cause Resistance to Favipiravir (T-705), a Broad-Spectrum Antiviral. *J. Antimicrob. Chemother.* **2014**, *69*, 2770−2784.
(140) Chen, C.; Zhang, Y.; Huang, J.; Yin, P.; Cheng, Z.; Wu, J.; Chen, S.; Zhang, Y.; Chen, B.; Lu, M.; Luo, Y.; Ju, L.; Zhang, J.; Wang, X. Favipiravir versus Arbidol for COVID-19: A Randomized Clinical Trial. *medRxiv* **2020**, DOI: 10.1101/2020.03.17.20037432.
(141) Warren, T. K.; Wells, J.; Panchal, R. G.; Stuthman, K. S.; Garza, N. L.; Van Tongeren, S. A.; Dong, L.; Retterer, C. J.; Eaton, B. P.; Pegoraro, G.; Honnold, S.; Bantia, S.; Kotian, P.; Chen, X.; Taubenheim, B. R.; Welch, L. S.; Minning, D. M.; Babu, Y. S.;

Sheridan, W. P.; Bavari, S. Protection against Filovirus Diseases by a Novel Broad-Spectrum Nucleoside Analogue BCX4430. *Nature* **2014**, *508*, 402−405.
(142) Taylor, R.; Kotian, P.; Warren, T.; Panchal, R.; Bavari, S.; Julander, J.; Dobo, S.; Rose, A.; El-Kattan, Y.; Taubenheim, B.; Babu, Y.; Sheridan, W. P. BCX4430 - A Broad-Spectrum Antiviral Adenosine Nucleoside Analog under Development for the Treatment of Ebola Virus Disease. *J. Infect. Public Health* **2016**, *9*, 220−226.
(143) Urakova, N.; Kuznetsova, V.; Crossman, D. K.; Sokratian, A.; Guthrie, D. B.; Kolykhalov, A. A.; Lockwood, M. A.; Natchus, M. G.; Crowley, M. R.; Painter, G. R.; Frolova, E. I.; Frolov, I. *β*-D-N-4-Hydroxycytidine Is a Potent Anti-Alphavirus Compound That Induces a High Level of Mutations in the Viral Genome. *J. Virol.* **2017**, *92*, e019650-17.
(144) Toots, M.; Yoon, J. J.; Cox, R. M.; Hart, M.; Sticher, Z. M.; Makhsous, N.; Plesker, R.; Barrena, A. H.; Reddy, P. G.; Mitchell, D. G.; Shean, R. C.; Bluemling, G. R.; Kolykhalov, A. A.; Greninger, A. L.; Natchus, M. G.; Painter, G. R.; Plemper, R. K. Characterization of Orally Efficacious Influenza Drug with High Resistance Barrier in Ferrets and Human Airway Epithelia. *Sci. Transl. Med.* **2019**, *11*, eaax5866.
(145) Agostini, M. L.; Pruijssers, A. J.; Chappell, J. D.; Gribble, J.; Lu, X.; Andres, E. L.; Bluemling, G. R.; Lockwood, M. A.; Sheahan, T. P.; Sims, A. C.; Natchus, M. G.; Saindane, M.; Kolykhalov, A. A.; Painter, G. R.; Baric, R. S.; Denison, M. R. Small-Molecule Antiviral *β*-D-N-4-Hydroxycytidine Inhibits a Proofreading-Intact Coronavirus with a High Genetic Barrier to Resistance. *J. Virol.* **2019**, *93*, e01348-19.
(146) Ehteshami, M.; Tao, S.; Zandi, K.; Hsiao, H. M.; Jiang, Y.; Hammond, E.; Amblard, F.; Russell, O. O.; Merits, A.; Schinazi, R. F. Characterization of *β*-D-N4-Hydroxycytidine as a Novel Inhibitor of Chikungunya Virus. *Antimicrob. Agents Chemother.* **2017**, *61*, e023950-16.
(147) Yoon, J.-J.; Toots, M.; Lee, S.; Lee, M.-E.; Ludeke, B.; Luczo, J. M.; Ganti, K.; Cox, R. M.; Sticher, Z. M.; Edupuganti, V.; Mitchell, D. G.; Lockwood, M. A.; Kolykhalov, A. A.; Greninger, A. L.; Moore, M. L.; Painter, G. R.; Lowen, A. C.; Tompkins, S. M.; Fearns, R.; Natchus, M. G.; Plemper, R. K. Orally Efficacious Broad-Spectrum Ribonucleoside Analog Inhibitor of Influenza and Respiratory Syncytial Viruses. *Antimicrob. Agents Chemother.* **2018**, *62*, e00766-18.
(148) Toots, M.; Yoon, J.-J.; Cox, R. M.; Hart, M.; Sticher, Z. M.; Makhsous, N.; Plesker, R.; Barrena, A. H.; Reddy, P. G.; Mitchell, D. G.; Shean, R. C.; Bluemling, G. R.; Kolykhalov, A. A.; Greninger, A. L.; Natchus, M. G.; Painter, G. R.; Plemper, R. K. Characterization of Orally Efficacious Influenza Drug with High Resistance Barrier in Ferrets and Human Airway Epithelia. *Sci. Transl. Med.* **2019**, *11*, eaax5866.
(149) Wu, C.; Liu, Y.; Yang, Y.; Zhang, P.; Zhong, W.; Wang, Y.; Wang, Q.; Xu, Y.; Li, M.; Li, X.; Zheng, M.; Chen, L.; Li, H. Analysis of Therapeutic Targets for SARS-CoV-2 and Discovery of Potential Drugs by Computational Methods. *Acta Pharm. Sin. B* **2020**, *10*, 766−788.
(150) Elfiky, A. A. Anti-HCV, Nucleotide Inhibitors, Repurposing against COVID-19. *Life Sci.* **2020**, *248*, 117477.
(151) Sofia, M. J.; Chang, W.; Furman, P. A.; Mosley, R. T.; Ross, B. S. Nucleoside, Nucleotide, and Non-Nucleoside Inhibitors of Hepatitis C Virus NS5B RNA-Dependent RNA-Polymerase. *J. Med. Chem.* **2012**, *55*, 2481−2531.

https://dx.doi.org/10.1021/acs.jmedchem.0c01140
J. Med. Chem. 2022, 65, 2716−2746